PB82-260845

River Basin Validation of the Water Quality Assessment Methodology for Screening Nondesignated 208 Areas. Volume II Chesapeake-Sandusky Nondesignated 208 Screening Methodology Demonstration

Tetra Tech, Inc,
Lafayette, CA

Prepared for

Environmental Research Lab.
Athens, GA

May 82

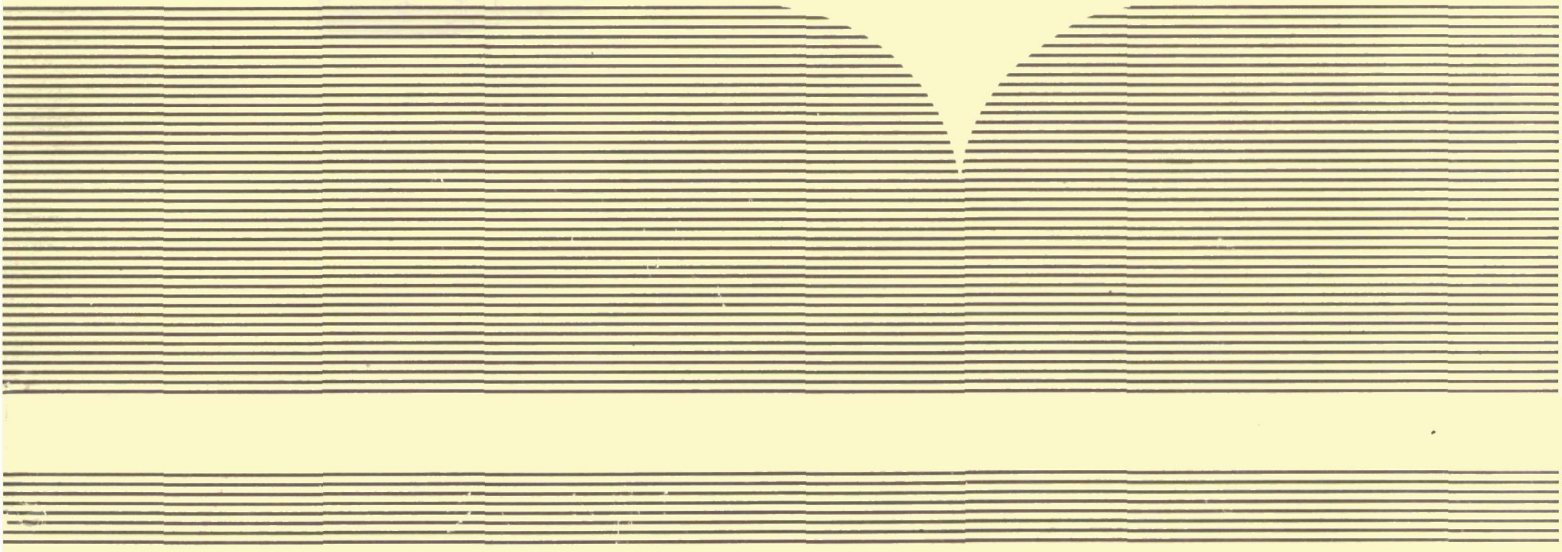

U.S. DEPARTMENT OF COMMERCE
National Technical Information Service
NTIS®

EPA 600/3-82-057b
May 1982

RIVER BASIN VALIDATION OF THE WATER QUALITY ASSESSMENT METHODOLOGY FOR SCREENING NONDESIGNATED 208 AREAS

Volume II: Chesapeake-Sandusky Nondesignated 208 Screening Methodology Demonstration

By

J. David Dean
Bob Hudson
William B. Mills

Tetra Tech, Inc.
3746 Mt. Diablo Boulevard
Lafayette, California 94549

Grant No. R806315-01-0

Project Officer

Robert B. Ambrose
Technology Development and Applications Branch
Environmental Research Laboratory
Athens, Georgia 30613

ENVIRONMENTAL RESEARCH LABORATORY
OFFICE OF RESEARCH AND DEVELOPMENT
U.S. ENVIRONMENTAL PROTECTION AGENCY
ATHENS. GEORGIA 30613

TECHNICAL REPORT DATA
(Please read Instructions on the reverse before completing)

1. REPORT NO.	2.	3. RECIPIENT'S ACCESSION NO.
EPA-600/3-82-057b	ORD Report	PB82 [illegible]

4. TITLE AND SUBTITLE	5. REPORT DATE
River Basin Validation of the Water Quality Assessment Methodology for Screening Nondesignated 208 Areas, Volume II: Chesapeake-Sandusky Nondesignaged 208 Screening Methodology Demonstration	May 1982
	6. PERFORMING ORGANIZATION CODE
7. AUTHOR(S) J. David Dean, Bob Hudson, and William B. Mills	8. PERFORMING ORGANIZATION REPORT NO.
9. PERFORMING ORGANIZATION NAME AND ADDRESS Tetra Tech, Inc. 3746 Mt. Diablo Boulevard Lafayette, California	10. PROGRAM ELEMENT NO. ACUL1A
	11. CONTRACT/GRANT NO. R806315-01-0
12. SPONSORING AGENCY NAME AND ADDRESS Environmental Research Laboratory--Athens GA Office of Research and Development U.S. Environmental Protection Agency Athens, Georgia 30613	13. TYPE OF REPORT AND PERIOD COVERED Final, 9/79-11/81
	14. SPONSORING AGENCY CODE EPA/600/01

15. SUPPLEMENTARY NOTES
River Basin Validation of the Water Quality Assessment Methodology for Screening Nondesignated 208 Areas, Volume I: Nonpoint Source Load Estimation

16. ABSTRACT

In earlier work under the sponsorship of EPA, a screening methodology was produced by Tetra Tech, Inc., for assessing water quality problems in areas not covered under Section 208 of the Federal Water Pollution Control Act Amendments of 1972, and loading functions were developed by Midwest Research Institute (MRI) for estimating the quantities of different diffuse loads entering receiving waters from nonpoint sources. The two methods had never been applied together under realistic conditions, however, to demonstrate how the combined techniques might be used for identification of water quality problems in U.S. rivers. In this volume, the successful application of the Tetra Tech-developed nondesignated 208 screening methodology under field conditions in five river basins is described, and the compatibility with the nonpoint source calculator is demonstrated. Outputs from the nonpoint source calculator were easily adapted and in some cases used directly in the mass balance equations of the screening methods. Loadings predicted with the nonpoint source calculator in conjunction with mass balance techniques employed by the screening methods provided reasonably accurate predictions of instream, lake, and estuary water quality constituent concentrations. Volume I describes the application of the MRI-developed nonpoint loading procedures in the same river basins (Sandusky River in Ohio and the Patuxent, Chester, Occoquan, and Ware Rivers in the Chesapeake Bay Basin).

17. KEY WORDS AND DOCUMENT ANALYSIS

a. DESCRIPTORS	b. IDENTIFIERS/OPEN ENDED TERMS	c. COSATI Field/Group

18. DISTRIBUTION STATEMENT	19. SECURITY CLASS *(This Report)*	21. NO. OF PAGES
RELEASE TO PUBLIC	UNCLASSIFIED	245
	20. SECURITY CLASS *(This page)*	22. PRICE
	UNCLASSIFIED	

EPA Form 2220-1 (9-73)

NOTICE

Mention of trade names or commercial products does not consititute endorsement or recommendation for use.

FOREWORD

As environmental controls become more costly to implement and the penalties of judgment errors become more severe, environmental quality management requires more efficient analytical tools based on greater knowledge of the environmental phenomena to be managed. As part of this Laboratory's research on the occurrence, movement, transformation, impact, and control of environmental contaminants, the Technology Development and Applications Branch develops management and engineering tools to help pollution control officials achieve water quality goals through watershed management.

In earlier work sponsored by EPA, water quality assessment techniques were developed for characterizing pollution problems in nondesignated 208 areas,and loading functions were developed for estimating quantities of different pollutants entering receiving water bodies from nonpoint sources. It appeared that these two tools used in concert might provide an adequate set of methods for screening nondesignated areas using simple hand calculation procedures. This report describes the application of both methods to the identification of water quality problems in several river basins in the United States.

David W. Duttweiler
Director
Environmental Research Laboratory
Athens, Georgia

ABSTRACT

In earlier work under the sponsorship of EPA, a screening methodology was produced by Tetra Tech, Inc., for assessing water quality problems in areas not covered under Section 208 of the Federal Water Pollution Control Act Amendments of 1972, and loading functions were developed by Midwest Research Institute (MRI) for estimating the quantities of different diffuse loads entering receiving water bodies from nonpoint sources. The two methods had never been applied together under realistic conditions, however, to demonstrate how the combined techniques might be used for identification of water quality problems in U.S. rivers.

In this volume, the successful application of the Tetra Tech-developed nondesignated 208 screening methodology under field conditions in five river basins is described, and the compatibility with the nonpoint source calculator is demonstrated. Outputs from the nonpoint source calculator were easily adapted and in some cases used directly in the mass balance equations of the screening methods. Loadings predicted with the nonpoint source calculator in conjunction with mass balance techniques employed by the screening methods provided reasonably accurate predictions of instream, lake and esturay water quality constituent concentrations. Volume I describes the application of the MRI-developed nonpoint loading procedures in the same river basins (Sandusky River in Ohio and the Patuxent, Chester, Occoquan, and Ware Rivers in the Chesapeake Bay Basin).

This report was submitted in fulfillment of Grant No. R806315-01-0 by Midwest Research Institute under the sponsorship of the U.S. Environmental Protection Agency. The report covers the period September 1979 to March 1981, and work was completed as of November 1981.

CONTENTS

FIGURES

FIGURES (Cont'd)

TABLES

TABLES (Cont'd)

TABLES (Cont'd)

TABLES (Cont'd)

TABLES (Cont'd)

CHAPTER 1

INTRODUCTION

1.1 BACKGROUND

In August, 1977 the U.S. Environmental Protection Agency (EPA) published a document entitled "Water Quality Assessment--A Screening Method for Nondesignated 208 Areas", EPA-600/9-77-023 (Zison et al., 1977). This document is a compendium of techniques designed to aid in the assessment of water quality problems in areas other than those covered under Section 208 of the Federal Water Pollution Control Act Amendments of 1972. Designated 208 areas are generally characterized by high concentrations of urban or industrial discharges while non-designated 208 areas may encompass a wider spectrum of human activities and, hence, a larger set of water quality conditions. These include agriculture and silviculture, as well as industrial and municipal activities. As a result, methods to assess water quality in nondesignated 208 areas must include not only the capability to predict impacts from point sources but also impacts from diffuse or nonpoint sources.

In the above document, Tetra Tech, Inc. brought together a number of methods designed to accommodate both urban and non-urban nonpoint sources, as well as municipal and industrial point sources of pollutants. In addition to the assessment of effluent water quality, the methodology provided for systematic routing of these pollutants through rivers and streams, impoundments, and estuary systems. All algorithms were designed to be used as hand calculation tools.

In 1976 Midwest Research Institute (MRI) developed a document entitled, "Loading Functions for Assessment of Water Pollution from Nonpoint Sources," for the U.S. Environmental Protection Agency (EPA-600/2-76-151). The loading functions described therein are used to

estimate the quantities of different diffuse loads that enter receiving water bodies. These methods do not route the pollutants through the receiving waters, however.

Thus, it appeared that the use of these tools in concert might provide an adequate set of methods for screening nondesignated 208 areas by simple hand calculation procedures. The methods developed by MRI for analysis of diffuse sources of water pollution and the parallel methodology developed by Tetra Tech had never been applied together in an actual field situation. This study represents an application of both methods under realistic situations for the purposes of demonstrating how the methodologies may be used for identification of water quality problem areas in nondesignated 208 areas.

1.2 PURPOSE AND SCOPE

The primary goal of this study is to demonstrate Midwest Research Institute's nonpoint calculator and Tetra Tech's nondesignated 208 screening procedures under authentic field situations. The demonstration is designed to subject the procedures to a wide range of data availability, water quality parameters, and hydrologic/hydraulic scenarios. In addition to this primary goal, there are several subgoals. They are:

1. Provide a report demonstrating the 208 screening methodology to be used as a guide by planners.
2. Show the degree of compatibility between the nonpoint loading analysis and the 208 screening methodology.
3. Develop firmer insight into the strengths and weaknesses of the nonpoint loading methodology.
4. Evaluate the sensitivity of nonpoint load estimates to varying degrees of data availability.

5. Determine how critical or necessary the quality and quantity of nonpoint source details are with regard to reliably modeling in-stream processes as they are affected by nonpoint loading.

6. Demonstrate strengths and weaknesses of the 208 screening methodology.

1.3 FORMAT AND ORGANIZATION

The nondesignated 208 screening methods are an extremely versatile set of procedures. Because of their breadth of scope, some of the methods are not applicable in every planning situation. Consequently, some techniques are not covered in these demonstrations. Conversely, some techniques have been used which are not found in the original screening procedures. When this occurs these additional techniques have been fully explained.

The applications pursued in this demonstration are not exhaustive of the ways that the methods can be used. For instance, the user may not wish to predict water quality on the basis of a specified low flow as has been done in this document. Or, the user may choose to evaluate planning alternatives which have not been investigated in these demonstrations. The approaches presented here are reasonable ones for the water quality constituents under investigation but the utility of the methods may be enhanced by innovation coupled with sound judgment on the part of the user.

This document has not been written in the tutorial style of the original non-designated 208 screening methodology document. For brevity's sake, not all calculations are shown. For in-depth documentation of the methods, the reader is referred to "Water Quality Assessment: A Screening Methodology for Nondesignated 208 areas" (Zison, et. al., 1977). Reference is frequently made to this document in these demonstrations as simply the "screening manual." To assist in obtaining values of rate

constants, the user may find the following document useful: "Rates, Constants, and Kinetics Formulations in Surface Water Quality Modeling" (Zison et al., 1978).

Almost without exception, numerical values appearing in this document are given in metric units. Exceptions are made when:

- the values are used in equations which were assigned different units in the original screening manual, or
- when non-metric units are used as indices for table look-ups in the original screening manual.

This report is divided into three chapters. The first is the introduction. The second chapter lists the major results of the demonstrations and the conclusions reached concerning both the methods themselves and the systems to which they were applied. The third chapter deals with the demonstration of the methods in each of five watersheds. It begins with a short description of each system followed by discussions of the methodology applications. The most detailed demonstrations for user orientation are the Sandusky River (for streams), Patuxent River (for estuaries), and the Occoquan Reservoir (for impoundments). The remainder of the demonstrations emphasize comparison of predicted and observed results.

CHAPTER 2

RESULTS AND CONCLUSIONS

Elements of the non-designated 208 screening methodology were applied to each of five basins for water quality assessment. The rivers and streams methods (Chapter 4 in the screening manual) were applied to the Sandusky and Patuxent river basins. Impoundment methods (Chapter 5 in the screening manual) were applied to the Occoquan Reservoir. Estuary methods (Chapter 6 of the screening manual) were applied to the Chester, Patuxent, and Ware rivers. Certain conclusions can be drawn concerning both the applicability of the methods and the screening results for each individual basin. First, however, some general conclusions concerning both the screening methodology and the nonpoint source calculator are presented. Specific conclusions of the demonstration are then listed by screening method (river, lake, or estuary) and by each basin studied.

2.1 GENERAL CONCLUSIONS

- The nonpoint source calculator (Midwest Research Institute) and the non-designated 208 screening methodology (Tetra Tech) are highly compatible. Outputs from the nonpoint source (NPS) calculator are easily adapted and in some cases are used directly in the mass balance equations of the screening methods. Event-based urban nonpoint loads are not readily predictable by the nonpoint calculator, but it is questionable if the non-designated 208 screening methods are applicable under these high flow - unsteady loading scenarios except to provide approximate upper and lower limits of instream pollutant levels.

- Loadings predicted by the nonpoint source calculator in conjunction with mass balance techniques employed by the non-designated 208 screening methods provided reasonably accurate predictions of instream, lake, and estuary water quality constituent concentrations. No effects due to basin size or location were noted that detracted from either the applicability or accuracy of the methods.

Generally, loss of accuracy due to a loss in resolution was mitigated by the averaging effects intrinsic to larger systems.

A qualitative assessment of the rivers, estuaries and impoundments methods is shown in Tables 2.1-1 to 2.1-3. In general, the tables imply that the river methods are the most accurate followed by estuaries and then impoundments. Within each method it should be mentioned that low flow - steady state conditions are more readily reproducible than high flow - unsteady loading situations. The impoundment methods probably require the least time and background skills to apply. The riverine methods will usually require more time to apply than the estuary methods. The results, however, should be easier to interpret for the uninitiated user than the results of the estuary methods.

- Loadings predicted by the nonpoint source calculator in which all parameters are assumed to be correlated with sediment loss were more accurate for sediment and phosphorus than for nitrogen and BOD_5. This is an expected result. In general, predicted nonpoint source nitrogen and BOD_5 loads were too low based on comparison of observed and predicted instream concentrations.

- For conservative parameters, linear increases or decreases in load estimates (either point or nonpoint) result in approximately linear changes in the concentrations of those constituents in the water bodies. Therefore, an approximate error analysis can be performed directly using load estimates. For nonconservative parameters, changes in stream, lake, or estuary concentrations caused by increases or decreases in loadings can only be determined by routing the pollutants through the receiving water system. An error analysis using loading changes and assuming the constituents behave conservatively will give an upper limit for the concentration changes likely to be encountered.

- While the methods appear to be a powerful tool for quickly identifying water quality problem areas, the use of the predictive techniques in conjunction with observed data further adds to their effectiveness. By doing this, the planner can identify specific problem areas in which quality cannot adequately be described by the simple techniques. In most cases, the planner will be able to recommend action, based

TABLE 2.1-1. WATER QUALITY SIMULATION RESULTS SUMMARY FOR RIVERS

	SYSTEM	
	SANDUSKY	PATUXENT
LOW FLOW		
Temperature	●	●
BOD	✸	●
Dissolved Oxygen	●	●
Coliforms	✸	✸
HIGH FLOW		
Sediment	◐	
BOD		
Total N		
Total P	◐	

Key:

●	Results good to excellent
◐	Results fair to good
✸	Simulation performed, no comparative data available
(blank)	No simulation performed

TABLE 2.1-2. WATER QUALITY SIMULATION RESULTS
SUMMARY FOR IMPOUNDMENTS

	OCCOQUAN
IMPOUNDMENTS	
Temperature	●
BOD	◐
Dissolved Oxygen	◐
Sediment	●
Total N	●
Total P	●

Key:

● Results good to excellent

◐ Results fair to good

TABLE 2.1-3. WATER QUALITY SIMULATION RESULTS SUMMARY FOR ESTUARIES

	SYSTEM		
	CHESTER	PATUXENT	WARE
LOW FLOW			
BOD	◐		◐
Coliforms	✸		
Total N		●	●
Total P		●	
HIGH FLOW			
Sediment	✸		◐
BOD	○		○
Total N	◐	✸	◐
Total P	✸	✸	◐

Key:

●	Results good to excellent
◐	Results fair to good
○	Results poor to fair
✸	Simulation performed, no comparative data available
(blank)	No simulation performed

on an understanding of the methods he has already applied, to investigate the problem area more closely. These further investigations may include sampling programs or the use of a more sophisticated analytical tool.

2.2 RIVERS AND STREAMS

- Hydraulic characterization of rivers and streams is one of the most error-prone steps in the methods. A major reason for this is that flow is in many cases a function of subsurface phenomena which are not directly estimatable from the surface topography. Unless the user has ground water measurements or detailed potentiometric maps, these effects will not be properly characterized in the system description.

  Neither is the user given any direct guidance in the screening manuals as to appropriate techniques which can be used to characterize his system hydraulically. Often only limited geometric data are available for a given river system. Measurements of channel geometry and collection of stage-discharge data are commonly done at bridges or other easily accessible locations. These locations are often not representative of the conditions in the remainder of the river. Regardless of where these measurements are made, the problem of estimating flows, geometries, and flow depths at locations between gaging stations still persists. It was found in these demonstrations that simple areal proportioning was adequate for interpolating and extrapolating streamflows. Hydraulic depths or radii were used successfully in the mass balance equations for the flow depth dependent terms. Hydraulic depth is the preferred characteristic depth to use in reaeration equations since it represents the ratio of oxygen transfer capacity at a cross section of the river (the surface width) to the oxygen storage capacity (the cross sectional area). The hydraulic radius is used in the Manning equation to estimate flow velocities.

- Dissolved oxygen prediction is far more sensitive to errors in estimating reaeration rates than in estimating deoxygenation rates. An inspection of the range of these rates indicates why this is true. The methods used to predict reaeration rates can yield answers which vary by an order of magnitude. Deoxygenation coefficients are generally predicted with greater accuracy.

- Predictive techniques for stream reaeration deserve further attention. The three methods primarily used in these demonstrations are those of Tsivoglou-Wallace, O'Connor and Owens. Of the three, the O'Connor and Owens formulations are similar, each having the stream velocity in the numerator raised to a power and stream depth in the denominator raised to a power. The Tsivoglou-Wallace approach takes into account the slope and travel time through the reach. The remainder of the commonly used formulations for reaeration are of the O'Connor and Owens type.

  Given that BOD loading rates and stream hydraulics are known with some accuracy in the demonstration systems, it appears that the O'Connor and Owens formulations give estimates which are too high and the Tsivoglou-Wallace predicts reaeration rates which are too low.

  The use of the formulations of O'Connor and Owens usually kept dissolved oxygen profiles at saturation, so it is difficult to determine how much they overestimated reaeration rates. Use of Tsivoglou-Wallace rates rarely allowed the prediction of anoxic conditions, however. A value in between the Tsivoglou-Wallace and Owens or O'Connor predictions is more likely to be appropriate.

- Comparison of predicted instream fecal or total coliform concentrations with observed data is impractical. Although the techniques presented in the screening manual are adequate, the use of average loading data for coliforms does not readily reproduce individual instream measurements. Loadings of fecal or total coliforms from sewage treatment facilities are extremely unsteady and are subject to very large perturbations. When disinfection equipment is malfunctioning, coliform concentrations in the effluent may reach 10^8/100 ml; when disinfection is successful, the concentrations are negligible. The methods in the manual can be best used for worst case analyses to give upper limit concentrations. Attempts to identify bacterial problems resulting from municipal sewage treatment plant and septic tank failures, or combined sewer overflows, should probably proceed with a time to failure or probability approach for the systems involved.

2.3 IMPOUNDMENTS

2.3.1 Stratification

- Thermal plots from the impoundment thermal model accurately describe water temperature, thermal gradients, and time of the onset of stratification. Epilimnion depths are modeled less reliably. Although conditions for the Occoquan do not exactly match the parameter values in any one set of thermal plots, the excellent results in the demonstration show the utility of the information that can be derived from these plots.

- The greatest difficulty in using the thermal profiles lies in the selection of the correct plot to apply in a borderline case. When several impoundment paramters have to be bounded, a large number of plots may have to be considered. Some cases may be eliminated if they predict a physically unreasonable result (e.g., a thermocline depth is predicted which is greater than the mean depth of the impoundment). If the occurrence of stratification is uncertain, the user may want to proceed as if the impoundment does stratify. Climatic variation will almost certainly cause stratification to occur in some years in these borderline cases.

- In borderline cases, selection of the maximum depth parameter may be aided by also considering mean impoundment depth. The mean depth represents the ratio of the volume of the impoundment to its surface area. Because the volume and surface area are proportional to the thermal capacity and heat transfer rate respectively, the mean depth should be useful in characterizing the thermal response of the impoundment.

- The hydraulic residence time strongly affects the thermal profile of an impoundment. In the demonstration, two- to threefold changes in the magnitude of the thermal gradient were observed when the residence times varied by 25 percent. It was shown that interpolation between thermal plots successfully predicted the effects of variation in hydraulic residence times on the thermal gradient.

2.3.2 Sedimentation

- Accuracy of sedimentation calculations depends primarily on accurate load estimates. Predictions based on the Universal

Soil Loss Equation (USLE) can vary greatly due to the uncertainty in the sediment delivery ratio. If possible, on-site data should be utilized. However, the good agreement of the predicted and measured loads in the demonstration watershed indicates that the USLE may be used with some confidence.

- Trapping efficiencies are most sensitive to particle size. This arises from the quadratic relationship of particle diameter to its settling velocity. Consequently, accurate knowledge of sediment diameters is required. Often a very large portion of the range of particle sizes is completely trapped, so errors tend to be relatively small.

2.3.3 Eutrophication

- The ability of the methods to quantitatively predict parameter values associated with eutrophication is limited. If nutrient concentrations are estimated from average annual loads, plant growth can only be approximated. Seasonal effects cannot be represented adequately. Prediction of algal growth may also be confounded by factors such as toxicants in the water. The relationship used in the impoundment methodology to calculate water column total phosphorus levels requires site-specific knowledge of rate constants which may only be determined through measurement.

2.3.4 Dissolved Oxygen

- The hypolimnion dissolved oxygen calculations are very sensitive to the BOD loading rate (k_a) and decay rates. The dissolved oxygen level has an exponential dependence on the first-order BOD decay rate constants for the water column (k_1) and in the benthic layer (k_4). The decrease in dissolved oxygen at any time is directly proportional to k_a. As a consequence, any uncertainty in the value of these constants will greatly broaden the range of predicted oxygen depletion rates. Because the reported values of the constant vary widely or are few in number, on-site measurements of these constants are required in order to make quantitative projections of dissolved oxygen levels.

- Qualitatively useful results are predicted by the simplified hypolimnion dissolved oxygen model even when BOD decay rate constants are not accurately known. By using estimated upper

and lower bounds for these constants, dissolved oxygen versus time curves can be obtained. These curves indicate the likelihood of experiencing low dissolved oxygen levels in the hyplimnion. When applied to the demonstration impoundment, the method predicted a range of oxygen depletion rates that was shown to bracket the actual behavior of the impoundment. This agreement demonstrates the qualitative value of the model.

2.4 ESTUARIES

2.4.1 Classification

- The use of the flow ratio method underestimates the degree of vertical stratification. According to most sources, the Chesapeake Bay and its tributaries are partially mixed. The flow ratio method predicts well mixed conditions for both low and high flows in both the Patuxent and Chester Rivers.

- The Stratification-Circulation method is preferred for estuarine classification, but the required data may not be available. Surface velocity data were available for only one estuary (the Chester River). These data were taken from a special study. Similar data may not be routinely available for other estuaries. Salinity and net fresh water flow rates are usually obtainable or can be estimated. To obtain a complete picture of the hydrodynamic variation that the estuary might undergo, the surface velocity, net fresh water velocity, and surface and bottom salinity should be available for high and low fresh water inflows both at the mouth and head of the estuary.

2.4.2 Flushing Calculations

- The tidal prism and modified tidal prism flushing times are related, and their ratio seems to be dependent upon the estuary volume. The flushing times at the $7Q_{10}$ (seven-day low flow that occurs once in 10 years) for several estuaries tributary to and including the Chester River were evaluated by both methods. A log-linear regression of the ratio of modified tidal prism method to tidal prism method versus the mean low tide volume of the estuary

was performed. The regression predicted the same ratio for the Patuxent and Ware rivers with accuracy.

- The fraction of fresh water method is fairly insensitive to the number of segments used to estimate flushing times. Flushing times in the Chester River were calculated by the fraction of fresh water method using a 1 ppt and 2 ppt segmentation scheme. The results were essentially equal.

- For flushing times derived by the modified tidal prism method that are similar at high and low flows, mechanisms other than advective flow are more important in flushing the estuary. This will generally be the case for large estuaries with small drainage basins. One might also infer from this that the water quality in such a system is dominated by the quality of the replacement waters during tidal exchange rather than the surface runoff waters.

- The fraction of fresh water and modified tidal prism methods predict more similar flushing times for smaller estuaries. The longer the residence time in the estuary, the more likely it is that antecedent runoff conditions will affect salinity profiles. The fraction of fresh water method inherently accounts for antecedent flow conditions whereas the modified tidal prism method does not. The methods will compare more consistently if salinity data are taken during a period of steady inflow. The salinity profile should be averaged over the sampling period. The length of the period of sampling should be determined by the residence time in the estuary. The problems of estimating accurate flushing times in large estuaries with short term flow or salinity data should be obvious. For these estuaries a flushing time should be computed from an expected quarterly, semi-annual or annual flow rate. Flushing times calculated for long residence estuaries using very low or very high short term flows or salinities should be used only for comparisons of the relative flushing characteristics.

2.4.3 Pollutant Distribution

- Low flow predictions of pollutant distributions in estuaries are good for conservative constituents. As long as the steady state assumptions for flow and loadings are met, the fraction of fresh water method is adequate to predict distributions.

- The modified tidal prism method must be used for non-conservative constituents. The calculation of decay for non-conservative constituents is based on a development using the modified tidal prism method (Officer, 1976). If a segmentation other than that determined by the modified tidal prism is used, the results will be erroneous.

- Pollutant distributions predicted for unsteady flow or unsteady loading represent upper and lower limit concentrations. Such cases include prediction of concentrations due to storm water carrying nonpoint source contaminants into the estuary or other impulse type discharges (chemical spills, etc.). For storm events, the user can assume that the full storm load enters the estuary during each tidal cycle, providing upper limit concentrations for the pollutant. This is reasonable since the duration of most events is less than the approximate 12-hour tidal cycle in duration. Alternatively, the user can assume that the storm load is equally distributed over each tidal cycle occurring during the time base of the runoff inflow hydrograph. This alternative will give lower limit concentrations for pollutants. More exact predictions require the use of advection-dispersion equations.

- Estuarine contamination from tidal exchange with polluted background waters can be ascertained. The modified tidal prism and fraction of fresh water methods assume that the replacement waters on each tidal exchange have no residual contamination. Since this is usually not the case, especially for estuaries which may be tributary to other estuaries, the degree of contamination in the estuary due to replacement waters can be estimated by comparing observed profiles to those predicted by the estuarine methods.

2.4.4 Eutrophication

- The two parameter light extinction model which regresses Secchi depth on contaminant concentration data can be used to investigate light limitation of algal growth in estuaries. Values of the background extinction coefficient calculated from raw data are of the same magnitude as those measured by others (3.4 to 3.6).

2.5 THE SANDUSKY RIVER

- No critical temperature problems exist in the basin except in Spring Run where an industrial effluent enters at a high temperature. In general, temperature is not a problem in other subbasins in the system.

- High BOD and low dissolved oxygen occur concurrently in this system and are bracketed if not accurately predicted by reasonable choices of BOD decay rates and reaeration coefficients. The exception is below Fremont where dissolved oxygen levels were not adequately predicted. Here, the methods have indicated that a more detailed analysis should be conducted which should include measurement of benthic oxygen demand, photosynthesis and respiration rates.

- Dissolved oxygen profiles support the conclusions drawn from field data by the Ohio EPA (1978) with respect to river segments in which dissolved oxygen sags normally occur.

- Data indicate that suspended sediment is not a problem at low flows.

- When suspended sediment and total phosphorus are treated as conservative constituents, the predicted concentrations at high flows are accurate. Using urban and non-urban loads, it appears that urban controls are more appropriate in the upper basin for reduction of instream concentrations while agricultural controls would be more appropriate in the lower basin.

- Prediction of available nitrogen was poor, but the same recommendations as for sediment and phosphorus are indicated.

2.6 THE CHESTER RIVER

- Even with the "worst-case" assumption of no enroute decay for non-conservative constituents, initial pollutant concentrations in the Chester due to point sources were small. Initial concentrations of total nitrogen and total phosphorus due to sewage treatment plant (STPs) and industrial effluents were also negligible.

- Degradations may well occur in small estuaries tributary to the Chester into which effluents from STPs or small commercial seafood operations flow, but a lack of salinity and hydraulic data prevented an in-depth analysis of these estuaries.

- Modified tidal prism flushing times under both high and low flows were very nearly equal, indicating that in the Chester River tidal action, as opposed to advective flow, is the dominant flushing mechanism.

- Phosphorus concentrations that result from high flow events are of sufficient magnitude to cause algal problems. These are more likely to occur in the upper estuary where concentrations are higher. Algal growth at the estuary head may be residence time limited due to the good flushing characteristics there.

- Nitrogen also appears to be plentiful enough after high flow events to support a large algal crop.

- The fact that high coliform counts have been observed in the estuary should lead naturally to an investigation of the effectiveness of disinfection at the sewage treatment plants and the effects of combined sewer overflows from municipalities. No estimates were made of the frequency of combined sewer overflows, septic tank, or sewage treatment plant failures in the basin. It is felt that due to the limited urban or suburban development in the basin, other factors must be contributing to the high bacterial counts. Chief among these other factors are probably untreated loadings from boat latrines and waterfowl.

- Although the methods contain no technique for assessing dissolved oxygen levels in the estuary, observed data indicate nearly anoxic conditions on occasion near the bottom. Investigations of this problem should include estimation of benthic oxygen demand and solids loadings from boating and waterfowl which may settle.

- There appears to be a seasonal shift in the N:P nutrient ratios in the estuary based on a limited number of observations. Higher N:P ratios tend to occur in the spring with lower N:P ratios occurring in the summer. The high N:P ratio in the spring indicates that spring phosphorus control from nonpoint sources may be appropriate for managing the size of the algal crop.

- If it is assumed that the Chester River is a well mixed estuary, application of the two parameter light model indicates light limitation of algal growth.

2.7 THE PATUXENT RIVER

2.7.1 Riverine Portion

- No temperature problems due to heated effluents are observed or predicted.

- Deoxygenation coefficients calculated by the Bosko equation (see Zison, et al., 1978, p. 180) were in the range of those calculated by graphical analysis of field data.

- NBOD estimates based on the type of treatment that the sewage facilities employed generally overestimated NBOD loadings as compared to estimates based on measured total Kjeldahl nitrogen at each plant.

- BOD in the Little Patuxent River is higher during low flows than in the Patuxent above their confluence.

- BOD and dissolved oxygen predictions are not extremely sensitive to background values used in the mass balance equations. Usually, loadings from sewage treatment facilities are of great enough magnitude that the background BOD becomes negligible after the first point source enters the river. Similarly reaeration rates are sufficiently large so that the initial value chosen for the oxygen deficit in the most upstream reach is not critical.

- As in the Sandusky River, the use of the Tsivoglou-Wallace and O'Connor formulations for predicting reaeration rates results in a bracketing of observed dissolved oxygen profiles.

2.7.2 Estuarine Portion

- Non-conservative constituents can be effectively dealt with by using simple mass balance with decay in the tidal fresh water portion of the Patuxent River. The tidally influenced fresh waters should be segmented as in the riverine portion and waste concentrations estimated by flow weighting. These concentrations should then be decayed instream by first order kinetics. Excursion times for each segment can be estimated by dividing the length of the section by the net velocity in that section.

- A problem area was identified in the tidally influenced fresh water portion of the Patuxent. At flows near the $7Q_{10}$ for the system, total nitrogen and total phosphorus act non-conservatively in this portion. Just before the

riverine flow meets the density-gradient flow total nitrogen and total phosphorus both drastically decrease. This may be explained by macrophyte uptake or algal growth with concurrent predation by zooplankton. At slightly higher flow rates earlier in the summer these losses of total nitrogen and phosphorus were not observed.

- The seasonal trend in N:P ratios is very pronounced in the Patuxent estuary. N:P ratios estimated by the screening method adequately predict the seasonal trend. This strong seasonal trend also implies that nonpoint controls for phosphorus in the spring and control of nitrogen from point sources in the fall may be used for managing the size of the algal crop. Given the range of the N:P ratio observed in the estuary it may be concluded that nitrogen control is the more important of the two.

- Predicted N:P ratios are lower than those calculated from observed data in the Patuxent River estuary during high flows. This appears to be due to low predicted total nitrogen values. Even so, the observed N:P ratios and those predicted would lead to the conclusion of nitrogen limitation in the estuary.

2.8 THE WARE RIVER

- Estuarine methods were applied to a very small tidal creek, Fox Mill Run, and yielded reasonable predictions for conservative and non-conservative parameters.

- Nonpoint source loads dominate the quality of the Ware River. This is logical since there is essentially no urbanization in the basin.

- Similar values of flushing times for high and low flow periods indicate that the Ware River is probably dominated by tidal exchange as opposed to advective flow, although not to the same extent as the Chester.

- Average nitrogen and phosphorus concentration predictions are good for this estuary at high flows. Predicted sediment concentrations are high while BOD_5 concentrations are low.

- N:P ratios computed for the estuary were much lower than the observed ratios. In this case, these ratios were so different that an improper conclusion would have been drawn concerning nutrient limitation had data not been available.

Observed ratios indicate a trend toward phosphorus limitation while predicted ratios indicate definite nitrogen limitation.

- Almost no seasonal trend is observed in the N:P ratios for this system. This is as expected since no major urban areas exist in the basin and nonpoint sources dominate the nutrient input to the river.

- Background extinction coefficients determined by fitting a two parameter light model to Secchi Disc data are consistent with those calculated for the Chester River and those observed by other researchers for a turbid coastal inlet.

- The two parameter light model predicts that the Ware River is light limited for algal growth, assuming a fully mixed estuary.

2.9 THE OCCOQUAN RESERVOIR

- Thermal profiles predict that stratification in Occoquan Reservoir may occur. The uncertainty is a result of the mean hydraulic residence time falling between 10 and 30 days. During years with low rainfall, stratification should occur. During years with a higher than average rainfall, stratification will be weak or nonexistent.

- The Occoquan Reservoir traps approximately 90% of the sediment entering the impoundment from the Bull Run sub-basin and 80% of the sediment entering from Lake Jackson. Any future land use that would significantly increase sedimentation should be carefully examined.

- Based on predictions of both the Vollenweider plot and the Chiaudani curve, the Occoquan Reservoir is eutrophic. This prediction is confirmed by field data.

- Water quality should not change significantly during high flow events. The MRI loading functions predict pollutant loads will be significantly higher during a high flow event than during a seven-day period under average flow conditions. The high loads are offset by a threefold increase in the volumetric flow rate over that of an average seven-day period.

- Nutrient loads predicted using the MRI nonpoint calculator were quite accurate. The total nitrogen and phosphorus loads

reported by one source were within twelve percent of those calculated using a delivery ratio of 0.2. Another source reported loads 2.3 and 1.9 times larger than the calculated loads.

- Predicted mean nutrient concentrations were comparable to observed summer values. The ratios of observed to predicted concentrations of total nitrogen and phosphorus were 1.2 and 0.9, respectively, for a delivery factor of 0.1, and 0.7 and 0.5, respectively, for a delivery factor of 0.2. The calculated ratio of nitrogen to phosphorus concentrations was 27 percent lower than observed in the Occoquan Reservoir.

- Anoxic conditions are likely to occur during the period of stratification. The dissolved oxygen calculations predict that dissolved oxygen will be absent near the bottom for 20 to 95 days during the summer.

- The primary cause of oxygen depletion is algal growth, the algal BOD contribution being approximately five times greater than the BOD load from the tributaries.

CHAPTER 3

DEMONSTRATION OF METHODS

3.1 STUDY AREA DESCRIPTION

In order to demonstrate the screening methods under a wide range of watershed conditions, types of discharges, and date availability, five watershed systems were chosen for analysis. They were:

- Sandusky River, Ohio
- Chester River, Maryland and Delaware
- Patuxent River, Maryland
- Ware River, Virginia
- Occoquan River, Virginia

3.1.1 The Sandusky River

The Sandusky River rises near Crestline, Ohio, where it first flows west, and then north. It empties into Muddy Creek Bay, Sandusky Bay, and finally into Lake Erie (Figure 3.1-1). The drainage area is 4404 km^2, making it the largest basin under consideration for this demonstration. The river is approximately 209 km long and drops an average of .74 m/km over that length. Over most of its length the river is lined by a vegetative corridor which provides a buffer for runoff from agricultural areas adjacent to it. About 88% of the land use in the drainage basin is agricultural. Crops grown are mostly corn, soybeans, wheat, oats, hay, orchards and some specialty crops. There are four municipalities in the study area with populations over 5,000. These towns are Bucyrus, Tiffin, Upper Sandusky, and Fremont.

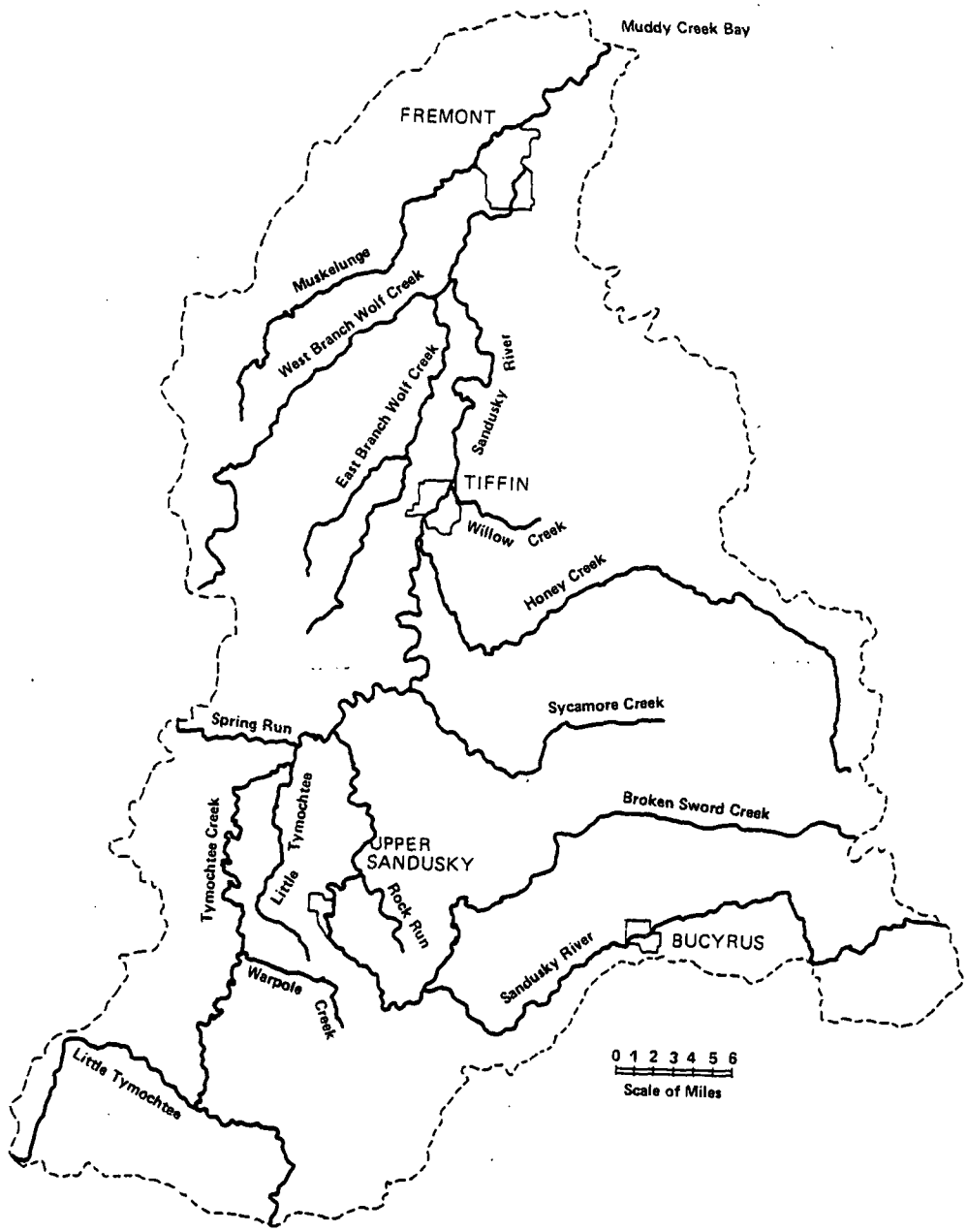

Figure 3.1-1. The Sandusky River basin.

The basin lies within the Till Plains and Lake Plains adjacent to Lake Erie. Within the Till Plains, covering approximately the lower two-thirds of the basin, end morraines left by retreating ice control the surface drainage. These morraines are roughly parallel to the Lake Erie shoreline. The northern third of the Lake Plains was formed when the area was inundated by an ancient lake. Their topography is flat to gently rolling.

The climate is humid continental with an average annual temperature of about 10.6 °C. The basin receives about 86 cm of precipitation annually. The months of February and October typically receive the lowest amounts of precipitation, while April through July are the months with the highest amounts. Further climatological and other descriptive data will be presented in the demonstration sections as needed.

3.1.1.1 Water Quality

Table 3.1-1, taken from the Sandusky River Basin portion of the Ohio State Water Quality Management Plan, shows the major water quality problem areas in the basin (Ohio EPA, 1978).

The two most seriously affected segments are immediately below the Bucyrus and Fremont Waste Water Treatment Plants. Bucyrus has secondary treatment facilities, but the fact that the plant discharges roughly half the streamflow below the effluent outfall creates problems. Bucyrus also has combined sewer overflow problems. It has been estimated that a 20-minute rainfall of greater than 0.13 cm would cause overflows to occur. The probability of occurrence of this event is one in every five days (Ohio EPA, 1978).

The river below Fremont sometimes shows anaerobic conditions during summer low flows. This apparently is the result of overloading treatment facilities by food processing plants.

TABLE 3.1-1. MAJOR WATER QUALITY PROBLEM SEGMENTS IN THE SANDUSKY RIVER

Water Quality Problem Segment RKMI* of Segment	Sub-Basin Name	Problematic Parameters	Source of Problem/RKMI*
Paramour Creek (211.4 - 208.3)	Upper Sandusky River	Dissolved Oxygen Ammonia	Crestline STP/211.4
Sandusky River (177.9 - 170.2)	Upper Sandusky River	Dissolved Oxygen Ammonia	Bucyrus STP/177.9
Sandusky River (222.5 - 124.5)	Upper Sandusky River	Dissolved Oxygen Ammonia	Upper Sandusky STP/127.6
Honey Creek (46.0 - 30.6)	Middle Sandusky River	Dissolved Oxygen	Attica STP/45.4
Spring Run (9.6 - 0.0)	Tymochtee Creek	Dissolved Oxygen	Carey STP/6.6 Budd Co./9.5

*RKMI - River Kilometer Index. The distance along the stream/river to the confluence with the next larger water body.

Otherwise, water quality degradation as a result of inadequate waste treatment is not considered a problem. The river is affected by secondary pollution problems such as sediment, turbidity, high coliform bacteria counts, and high nutrient levels resulting in occasional algal blooms. The high coliform counts are attributable to animal wastes, combined sewer overflows, and poor maintenance of rural septic tanks.

3.1.2 The Chester River

The Chester River empties into the Chesapeake Bay between Eastern Neck and the Northern end of Kent Island (Figure 3.1-2). Its headwaters are in Delaware and it meanders toward the Chesapeake Bay through Maryland's Eastern Shore. It drains approximately 1,140 km^2. The river is 81 km in length and is tidally influenced for 64 km upstream of the mouth. Agricultural uses of land are predominant in the basin. Corn, wheat, grains, soybeans, hay, vegetables, and potatoes are the major crops. The largest towns in the study area are Chestertown and Centreville. These municipalities had populations of 3,500 and 1,850, respectively, as of 1970. Wetlands are present in the basin, comprising about 34 km^2. Forestry and fishery operations are also found in the basin, with the processing of oysters, soft shell clams, blue crabs, and finfish being prevalent.

The topography is flat to gently rolling. The uplands in the Wicomico Plain have elevations of 27 to 30 meters and the lower basin, which lies in the Talbot Plain, has elevations from sea level to 18 meters.

The basin has a humid, temperate continental climate with mild winters due to climatic moderation by the Chesapeake Bay and the Atlantic Ocean. Summers are warm and humid. Temperatures average 26°C in July and temperatures of 0°C or lower occur an average of 73

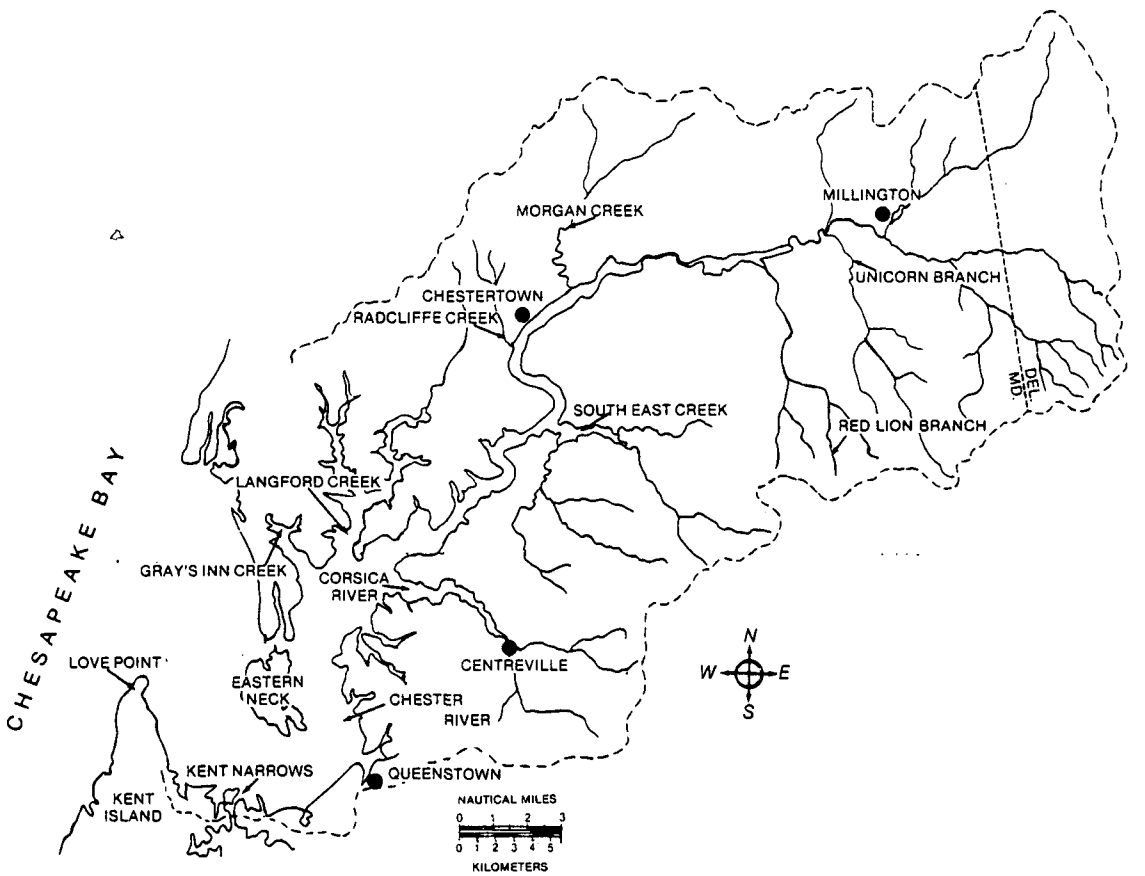

Figure 3.1-2. The Chester River basin.

days per year. Precipitation averages 107 cm per year and is distributed evenly throughout the year. Snowfall averages about 54 cm per year.

3.1.2.1 Water Quality

Three water quality factors are of primary concern in the Chester River Basin. These are:

- An unusually high mortality of oysters and other benthic organisms,
- Significant increases in nutrient concentration over the last decade,
- Bacterial levels which exceed the State of Maryland's shellfish harvesting standards.

In general, water quality in the Chester is good with the exception of coliform levels. High benthic organism mortality is suspected as being caused by a toxicant in the basin. Efforts by the Maryland Department of Natural Resources are currently underway to identify this agent.

Nutrient concentrations have been increasing since 1965. In 1974 phosphorus and nitrogen concentrations were of such magnitude to support a large algal bloom in the upper river from Chestertown to Crumpton (State of Maryland, 1975).

Closures of shellfish waters due to high indicator organism counts are extensive in the basin. Table 3.1-2 shows the extent of these closures and the suspected reasons for them.

3.1.3 The Patuxent River

The Patuxent River is located on Maryland's western shore and drains approximately 2,537 km^2. It originates in the hilly Piedmont

TABLE 3.1-2

CLOSED SHELLFISH HARVESTING AREAS IN CHESTER RIVER

Area	County	Acreage	Conditions for Closure
Chester River	Kent, Queen Anne's	4,642	Sewage treatment plant, storm water runoff
Reed and Grove Creeks	Queen Anne's	469	Storm water runoff, septic tanks overflowing
Corsica River	Queen Anne's	571	Treatment plant
Gray's Inn Creek	Kent	837	Overflowing septic systems
Langford Creek	Kent	531	Agriculture runoff, overflowing septic systems
St. Michael's Harbor	Talbot	61	Buffer zone - St. Michael's Treatment Plant
Kent Island Narrows	Queen Anne's	665	Waste from seafood processing plants
Queenstown Creek	Queen Anne's	316	Buffer zone - treatment plant
Cox Creek	Queen Anne's	142	Storm water runoff
Rock Hall Harbor	Kent	1,591	Storm water runoff, sewage violations
Spencer and Little Neck Creeks	Talbot	61	Storm water runoff, sewage violations
Oak Creek	Talbot	173	Storm water runoff, sewage violations
Leeds Creek	Talbot	387	Storm water runoff, sewage violations

After U.S. Army Corps of Engineers, Baltimore District, 1977.

Plateau between Washington, D.C., and Baltimore and flows southeasterly, entering Chesapeake Bay at Solomon's Island. The river itself can be divided into four distinct regions as indicated on the map in Figure 3.1-3. These regions are:

- Free flowing waters which extend from the headwaters to approximately Hardesty, Maryland,
- Tidal fresh waters which extend from Hardesty to about where Hall Creek enters the Patuxent River,
- Estuarine waters from Hall Creek to just below Sheridan Point, and
- Embayment waters which comprise the remainder of the river downstream.

The tidally influenced portion of the river ends about 89 km from the mouth.

As of 1977, over 50 percent of the basin was forested, with 35 percent being cultivated for agriculture and the remainder in urban or suburban developments. Major communities in the area include Laurel, Bowie and Savage (U.S. Army Corps of Engineers, 1977).

Two major tributaries contribute flow to the Patuxent. The largest is the Little Patuxent which joins the main stem at Bowie. The other is Western Branch which flows into the Patuxent just above Jug Bay. Two reservoirs are located on the Patuxent above Laurel. These are the Triadelphia and T. Howard Duckett (Rocky Gorge) Reservoirs. Their combined storage capacity is 13.4 billion gallons. They are used primarily to supply water to the Washington Suburban Sanitary Commission and Montgomery and Prince George Counties.

The Patuxent River basin, like the Chester, has a humid, temperate continental climate with warm summers and mild winters. The mean annual

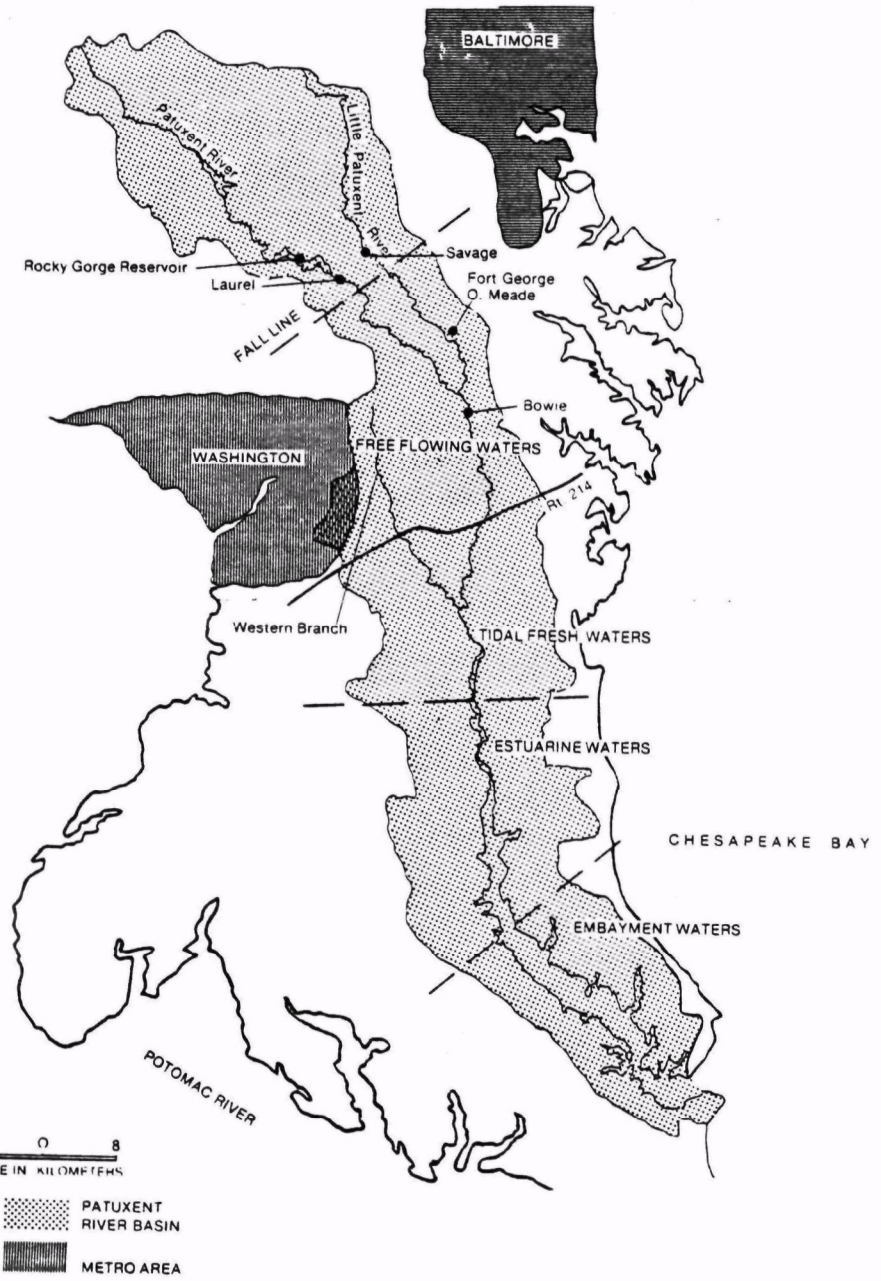

Figure 3.1-3. The Patuxent River basin.

precipitation at Washington, D.C., is 103.6 cm, which is distributed fairly evenly by season. Normal temperatures range from 2.7°C in January to 25.7°C in July with the annual average being 13.9°C.

3.1.3.1 Water Quality

Early water quality studies in the Patuxent River showed severe dissolved oxygen violations downstream of Laurel during periods of low flow and high temperature. Recently, due to sewage treatment plant modifications these problems have been mitigated somewhat. Current dissolved oxygen problems are attributed primarily to nitrogenous BOD demand. However, total nitrogen and phosphorus levels have continued to increase. There are eleven publicly owned sewage treatment plants of concern in the basin.

Industrial dischargers in the basin are in general small and do not significantly affect water quality (Pheiffer et al., 1976). The largest industrial discharger is the Potomac Electric Power Company Chalk Point Electric Plant with a discharge of approximately 720 mgd of cooling water to the Patuxent Estuary. According to a Corps of Engineers report (U.S. Army Corps of Engineers, 1977), tidal portions of the estuary do not meet Class II temperature standards. However, studies have not indicated problems attributable to this heated effluent.

Shellfish waters, as of 1977, were closed from river km 37.8 to river km 64.4 because fecal coliform standards were exceeded in most portions of the middle section of the main stem and in the tidal reaches of the river. Bacterial contamination has been primarily attributed to nonpoint agricultural and urban runoff.

Sedimentation has been and continues to be a problem in the basin, particularly with regard to navigation.

3.1.4 The Ware River

The Ware River is a small tidal river located in southern Virginia off Mobjack Bay adjacent to Chesapeake Bay. It lies between the York and the Rappahannock Rivers on the western shore. The 138 km^2 area is drained principally by two streams, Beaver Dam Swamp and Fox Mill Run as shown in Figure 3.1-4. These streams are meandering sloughs with ill-defined channels. Fox Mill Run has a drainage area of 34 km^2 above the outfall of the Gloucester Sewage Treatment Plant, the only municipal discharger in the basin. The land consists primarily of forests and swamps with limited agricultural development.

3.1.4.1 Water Quality

Water quality problems frequently associated with the Ware River are low dissolved oxygen concentrations (<5.0 mg ℓ), low pH values (<6.5), and high fecal coliform densities (>allowable log mean of 200/100 mℓ MPN). As of February 1, 1976, the Ware River waters were still open to shellfishing (U.S. Army Corps of Engineers, 1977).

3.1.5 The Occoquan River

The Occoquan River is a tributary to the Potomac River located in Northern Virginia. The watershed lies entirely in three counties: Fauquier, Prince William, and Loudoun. The map of Figure 3.1-5 shows that the 1,480 km^2 watershed is drained by three major streams which form the Occoquan River. These are Bull Run, Broad Run, and Cedar Run. The Occoquan River itself is dammed just below Hooes Run to form the only major water supply reservoir on the east coast downstream from an urbanized area.

There are three cities of consequence in or on the periphery of the watershed; namely, Fairfax, Manassas, and Warrenton, Virginia.

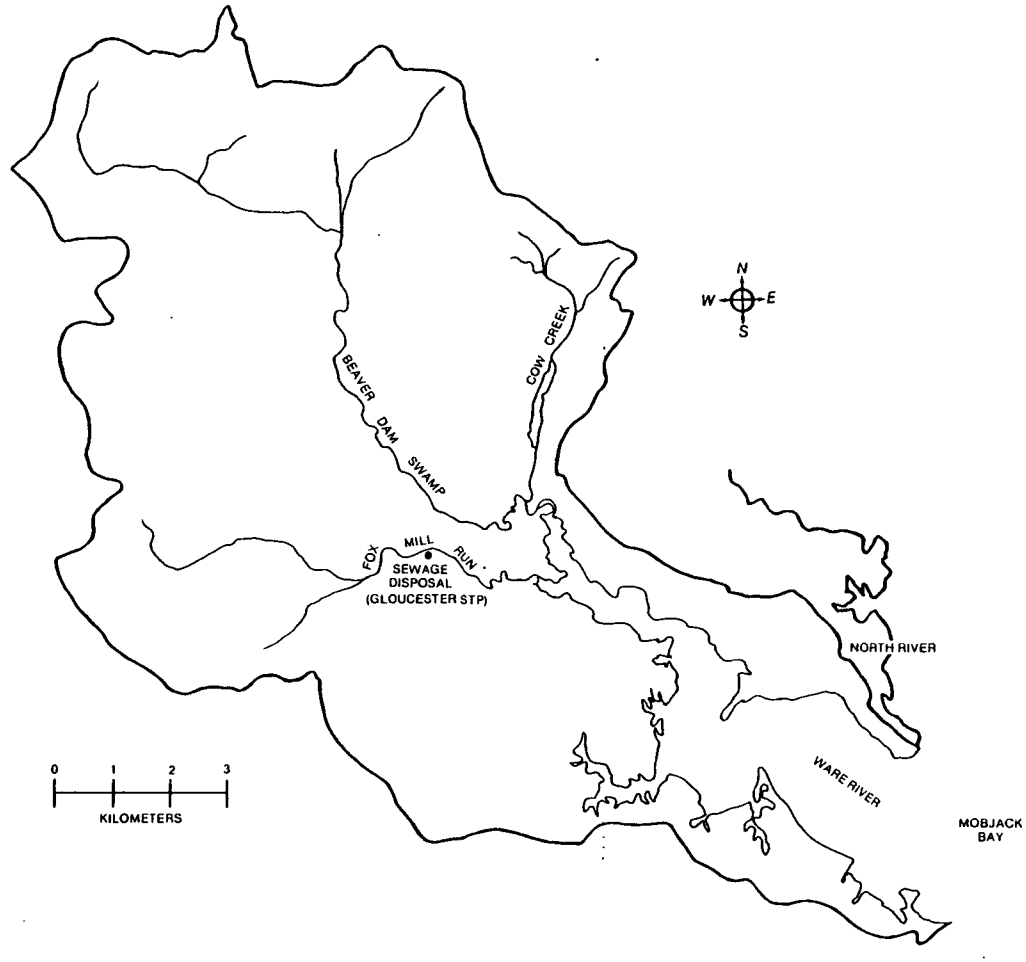

Figure 3.1-4. The Ware River basin.

Dulles Airport is also located on the boundary of the basin. Aside from these centers, the basin is relatively undeveloped, consisting mainly of agricultural land and forests. The climate is similar to that of the Patuxent basin.

3.1.5.1 Water Quality

By far the biggest problem area in the watershed is in the Bull Run sub-basin. As of 1977 there were eleven major sewage treatment plants located there. Plans were made to replace these facilities with an 84 million dollar regional tertiary treatment plant. Table 3.1-3 shows an annual history of the combined discharges of these plants.

Apparently, tertiary treatment of municipal waste has not alleviated the problem of high nutrient levels and occasional algal blooms which have occurred primarily in the Bull Run arm of the Occoquan Reservoir since the late 1960's. Grizzard et al. (1977) have pointed out that urban nonpoint loads may be the primary source of these nutrients and indicate that higher unit area loads originate from urban than from agricultural nonpoint sources.

Nutrient levels in the Occoquan Reservoir as a whole have also been high enough to create eutrophic conditions. Total nitrogen concentrations averaged 0.9 gm^{-3} during the months of April through October between 1973 and 1977. The mean total phosphorus concentration for the same period was 0.08 gm^{-3}. The mean summer (April through October) chlorophyll a concentration was held to 21 mg m^{-3} by the addition of copper sulfate during the period of measurement (1975-1977) (Northern Virginia Planning District Commission, March 1979).

As might be expected from its trophic status, the Occoquan Reservoir has oxygen depletion problems as well. Hypolimnion oxygen

concentrations in general begin to decrease with the onset of stratification in late April and are usually depleted by the end of May or June. Oxygen replenishment may not begin until the end of September in some cases, leaving the hypolimnion without oxygen for possibly three to four months.

3.2 DEMONSTRATION EXAMPLE: THE SANDUSKY RIVER

The analysis of the Sandusky River basin involved demonstrating the procedures contained in the Rivers and Streams section of the screening methodology manual. Killdeer Reservoir, an impoundment in the basin for which water quality data were available, is a pumped-storage reservoir. As such, most of the methods presented in the Impoundments chapter of the screening manual are not applicable and no analysis was performed.

The analysis of water quality in the river and some of its tributaries was performed for both a high flow and a low flow scenario. Under high flow conditions, nitrogen, phosphorus, and sediment concentrations resulting from both urban and non-urban nonpoint loadings were analyzed. Under the low flow scenario, temperature, dissolved oxygen, BOD, and fecal coliforms were analyzed. When possible, predicted instream levels of these constituents were compared to historial observations made under similar hydrologic conditions.

3.2.1 Data Collection

As a first step in data collection, 7½-minute topographic maps were obtained for the basin. The 7½-minute maps were necessary to obtain the more detailed slope and stream mileage information for hydraulic computations. Larger scale maps were extremely helpful in getting a good perspective on the general basin features,

TABLE 3.1-3. COMPARISON OF SEWAGE TREATMENT PLANT DISCHARGES IN BULL RUN SUB-BASIN: 1969 - 1977

Year	Flow mgd	BOD_5 lb/day	Total Nitrogen lb/day	Total Phosphorus lb/day
1969	2.43		483	250
1973[1]	5.54	669		217
1974[2]	6.09	459	560	163
1974[3]	5.62	260	599	75
1975[4]	6.64	349	750	89
1975[3]	6.69	315	608	77
1976[4]	6.26	356	691	85
1976[3]	6.2	320	632	56
1977[4]	5.1	315	575	50
1977[3]	6.5	402	710	72

[1]Jan.-Nov. [2]Jan.-Mar. [3]July-Dec. [4]Jan.-June

Source: Northern Virginia District Planning Commission, 1979.

The U.S. Geological Survey (USGS) provided daily flow information for each of the gaging stations in the basin. The period of record varied from over 50 years at some gages to only two at some others. Cross-section profiles and stage-discharge rating curves were also obtained.

The USGS provided temperature, pH, conductance, and dissolved oxygen data for those same stations. Additional water quality data for total phosphorus and orthophosphorus, nitrite, nitrate, ammonia, organic and total Kjeldahl nitrogen, and suspended solids were obtained from the U.S. Army Corps of Engineers (1978). Data on the effluent characteristics of industrial and municipal dischargers were obtained from an Ohio EPA preliminary report on the Sandusky River basin (Ohio EPA, 1978).

3.2.2 Data Reduction and Supplementation

Frequency analysis was performed on the low flow data to determine the $7Q_{10}$. This is the low flow of seven-day duration that occurs once every ten years (see Haan, 1977, for a comprehensive example). The $7Q_{10}$ low flow magnitudes were determined for all gaging stations in the basin. These values are shown in Table 3.2-1.

Once the $7Q_{10}$ low flows were determined, the flow depths were found from state-discharge curves. At Fremont, the depth at a flow of 2.35 $m^3 sec^{-1}$ is about 0.33 meters.

The hydraulic radius or hydraulic depth can be used as the characteristic depth of the stream in the mass balance equations for water quality constituents. For wide, shallow streams, the hydraulic depth and hydraulic radius are roughly equivalent. By using a wetted perimeter measurement from the cross-sectional profile at the Fremont gage (Figure 3.2-1) the hydraulic radius was determined for the channel at that point. For the Sandusky, use of the hydraulic depth (defined as cross-sectional area divided by flowing stream width) in lieu of the

TABLE 3.2-1. HYDRAULIC DATA FOR SANDUSKY RIVER GAGING STATIONS (LOW FLOW CONDITIONS)

Name	$7Q_{10}$ Flow (m^3 sec^{-1})	Characteristic Depth (m)	Area of Cross Section (m^2)	Characteristic Velocity (m sec^{-1})
Bucyrus	0.23	0.12	1.17	0.20
Crawford (Tymochtee Creek)	0.14	0.09	1.58	0.09
Upper Sandusky	0.33	0.14	1.61	0.20
Mexico	1.61	0.22	8.29	0.19
Fremont	2.35	0.21	4.92	0.48

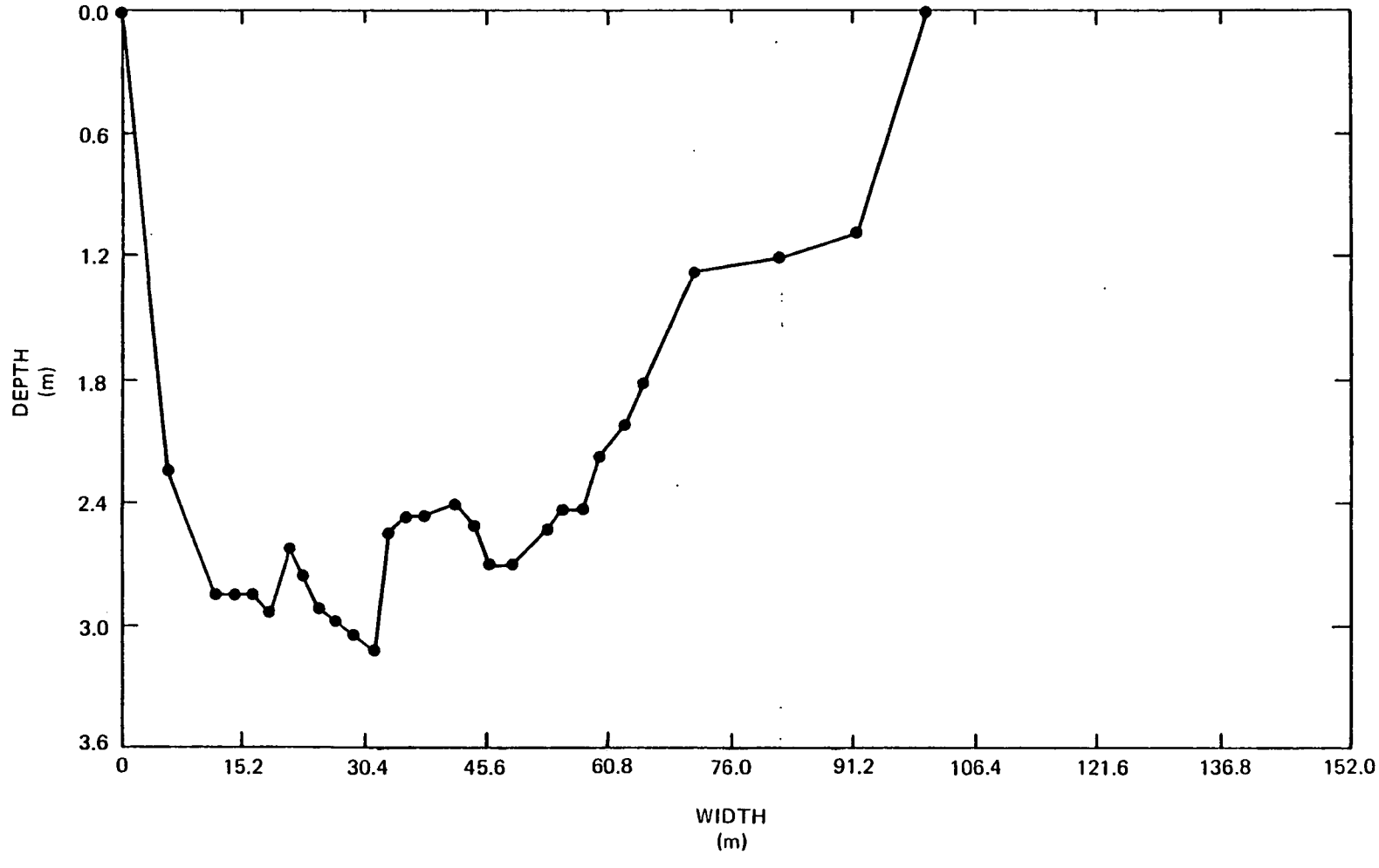

Figure 3.2-1. Cross-sectional stream profile of the Sandusky River near Fremont.

hydraulic radius (cross-sectional area divided by wetted perimeter) resulted in a 7 to 10 percent difference in the stream characteristic depth. The values shown in Table 3.2-1 are hydraulic radii.

From the continuity equation ($Q = AV$), the velocities in these sections were calculated and are also shown in Table 3.2-1. This was done by calculating the cross-sectional area in the channel corresponding to the $7Q_{10}$ flow. Dividing the cross-sectional area into the flow gives the velocity.

A word of caution is in order here. Many times the gaging stations are installed in sections of the stream which are nontypical of the rest of the stream. For instance, they may be installed in straight, uncluttered, narrow sections for ease of measurement, whereas most of the stream may be winding, debris-laden, and wide. Therefore, the velocities may be higher and the stream deeper in these sections. If other information is available, these depths and velocities should be adjusted accordingly. If not, there is generally no recourse but to use the available information as "representative" of the system.

For high flow periods a similar procedure was followed to characterize the channel system hydraulically. Instead of choosing the annual high flow event, however, selected high flow events were singled out during the period of record. The reason for this is that generally the annual high flow seven-day event takes place in conjunction with snowmelt conditions in this area. Under such circumstances it is difficult to estimate loads of nonpoint source pollutants since the waste load methods use the USLE (Universal Soil Loss Equation). The equation is designed to predict soil loss due to erosive rainfall-runoff conditions. (The reader is informed that the Screening Manual does provide a modification of the USLE for snowmelt events.) The "R" (rainfall-runoff erosivity) factor in the USLE is estimated for each rainfall event and averaged over all events, snowmelt events being excluded. Only those high flow events occurring from April to September inclusive were considered. Furthermore,

it is desirable that the rainfall events that produced the chosen high flow periods have a good areal coverage over the watershed. Because of the size of the Sandusky basin, the latter requirement was sometimes difficult to meet.

Keeping the above constraints in mind, 12 seven-day high flow periods were chosen. The loadings represent an average over those events. The flow data which represent the average seven-day high flow over all the events were supplemented as for the low flow periods to yield the hydraulic information given in Table 3.2-2.

3.2.3 River Segmentation

3.2.3.1 Low Flow

The Sandusky River system was initially broken down into a total of 76 reaches. The Sandusky River proper was made up of 21 reaches with an average length of 6.3 miles per reach. The divisions were made based on either the introduction of significant tributary flow or the introduction of flow from a point source of contaminants.

Reach segmentation is a partially subjective procedure. A point source may contribute insignificantly to the concentration of a contaminant once it is mixed with the flow of the river. In such cases, it can be ignored. It may be that the point source contributes a certain contaminant at significant concentrations but does not contribute a load of other contaminants under consideration. Therefore, the reach segmentation scheme may vary for certain water quality constituents.

In whatever manner the river is divided into reaches, slope and length are necessary to describe each reach. The user may interpolate slopes between the known points (stream gages) in the watershed or measure them from topographic maps. Again, slopes at the gaging stations may be nonrepresentative of the greater part of the river.

TABLE 3.2-2. HYDRAULIC DATA FOR SANDUSKY RIVER GAGING STATIONS (HIGH FLOW CONDITIONS)

Name	7-Day High Flow (m^3 sec^{-1})	Characteristic Depth (m)	Area of Cross Section (m^2)	Characteristic Velocity (m sec^{-1})
Bucyrus	24.0	1.68	27.0	0.89
Crawford (Tymochtee Creek)	10.4	0.79[a)]	30.5[a)]	0.34[a)]
Upper Sandusky	74.4	1.40	69.2	1.07
Mexico	192.3	0.31	172.8	1.13
Fremont	336.0	1.74	163.5	2.04

[a)] Estimated because of poor cross section profile information at high flows.

The reaches were numbered and the pertinent hydraulic information was organized into a matrix. A portion of this matrix is shown in Table 3.2-3. The information in this matrix with the exception of reach length and possibly slope, must be interpolated in some manner from the information at the stream gages.

3.2.3.2 High Flow

Because a different set of water quality parameters was under consideration during high flow events, the watershed was segmented differently. Specifically this segmentation scheme was dictated by the availability and resolution of land use data necessary for the estimation of nonpoint source loadings. Because the methodology treats nitrogen, phosphorus and suspended solids conservatively, much of the information necessary for mass balance of nonconservative constituents at low flows is not necessary. For conservative constituent routing, only flow and stream lengths are needed. These data are available from the information matrix provided in Table 3.2-3.

3.2.4 Temperature Profiles

Since the rate constants necessary for routing nonconservative constituents are temperature dependent, a stream temperature profile was first developed for the entire system.

The first step in using the methods for stream temperature is the calculation of the equilibrium temperature. (See Section 4.4.4 of the screening manual.) The month of October is the month when the annual seven-day low flow event usually occurs. From the Climatic Atlas of the United States (U.S. Department of Commerce, 1974) the following mean monthly climatic data for this month in the Sandusky area were obtained:

TABLE 3.2-3. SANDUSKY RIVER HYDRAULIC DATA BY STREAM REACH FOR A PORTION OF THE SYSTEM

Reach Number	Identifying Characteristic At Upstream End	Hydraulic Radius (m) Low	Hydraulic Radius (m) High	Cross Section (m^2) Low	Cross Section (m^2) High	Flow (m^3 sec^{-1}) Low	Flow (m^3 sec^{-1}) High	Slope (m km^{-1})	Velocity (m sec^{-1}) Low	Velocity (m sec^{-1}) High	Length (km)
1	Muskellunge Creek enters Sandusky River	0.24	2.13	5.57	167.2	2.61	378.5	0.47	0.46	2.26	15.1
2	Fremont WWTP	0.21	1.83	4.92	163.5	2.38	336.0	1.04	0.49	2.04	6.0
3	Indian Creek enters Sandusky River	0.20	1.87	5.20	164.3	2.35	323.1	1.91	0.49	2.04	11.1
4	Wolf Creek enters Sandusky River	0.21	2.40	6.50	167.9	2.2	268.5	0.85	0.30	1.62	3.2
5	Tiffin WWTP	0.21	2.41	6.50	167.9	2.01	268.5	1.56	0.30	1.62	25.7
6	Willow Creek enters Sandusky River	0.21	2.53	6.78	168.7	1.95	255.6	1.56	0.28	1.52	1.6
7	Point Source	0.21	2.53	6.78	168.7	1.93	255.6	0.15	0.28	1.52	1.3
8	Honey Creek enters Sandusky River	0.22	3.14	8.27	172.8	1.61	192.4	0.15	0.20	1.10	4.8

Mean daily incoming shortwave radiation =

280 langleys = 11,147, BTU m^{-2} day^{-1} = 1036 BTU ft^{-2} day^{-1}

Mean cloud cover = .55

Mean monthly air temperature = 12.8°C (dry bulb) = 55.0°F

Mean daily wind speed = 12.9 km hr^{-1} = 8.0 miles hr^{-1}

Mean daily relative humidity = 71%

The first four items can be used directly in the equilibrium temperature calculations. Mean shortwave radiation has to be converted from langleys to BTU ft^{-2}. The conversion factor is 3.7 BTU ft^{-2} per langley. The equilibrium temperature calculated for the Sandusky basin using these inputs is 16.2°C.

Temperature profiles for the Sandusky River were computed by beginning at the headwaters of the Sandusky and computing temperature successively for each downstream reach. (See Section 4.4.5 of the screening manual.) To start the calculations, an upstream temperature was estimated for the first reach. During low flow conditions a good estimate of this temperature was that of the ground water, approximately 10°C. At the junction of each reach, a resultant temperature was calculated due to the addition of wastewater or tributary inflow. This initial (resultant) temperature was used in the heat balance to compute a temperature at the beginning of the next reach. The procedure was repeated until the profiles for the entire river and all the major tributaries were computed.

Figures 3.2-2 and 3.2-3 show temperature profiles computed for the Sandusky River proper and a tributary, Spring Run. Included in the Sandusky plot are historical mean stream temperatures ± one standard deviation for gaged locations along the river. The computed temperature is always within the one standard deviation envelope of the historical observations. Spring Run had no historical temperature data with which

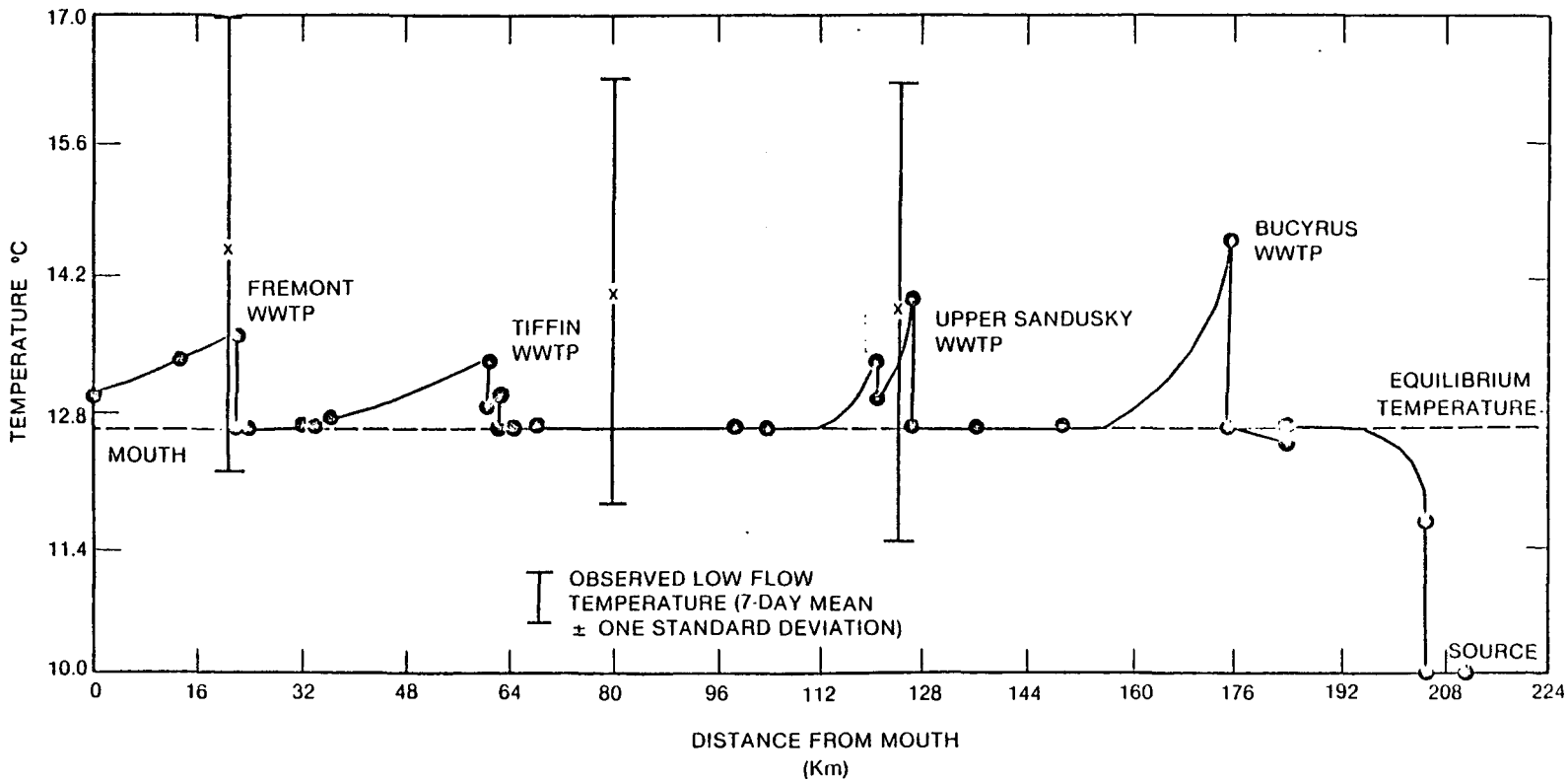

Figure 3.2-2. Observed and predicted temperatures in the Sandusky River (low flow).

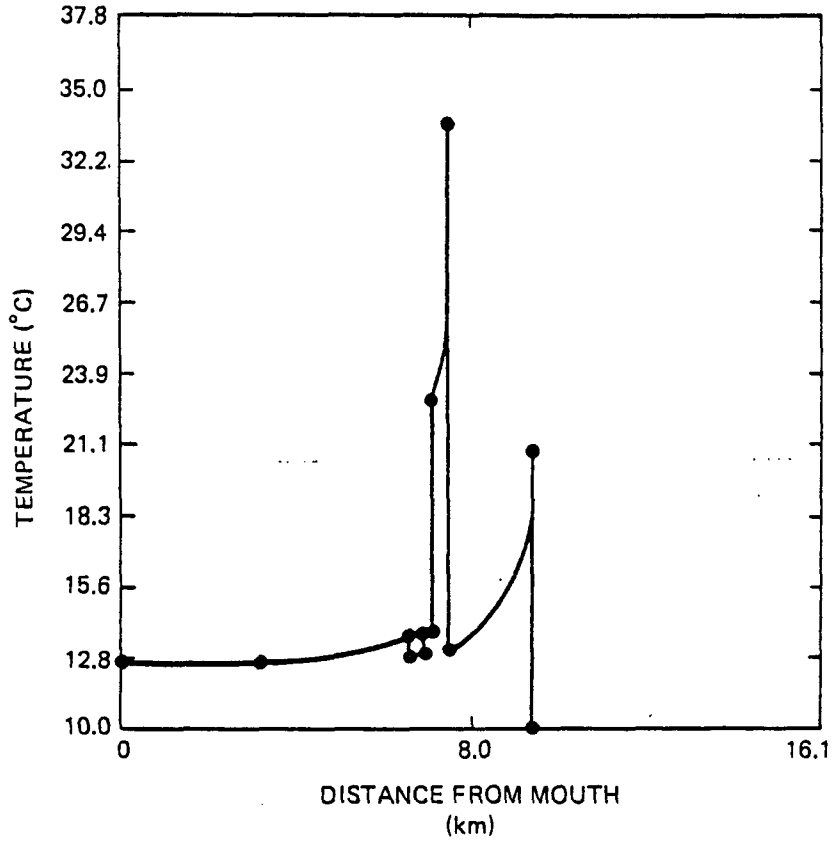

Figure 3.2-3. Calculated low flow temperature profile for Spring Run.

to compare the predicted values but is included because of the presence of an extremely high temperature effluent from an industrial source. At low flows, this effluent comes to equilibrium very rapidly and has no effect on the stream temperature after approximately three kilometers.

3.2.5 Estimation of BOD Decay Coefficients and Reaeration Coefficients

Since measured values of NBOD or CBOD (nitrogenous or carbonaceous biochemical oxygen demand) were not available, the decay coefficients for these two parameters could not be estimated directly. Additionally, no evidence was available to warrant making a distinction between the rates of decay of CBOD and NBOD. Therefore the decay of BOD was governed by a single decay constant. Using the methods of Hydroscience and Bosko described in the screening manual, a range of deoxygenation coefficients was established for each reach. Since the range of the deoxygenation rates from the Bosko equation was not large and the Hydroscience method predicted values close to the mean of the values from the Bosko equation, this mean value was used to predict BOD concentrations in the Sandusky system. The temperature corrected deoxygenation coefficients which were used in the routing equations are shown in Table 3.2-4 for reaches on the Sandusky River proper.

3.2.6 BOD Mass Balance

Biochemical oxygen demand was determined for all reaches in the system for the $7Q_{10}$ flow. Ultimate NBOD plus CBOD values were used as loads.

At low flows, the primary sources of BOD are sewage treatment plants discharging treated effluent directly into the river and to a lesser degree factories and food processing plants. Most of the industrial water users around Fremont discharge into the municipal sewage treatment facility.

TABLE 3.2-4. DEOXYGENATION RATE CONSTANTS FOR THE SANDUSKY RIVER

Reach(es)	Location	Deoxygenation Coefficient (day^{-1})
19, 20	Confluence of Paramour Creek and Allen Run to Bucyrus WWTP	.36, 2.38
18	Bucyrus WWTP to confluence of Broken Sword Creek and Sandusky River	.47
15, 16, 17	Confluence of Sandusky River w/Broken Sword Creek to Upper Sandusky WWTP	.46, .37, .37
14	Upper Sandusky WWTP to confluence of Sandusky River w/Tymochtee Creek	.36
12, 13	Confluence of Sandusky River w/Tymochtee Creek to confluence w/Honey Creek	.28, .28
8, 9, 10, 11	Confluence of Sandusky River w/Honey Creek to Tiffin WWTP	.45, .30, .29, .28
3, 4, 5, 6, 7	Tiffin WWTP to Fremont WWTP	.51, .68, .48, .41, .47
1, 2	Fremont WWTP to Muddy Creek Bay	.27, .45

Tables 3.2-5 and 3.2-6 show the computed ranges for BOD in reaches of the Sandusky and its tributaries on which there are important point sources of BOD. The range of values represents the variability from the upstream to downstream end of the reach or aggregation of reaches. By far the most degraded portion of the river considering this parameter is the segment below the Bucyrus Waste Water Treatment Plant followed by the segment downstream from the Upper Sandusky Water Treatment Plant. High values of BOD also occur in the headwater areas of the Sandusky and its tributaries where small sewage treatment plants are located in reaches with little instream diluting flow during low flow periods.

3.2.7 Dissolved Oxygen Profiles

Output from BOD routing and temperature routing were used to compute dissolved oxygen profiles for the Sandusky River system. Reaeration rate coefficients were computed by two methods, that of Owens and that of Tsivoglou and Wallace (1972). Since the results of these caltions often showed more than an order of magnitude difference in the rate coefficients, both sets of coefficients were used to determine dissolved oxygen profiles. Table 3.2-7 shows the reaeration coefficients computed by each method for reaches of the Sandusky River proper. These coefficients are not corrected for temperature as they appear in the table.

Generally, reaeration rates computed by the Owens equations are higher in the upstream portions of the river because of the shallow depths there. The depth term appears in the denominator of that equation, which drives up the calculated reaeration rate. Towards the mouth of the river depths become greater and the rates drop. Conversely, for the Tsivoglou-Wallace equation, reaeration rates are higher downstream generally than they are upstream. In this expression, stream velocity and slope are multiplied together. Although the slope remains relatively constant throughout the stream, velocity increases towards the mouth, causing predicted reaeration rates to increase. Other reaeration rate formulations

TABLE 3.2-5. EXPECTED BOD VALUES AT $7Q_{10}$ FLOW IN THE SANDUSKY RIVER

Reach(es)	Location	Ultimate BOD Concentration Range (mg ℓ^{-1})
19, 20	Confluence of Paramour Creek and Allen Run to Bucyrus WWTP	12.7 - 3.4
18	Bucyrus WWTP to confluence w/Broken Sword Creek	43.8 - 20.1
15, 16, 17	Confluence of Sandusky w/Broken Sword Creek to Upper Sandusky WWTP	14.3 - 5.6
14	Upper Sandusky WWTP to confluence w/Tymochtee Creek	30.4 - 9.1
12, 13	Confluence of Sandusky River w/Tymochtee Creek to confluence w/Honey Creek	7.50 - 6.1
8, 9, 10, 11	Confluence of Sandusky River w/Honey Creek to Tiffin WWTP	5.5 - 4.7
3, 4, 5, 6, 7	Tiffin WWTP to Fremont WWTP	7.4 - 3.3
1, 2	Fremont WWTP to Muddy Creek Bay	5.8 - 4.9

TABLE 3.2-6. EXPECTED BOD VALUES AT $7Q_{10}$ FLOW IN SELECTED SANDUSKY RIVER TRIBUTARIES

Reach(es)	Location	BOD Concentration Range (mg ℓ^{-1})
Spring Run-Tymochtee Creek		
54	Carey WWTP to confluence of Spring Run w/Tymochtee Creek	10.5 - 6.7
53	Confluence of Spring Run w/ Tymochtee Creek to confluence of Tymochtee Creek w/Sandusky River	4.1 - 2.8
Honey Creek		
26, 27	Attica WWTP to Bloomville WWTP	9.3 - 2.2
25	Bloomville WWTP to confluence w/Sandusky River	5.3 - 1.6

TABLE 3.2-7. REAERATION RATES COMPUTED BY TWO METHODS FOR THE SANDUSKY RIVER

Reach(es)	Reaeration Rates (day^{-1})	
	Owens	Tsivoglou-Wallace
19, 20	97, >100	1.28, 1.92
18	97	3.16
15, 16, 17	60, 67, 93	3.53, 1.61, 1.45
14	66	1.5
12, 13	20, 25	.40, .44
8, 9, 10, 11	28, 28, 25, 20	6.71, .65, .61, .45
3, 4, 5, 6, 7	45, 45, 42, 30, 30	7.63, 14.01, 5.61, 3.94, 7.22
1, 2	35, 40	3.31, 4.64

are included in the screening manual (Zison, et al., 1977) and in Zison, et al., 1978, but were not considered applicable here.

Figure 3.2-4 shows calculated dissolved oxygen profiles for the Sandusky River. The upper profile represents dissolved oxygen computed with the Owens reaeration rates. The lower shows the dissolved oxygen profile computed with the substantially lower reaeration rates calculated by the Tsivoglou-Wallace equation. Information on photosynthetic oxygen production rates and respiration and benthic demand were not available for any portions of the river. For this reason, these factors were not included in the analysis. These parameters can be estimated if desired. For guidance the reader is referred to Zison, et al., 1978.

An inspection of Figure 3.2-4 shows that the use of the Owens reaeration rates maintains the dissolved oxygen profile for the system almost always at the saturation dissolved oxygen value. This value decreases slightly from upstream to downstream due to temperature increases but is generally on the order of 10.4 to 10.6 mg ℓ^{-1}. The only segment in which the dissolved oxygen drops significantly is downstream from the Bucyrus Waste Water Treatment Plant (stream-km 177) where it is 9.0 mg ℓ^{-1}.

Using the Tsivoglou-Wallace reaeration rates, the dissolved oxygen values remain between 6 and 9 mg ℓ^{-1} for most of the river. At about km 59 the predicted dissolved oxygen begins to climb and almost reaches the level attained using the higher reaeration rates. This is due primarily to the fact that the Tsivoglou-Wallace reaeration rates approach values similar to the Owens rates in these reaches.

Once errors are introduced into the oxygen balance calculations, they remain although their influence generally decreases as computations for additional reaches are done. These errors may be related, for instance, to the hydraulic description of the system. It is also important to

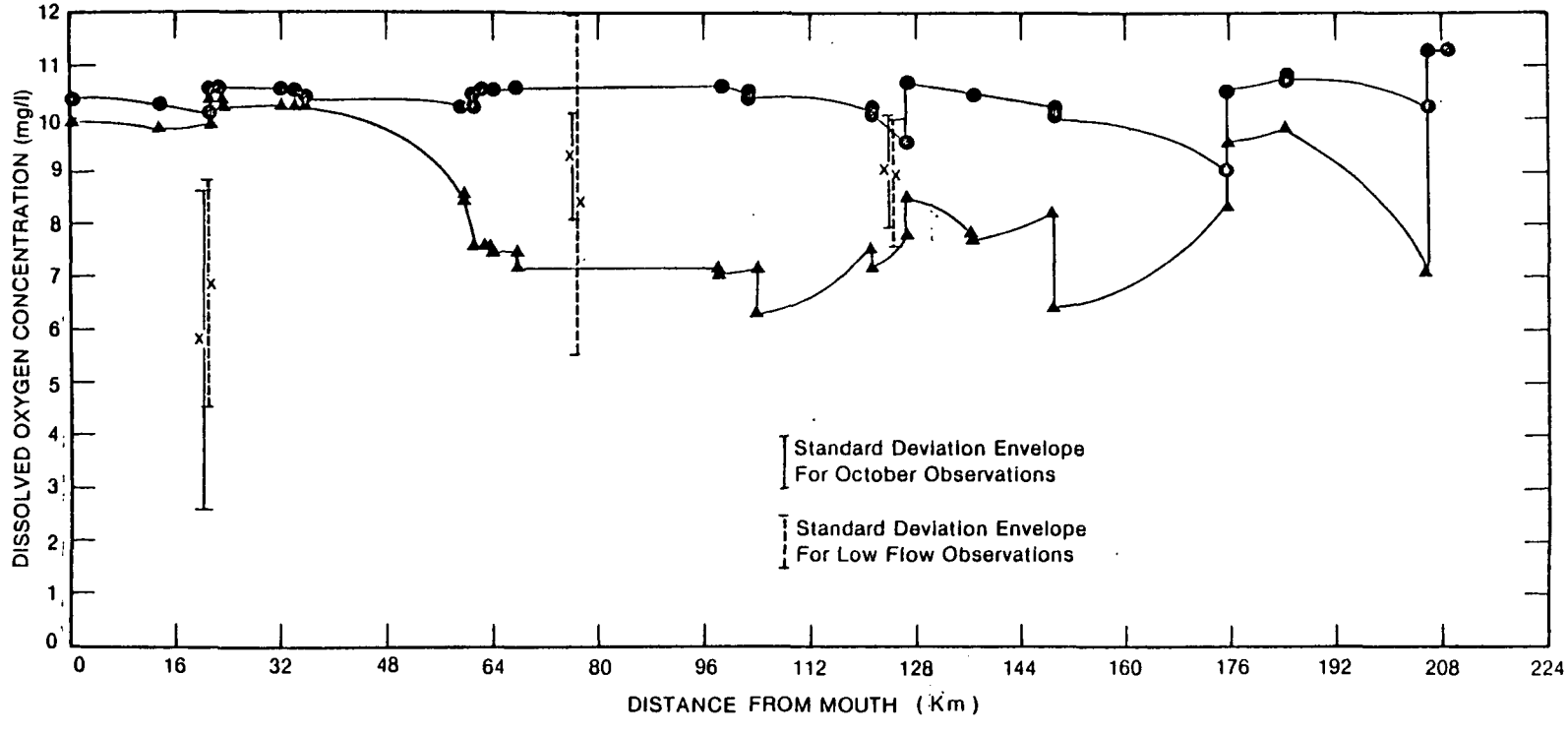

Figure 3.2-4. Computed vs. historical dissolved oxygen for the Sandusky River.

note that in the dissolved oxygen calculation, errors accrued in the computation of temperature and BOD levels are present. Therefore, results of dissolved oxygen calculations are more subject to error because the calculations are based on information that is estimated with some degree of uncertainty. Still, Figure 3.2-4 shows that the methods used bracket the observed water quality data (with the exception of the Fremont station at km 19).

The historical observations merit some discussion here. There is some question when making comparisons between predicted and historical observations regarding which historical data to use. Historical dissolved oxygen data exist for some of the low flow periods that were used to determine $7Q_{10}$ flows, flow depths, velocities, and deoxygenation and reaeration rates. However, temperature predictions were made using meteorological data exclusively for the month of October. This temperature information is used in the correction of the rate coefficients and also has a direct influence on the dissolved oxygen saturation concentration. Therefore, historical mean dissolved oxygen values and their respective standard deviation envelopes are plotted in Figure 3.2-4 for the observed annual low flow periods (irrespective of when they occurred) and the October low flow data (whether or not they went into the $7Q_{10}$ computation). The plotted standard deviation envelopes show that for the Upper Sandusky gage (stream km 125) these two means are almost equal with little difference in the dispersion of the observed data. At the Mexico gage (stream km 77) the observed means are still similar although the annual low flow dissolved oxygen values are far more dispersed than the October low flow observations. At the Fremont gage (stream km 20) the mean of the October observations is lower while its standard deviation is larger.

While the predicted results at the Upper Sandusky and Mexico gages are encouraging, the results at the Fremont gage suggest that the computational approach may be in error. One possibility for error is that parameters external to the method used may have a large influence on

dissolved oxygen levels in the Tiffin to Fremont segments. For instance, there may be a substantial benthic demand which is unaccounted for in the equation used. It is also possible that errors in hydraulic information have been compounded through repeated use in the estimation of temperature, BOD levels and rate coefficients. Additionally, it is possible that information is missing; i.e., a substantial source of BOD may have been omitted from the list of point sources, or, perhaps, a source thought to discharge via the sewage treatment plant discharges directly into the river. In instances where the methods are applied locally by personnel familiar with or having direct access to the study area, this latter possibility would be substantially reduced.

The fact that these methods do not reproduce historical observations in these reaches, however, does not vitiate them. On the contrary, the methods have served one of the purposes for which they were designed; that is, to point out areas requiring special attention and further, more detailed investigation.

Figure 3.2-5 shows dissolved oxygen profiles developed for Honey Creek using Tsivoglou-Wallace and Owens reaeration rates along with its temperature profile. The plot shows that neither temperature nor dissolved oxygen effects are likely to be of concern at low flows on this stream with its two small wastewater treatment plants. It was assumed in this calculation that the stream temperature above the Attica Waste Water Treatment Plant was at the temperature of the groundwater and that the dissolved oxygen was at saturation. Unfortunately, no historical dissolved oxygen data were available for comparison on this stream.

3.2.8 Fecal Coliform Mass Balance

Total coliform and instream fecal coliform data were unavailable for the Sandusky River. However, effluent data measurements for sewage treatment plants often included fecal coliforms. Since this parameter was being investigated under low flow conditions sewage treatment plants

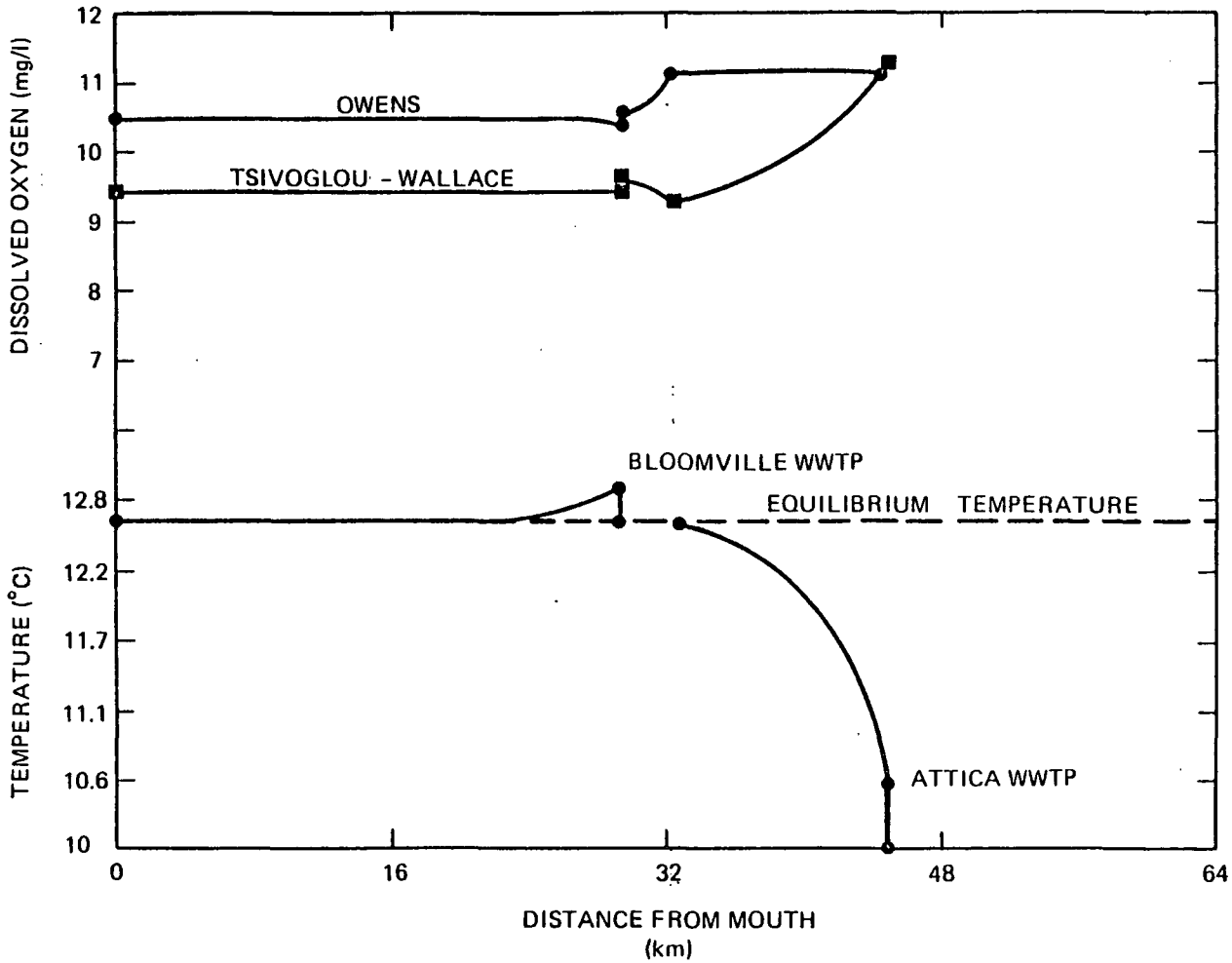

Figure 3.2-5. Dissolved oxygen and temperature profiles for Honey Creek.

were considered to be the only source. In cases where fecal coliforms were not measured estimates were made based on data from other treatment plants with similar flow and treatment type characteristics.

Table 3.2-8 gives the results of the fecal coliform mass balance for the Sandusky River system. Computations show that in many areas the fecal coliform count due to sewage treatment facilities are near the drinking water standard (1.0/100 ml) and well below the surface water standard of 2000/100 ml. Of course, the estimates of instream fecal coliform concentrations do not include the fecal coliform loading dur to waterfowl and other wildlife or from agricultural operations. McElroy, et al., (1976) show that the background total coliform concentration in this area is approximately 2000/100 ml. The U.S. Environmental Protection Agency reported that the fecal to total coliform ratio for the Ohio River was in the range of 0.2 to 12 percent (U.S. EPA, 1973), suggesting that background fecal coliform concentrations might be on the order of 4 to 240/100 ml.

The survival of fecal coliforms passing through a sewage treatment plant can be highly variable. When chlorination processes are functioning properly virtually all coliform bacteria may be eliminated. However, under situations in which such a process fails, concentrations on the order of 10^6/100 ml may be found in the effluent. Effluent characteristics such as those provided by the plant may be quite nonrepresentative of the actual stream loadings over a given 7-day period. Fecal coliforms are often of greater concern during high flow events when heavy rains may cause combined sewers or animal feeding operations to discharge raw sewage into the river system.

3.2.9 Sediment Mass Balance

Previous sections in this example have dealt exclusively with parameters which are of concern primarily at low flow conditions. In

TABLE 3.2-8. CALCULATED FECAL COLIFORM CONCENTRATIONS FOR THE SANDUSKY RIVER SYSTEM

Reach(es)	Location	Fecal Coliform Concentration (MPN/100 mℓ)
Sandusky River		
19, 20	Confluence of Paramour Creek and Allen Run to Bucyrus WWTP	8.6 - 4.6
15, 16, 17, 18	Bucyrus WWTP to Upper Sandusky WWTP	3.6 - 0.2
12, 13, 14	Upper Sandusky WWTP to Confluence w/Honey Creek	6.3 - 0.2
8, 9, 10, 11	Confluence of Sandusky and Honey Creek to Tiffin WWTP	0.4 - 0.03
3, 4, 5, 6, 7	Tiffin WWTP to Fremont WWTP	2.5 - 1.5
1, 2	Fremont WWTP to Muddy Creek Bay	1.8 - 1.3
Honey Creek		
26, 27	Attica WWTP to Bloomville WWTP	2.6 - 1.9
25	Bloomville WWTP to Confluence w/Sandusky River	2.7 - 1.6
Tymochtee Creek - Spring Run		
54-63	Carey WWTP to Confluence of Spring Run w/Tymochtee Creek	4.1 - 3.8
53	Confluence of Tymochtee Creek and Spring Run to Confluence of Tymochtee Creek and Sandusky River	2.3 - 0.9

the Sandusky River, sediment, phosphorus and nitrogen were investigated only at high flows. Sediment, nitrogen and phosphorus loadings were provided by the Midwest Research Institute's nonpoint calculator.

In the Sandusky River system velocities are of such low magnitude during low flow periods that sediment concentrations are a relatively unimportant aspect of water quality. Figure 3.2-6 shows a representative sediment rating curve for the month of October, 1976, at Fremont. The flows shown in the figure are reasonably close to the $7Q_{10}$ low flow estimated for the system. Most stations in the system for this month had suspended sediment concentrations under 30 mg ℓ^{-1} with the exception of the Upper Sandusky gage whose concentrations were consistently in the 20 to 130 mg ℓ^{-1} range.

A sediment balance for high flow conditions was performed for the entire Sandusky system. The mass balance equations for conservative constituents were utilized. Velocities in the Sandusky River ranged from about 0.88 to 2.3 m sec^{-1} so that the assumption of conservation of mass throughout the system is reasonable for the particle sizes of concern.

One large source of uncertainty when making predictions of pollutant concentrations based on flow frequency data or any method in which temporal continuity is ignored is the antecedent condition of the system. For instance, in using the Soil Conservation Service runoff curve number method to predict water yield, the antecedent soil moisture must be estimated. An analog can be drawn to estimating sediment yield from either an agricultural or an urban area.

On agricultural lands the amount of sediment available for transport can depend on a variety of factors. Among these are the method of planting, time elapsed in the growing season, time since last rainfall, magnitude of the previous rainfall, and time since the last cultivation. All these factors are time variant. For instance, in one year

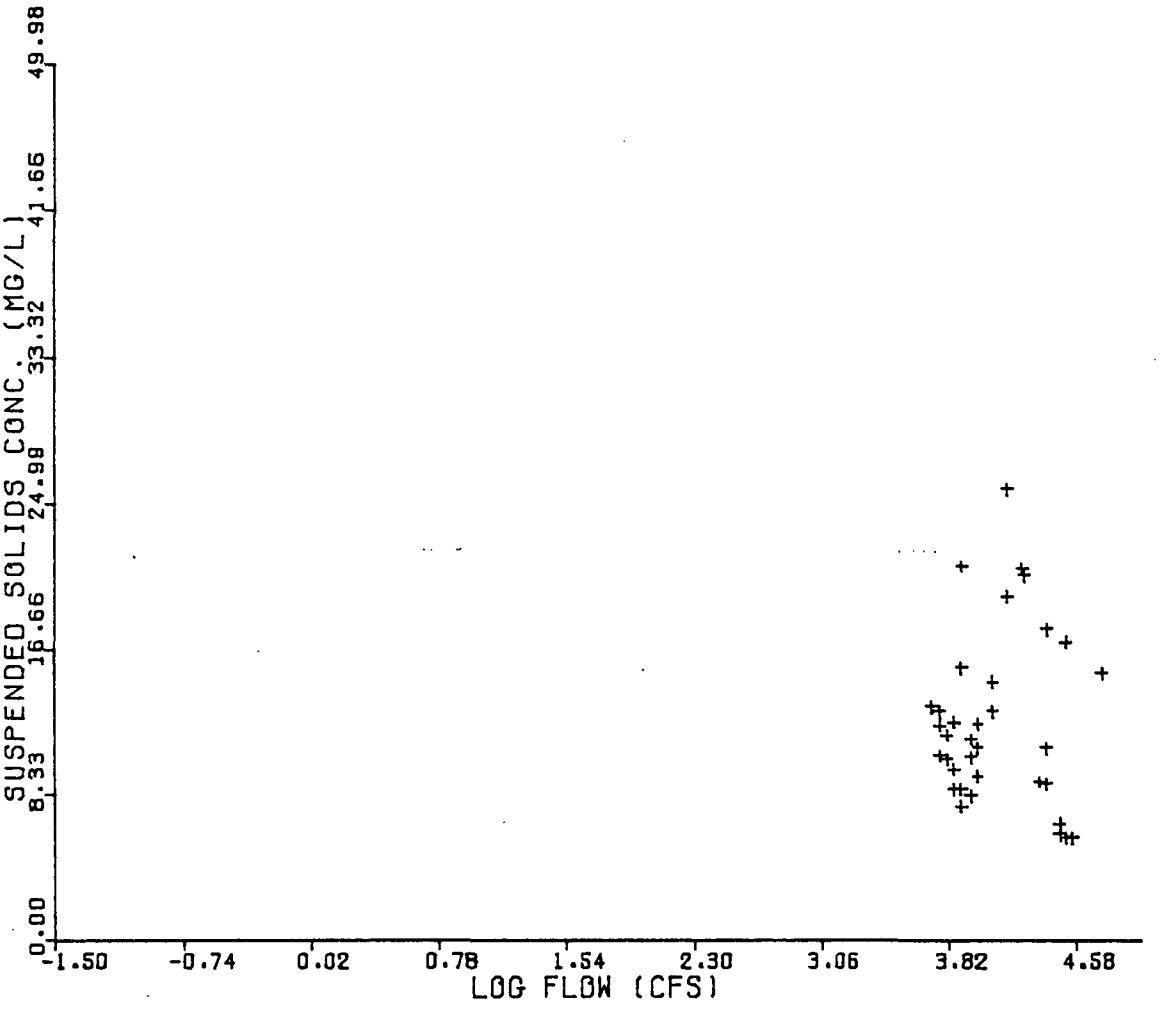

Figure 3.2-6. Sediment rating curve for Sandusky River near Fremont, October 1-31, 1976.

a farmer may choose to use conventional tillage methods whereas the next, he may use a no-till method of planting. Timing and magnitude of rainfall events vary considerably from year to year. Erosive rainfall events not only wash sediment from watershed surfaces but also break up soil aggregates making more fines available for transport. Cultivation also breaks up clods and surface crusts and generates soil fines. Thus sediment yields for any given event depend largely on the activities that occurred perhaps weeks before the event itself. It is easy to see why sediment yields are so variable and consequently difficult to predict from agricultural areas.

In urban areas the situation is similar. Here, deposition of solid matter onto streets and concrete surfaces may be a function of traffic, street cleaning frequency, and atmospheric conditions. Timing and magnitude of previous rainfalls are particularly important in urban areas to set initial conditions for sediment yield simulation, because deposition is more uniform in time than the generation of soil fines in agricultural areas. Thus the available amount of solids for washoff is largely a function of the time elapsed since the last major washoff occurred.

For non-urban loads, the "R" factor in the USLE was used to predict loadings for each event. The "average" high flow event loads were then computed. However, urban loads could only be estimated on an annual basis. (Techniques are available to estimate single event urban loads but are not included in this demonstration. See Amy, et al., 1974. The user should note that if this technique were used, the following assumptions would be unnecessary.) On this level of complexity, determination of what portion of the annual urban load can be assigned to the "average" high flow washoff event is tenuous at best. As a result, two extreme cases were considered. For the first, the annual urban sediment load is assumed to enter the stream equally distributed over each day of the year. For the second, the annual urban load is assumed to enter the river equal-

ly distributed over the single seven-day "average" high flow period. These two cases should represent reasonable upper and lower bounds for calculation of the instream concentration.

The urban loads were superimposed on the non-urban sediment loads. As a result three concentrations were calculated for each high flow reach. Figure 3.2-7 shows these concentrations predicted for the Sandusky River at Bucyrus. The smallest concentration is the contribution from non-urban loads alone. Next in magnitude is non-urban plus the urban load equally distributed over each seven-day period in the year. The largest concentration results from the assumption that all the urban loads are released during the average seven-day high flow period. Historical flow weighted means and standard deviations are also shown on the figure.

In the figure the non-urban loads appear to make up a substantial portion of the maximum "probable" instream concentration (the non-urban plus the seven-day annual urban load release). Table 3.2-9 shows the percent of the non-urban contribution to this maximum probable concentration for several gage locations in the system. Based on this analysis it is concluded that the control of sediments from agricultural areas has a definite impact in the lower reaches of the river and less impact in the upper reaches. At the Bucyrus location, controlling urban washoff appears to have more impact on local water quality.

3.2.10 Nitrogen and Phosphorus Balance

The methodology for routing nutrients at high flows is similar to that used for suspended sediment. The same sources of error are present due to the lack of definition of initial conditions. For example, application times for fertilizer and the formulation of the fertilizers used may change. The variability of rainfall also remains a problem.

With nutrients, however, there are additional sources of error that tend to make predictions more difficult. The first is that the correct-

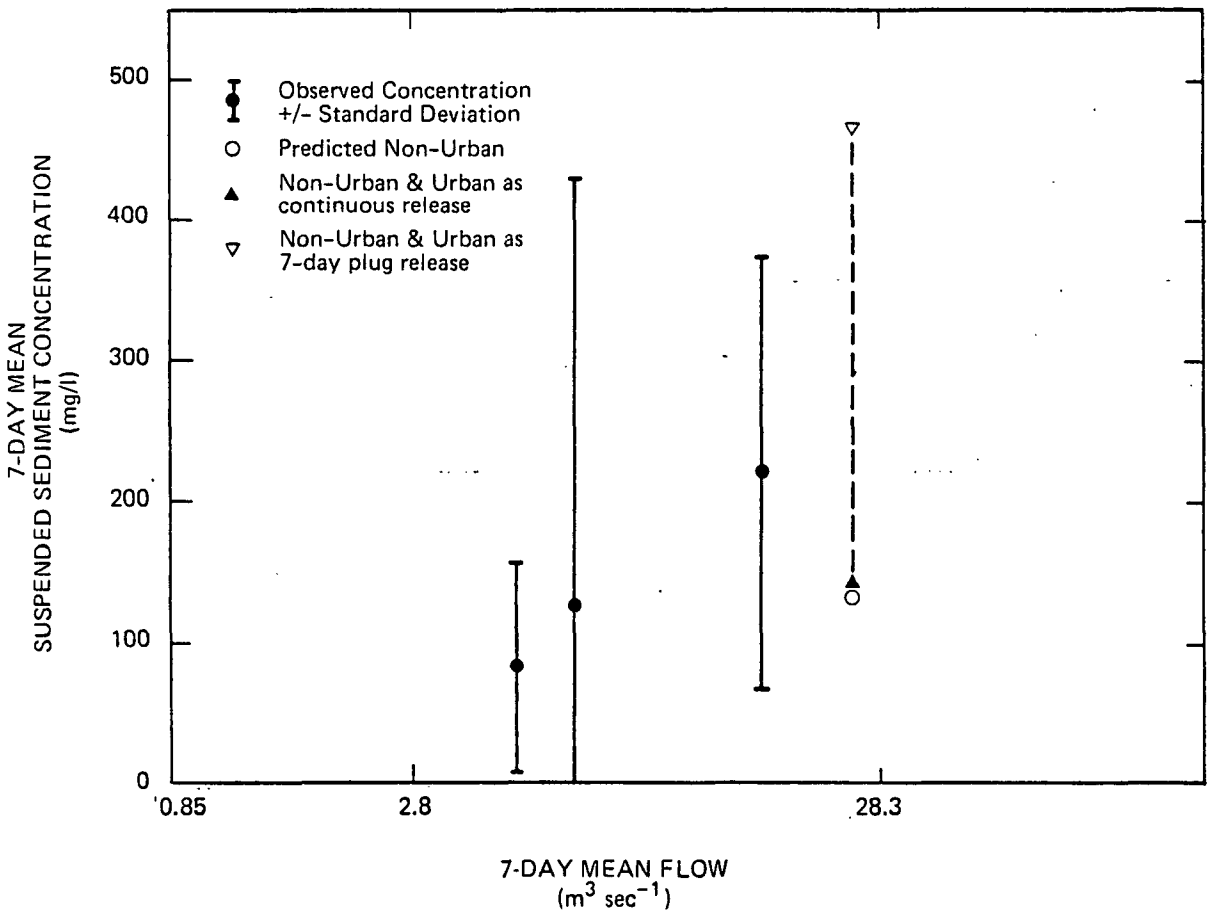

Figure 3.2-7. Predicted and observed suspended sediment concentrations for the Sandusky River at Bucyrus.

TABLE 3.2-9. EXPECTED PERCENT OF NON-URBAN CONTRIBUTION TO "WORST CASE" CONCENTRATION OF SUSPENDED SEDIMENT AT HIGH FLOWS

Location	% Non-Urban Contribution
Bucyrus	29%
Upper Sandusky	57%
Mexico	71%
Fremont	60%

ness of nonpoint source loading estimates is predicated on accurate prediction of sediment loadings. Second, the assumption of conservation of nutrient forms other than total nitrogen or total phosphorus is generally not valid.

The nonpoint loadings supplied for the Sandusky system were given as available nutrient forms; that is, forms available for uptake by terrestrial or aquatic plants. Typically, these forms include the ammonia, nitrite, and nitrate nitrogen and dissolved orthophosphorus (PO_4) forms. The question which must be addressed is how to convert these loadings given as available forms to total nitrogen or total phosphorus which can then be treated conservatively.

There is no definable relationship between total and orthophosphorus which can be extrapolated from one watershed to the next because of the differences in soil types, chemical watershed processes and degrees of urbanization that exist between different basins. For instance the total and orthophosphorus in the effluent from sewage treatment plants will very likely have similar values. From nonpoint sources, mineralized forms and organic phosphorus forms will likely be present in significant quantities. Thus, for a highly urbanized watershed, the ratio of instream ortho- to total phosphorus should be higher than for a non-urban watershed.

Fortunately, in the Sandusky Basin some relatively extensive phosphorus monitoring has been done. Both orthophosphate and total measurements have been made. The Ohio EPA (1978) has presented weighted average orthophosphorus and total phosphorus concentrations for several locations in the watershed. These are shown in Table 3.2-10. These ratios have been used for conversion between the two parameters. The background total phosphorus concentration in natural waters was taken to be 0.4 mg ℓ^{-1} for use in the mass balance equations.

Some results of the total phosphorus mass balance are shown in Figure 3.2-8. The smallest predicted value represents the non-urban contribution. As for the suspended sediment plots, the next greater value represents the non-urban plus wastewater treatment plant effluent and the annual urban nonpoint loads distributed over the entire year.

TABLE 3.2-10. ORTHO AND TOTAL PHOSPHORUS RELATIONSHIPS IN THE SANDUSKY RIVER BASIN

Station	Parameter	Number of Observations	Weighted Mean Concentration (mg ℓ^{-1})	Ratio (ortho/total)
Tymochtee	Ortho	563	.071	0.14
	Total	593	.499	
Bucyrus	Ortho	309	.230	0.41
	Total	303	.563	
Upper Sandusky	Ortho	570	.139	0.24
	Total	554	.580	
Mexico	Ortho	336	.098	0.17
	Total	360	.563	
Tiffin	Ortho	144	.102	0.19
	Total	203	.550	

After: Ohio EPA (1978)

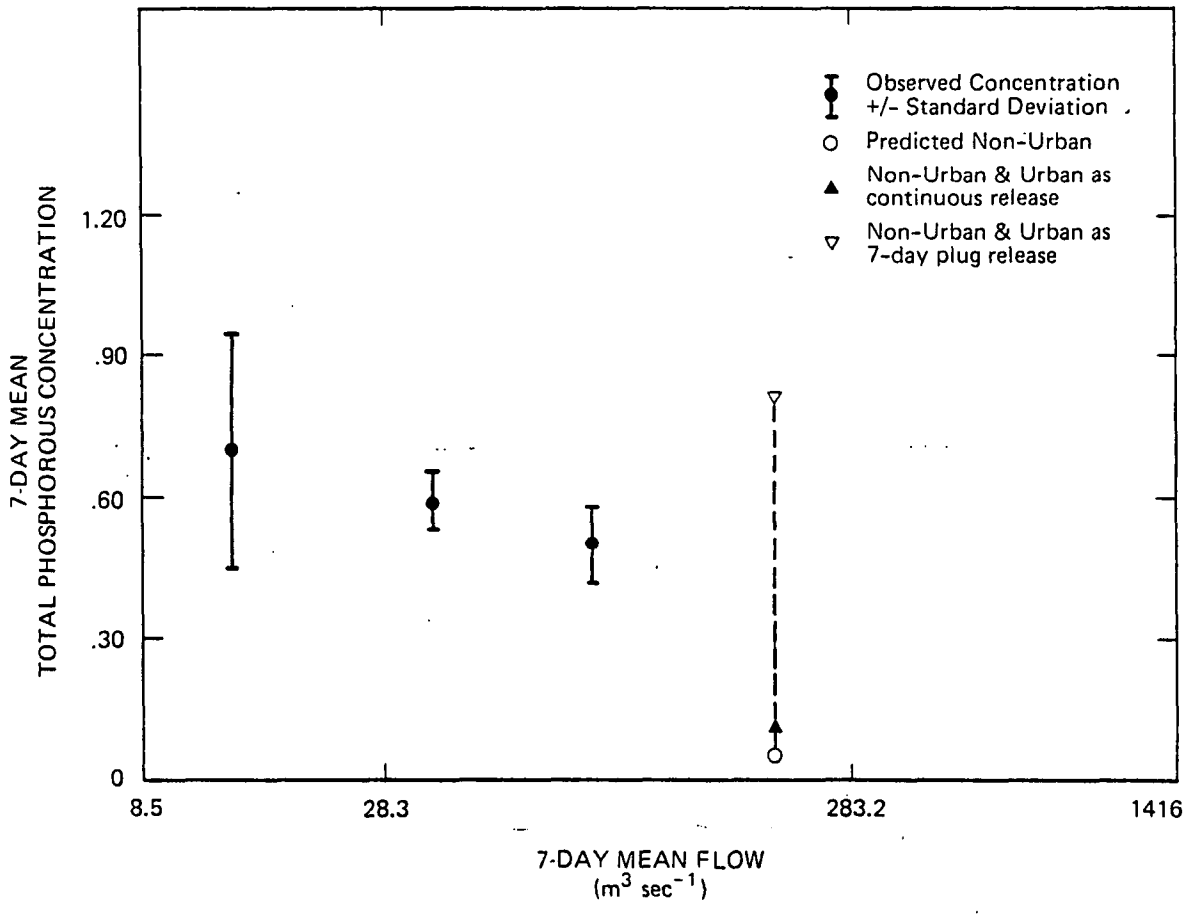

Figure 3.2-8. Observed and predicted total phosphorus concentrations for the Sandusky River at Mexico.

The highest value is the sum of the non-urban, waste water treatment plant effluent and urban diffuse loads assuming the total annual accumulation is washed off in one seven-day period.

The estimated contribution from non-urban areas appears to be small compared to the contribution from urban areas. However, inspection of the predicted values for stations upstream from which there is no substantial urbanization suggests that the predicted values of total phosphorus are probably low. Even so, the phosphorus concentrations appear to be moderately high with regard to eutrophication potential, even from only the non-urban sources. The U.S. EPA (1973) has suggested that 50 $\mu g\ \ell^{-1}$ may be an upper bound for limiting noxious plant growth in flowing waters. However, concentrations as low as 20 $\mu g\ \ell^{-1}$ are not uncommon in eutrophic lakes. The total phosphorus predicted concentrations in the Sandusky system from non-urban sources are above this value. Observed water quality data, however, suggest even higher concentrations. The addition of urban point and nonpoint loads places the Sandusky River waters well into the potential range for eutrophy.

As with suspended sediment, the control of urban discharges seems more critical than the control of non-urban sources for phosphorus control in this watershed.

No exact relationships exist for converting available nitrogen to total nitrogen and no data were available to calculate empirical relationships as was done with phosphorus. Nitrogen was routed as inorganic forms only (ammonia and nitrate-nitrogen) because total nitrogen water quality data were unavailable for making comparisons.

Nitrogen levels were not predicted as accurately as phosphorus and suspended sediment. Table 3.2-11 shows the relative contribution of non-urban nitrogen to the total predicted concentration assuming all the annual nonpoint urban loads washed off in one seven-day period. Once again, urban sources appear to have the greater influence on possible

TABLE 3.2-11. EXPECTED PERCENT OF NON-URBAN CONTRIBUTION TO "WORST CASE" CONCENTRATION OF INORGANIC NITROGEN

Location	% Non-Urban Contribution
Bucyrus	5%
Upper Sandusky	15%
Mexico	25%
Fremont	16%

available nitrogen concentrations. Figure 3.2-9 shows predicted versus observed available nitrogen levels at Bucyrus in the Sandusky River. The trend indicated in this figure is representative of the other locations; that is, predicted nitrogen concentrations were low compared to observed instream data even using the "worst case" assumptions.

Typically the epilimnetic inorganic nitrogen threshold for meso-eutrophic waters is 0.30 to .650 mg ℓ^{-1} and for eutrophic waters, 0.50 to 1.50 mg ℓ^{-1}. Predicted nitrogen levels place the Sandusky River waters into these categories. Historical observations place nitrogen levels in the 4.0 to 9.0 mg ℓ^{-1} range.

3.3 DEMONSTRATION EXAMPLE: THE CHESTER RIVER

The Chester River system was utilized principally to demonstrate the estuarine water quality section of the nondesignated 208 screening manual. The methodology as set forth in the manual calls for assessment of existing water quality followed by projected water quality under new conditions. Typically, this is the direction a 208 planner would take. The methodology is demonstrated, however, without fabrication of "future" scenarios by analyzing existing water quality with regard to the possible causes of degradation. The estuarine calculations were made both under low and high flow scenarios just as for the rivers and streams demonstration on the Sandusky River system.

3.3.1 Data Collection

Topographic maps (7½ minute) were obtained for the Chester River basin from the U.S. Geological Survey. The USGS also provided flow records and stage-discharge curves for streams flowing into the estuary. Ten years of recent streamflow data were obtained. The

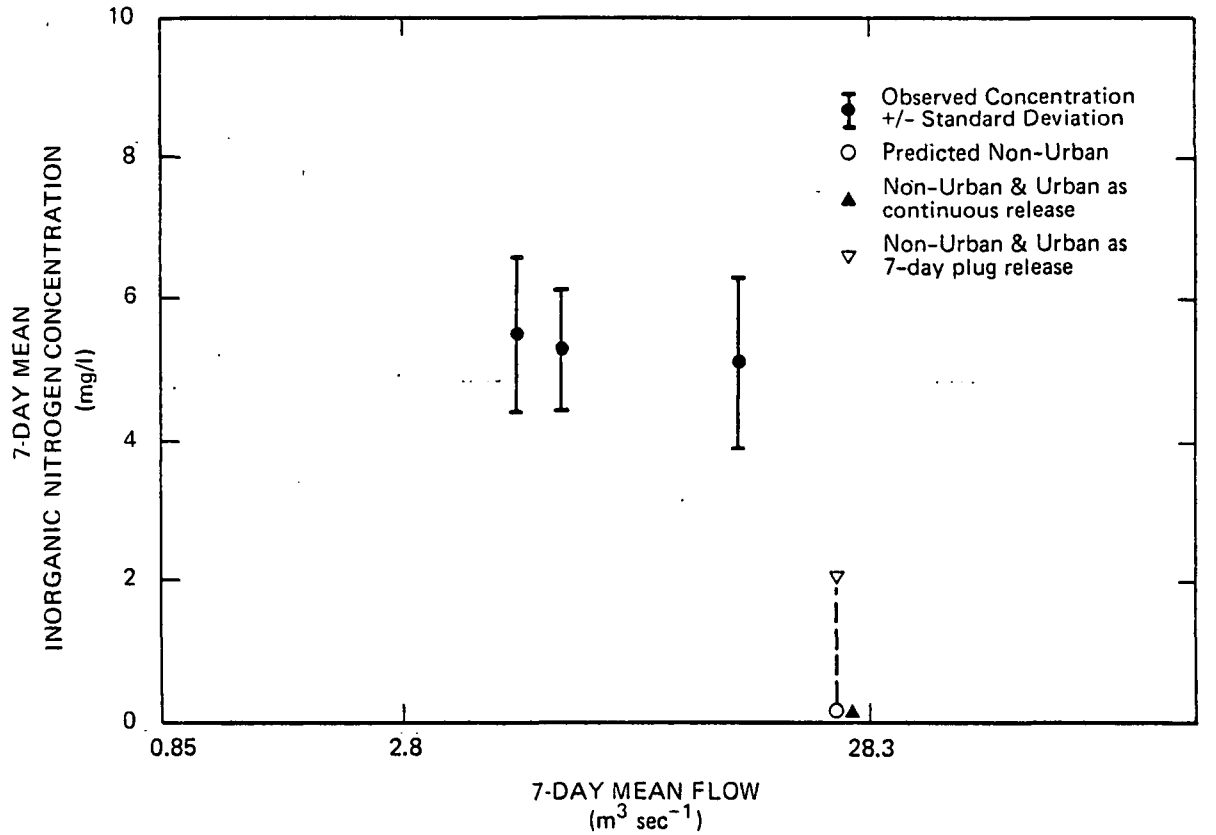

Figure 3.2-9. Observed and predicted inorganic nitrogen in the Sandusky River.

U.S. EPA's STORET system was the primary source of water quality data. Additional data were also found in a three volume series of reports on pollutants and sediment in the Chester River done by the Westinghouse Electric Corporation in cooperation with the State of Maryland (1972). Listings of industrial and municipal point sources in the basin and effluent characteristics for those of import were also obtained from the Maryland Department of Natural Resources.

3.3.2 Data Reduction and Supplementation

3.3.2.1 Hydrologic and Hydraulic Data

Streamflow data were available for two tributaries to the Chester: Unicorn Branch and Morgan Creek. Unicorn Branch is one of four creeks with their confluence at or near Millington which form the headwaters of the Chester. Morgan Creek enters the Chester just above Chestertown.

For the purposes of evaluating estuarine conditions under low flow, the $7Q_{10}$ flows were estimated for these two creeks. Figure 3.3-1 shows the flow frequency plot. Although the flow in Morgan Creek appears smaller, actually it is not. The gage on Unicorn Branch is located at the subshed outlet while the Morgan Creek gage is located at Kennedyville, several miles upstream of the outlet. From this information the $7Q_{10}$ flows for the major creeks in the basin were estimated (by areal weighting) and are shown in Table 3.3-1.

Because of the paucity of hydraulic data for streams tributary to the Chester River it was decided to perform a "worst-case" water quality analysis for the low flow condition. Loadings for the point sources in the basin were estimated and were assumed to enter the Chester River at full strength; that is, with no decay instream and

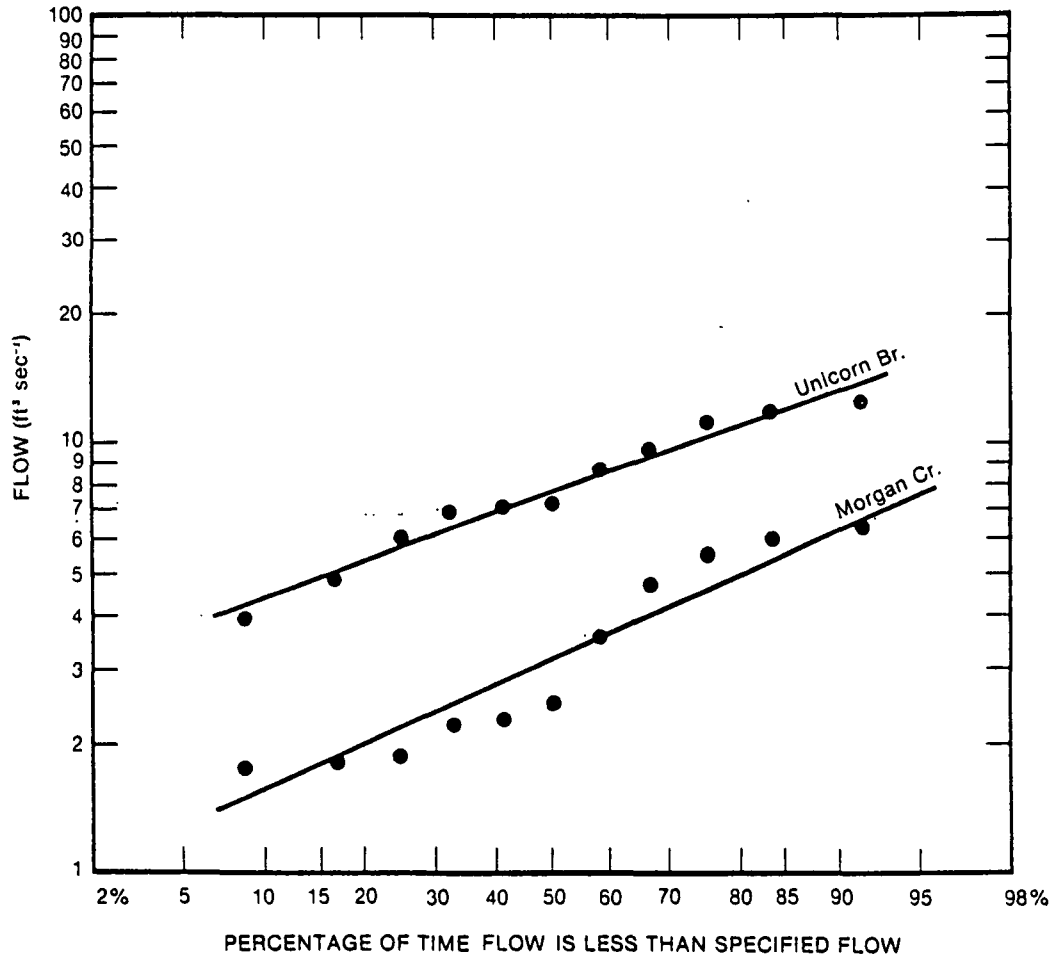

Figure 3.3-1. Frequency analysis of 7-day annual low flows.

TABLE 3.3-1. LOW AND HIGH SCENARIO FLOWS FOR CHESTER RIVER TRIBUTARIES

Creek	$7Q_{10}$ Flow ($m^3\ sec^{-1}$)	High Flow ($m^3\ sec^{-1}$)	Area of Sub-basin (km^2)
Langford Creek	0.23	8.69	110.0
Radcliffe Creek	0.04	1.56	19.7
Corsica River	0.20	7.62	109.8
Reed Creek	0.07	2.61	33.1
Southeast Creek	0.23	8.64	99.7
Red Lion Branch	0.15	3.34	63.2
Sewell Creek	0.10	2.29	48.7
Andover Creek	0.25	5.49	116.5
Cypress Creek	0.19	4.28	90.6
Mills Branch	0.07	1.53	32.6
Gray's Inn Creek	0.04	1.44	18.1
Morgan Creek	0.18	6.51	82.3
Unicorn Branch	0.12	2.78	58.8
TOTAL	1.88	56.78	883.1

only diluted by the flow of the tributary (if any) by which they are carried. As such, velocities and depths of flow were not calculated for these streams.

High flows were developed by selecting fifteen high flow events. The criteria for the selection were the same as used in the Sandusky, i.e., only events occurring from April to September were considered and storms with good areal coverage were preferred. There was no minimum flow criterion. The flows from these storms were averaged for Morgan Creek and Unicorn Branch and areal weighting was used to determine the flows in other creeks. The results are also shown in Table 3.3-1.

3.3.2.2 Water Quality Data

Water quality data for the Chester River, collected principally in 1970 and 1972, were tabulated to indicate which water quality parameters would be used in the demonstration and where water quality problems existed. Salinity profiles were plotted for each of the dates available and were grouped into categories representing "high" and "low" flow regimes based on flow records at the Unicorn Branch gage. From this grouping a representative high and low flow salinity profile was developed. These profiles indicate how pollutants are distributed in the estuary under certain flow regimes and are useful for other estuarine computations. Figures 3.3-2 and 3.3-3 show typical salinity profiles for the high and low flow conditions, respectively. The profile of June 30, 1972 was taken after the passage of Hurricane Agnes. The mean daily flow in Unicorn Branch was 3.82 m^3 sec^{-1} and followed a period of 14 - 17 m^3 sec^{-1} mean daily flows at that gage. The profile of October 30, 1972 is a typical low flow salinity profile for this system. The salinity differences between surface and bottom at this time are only about one-half ppt while during high flows the difference may be two to three ppt. The flow at Unicorn Branch on October 30 was 0.42 m^3 sec^{-1}.

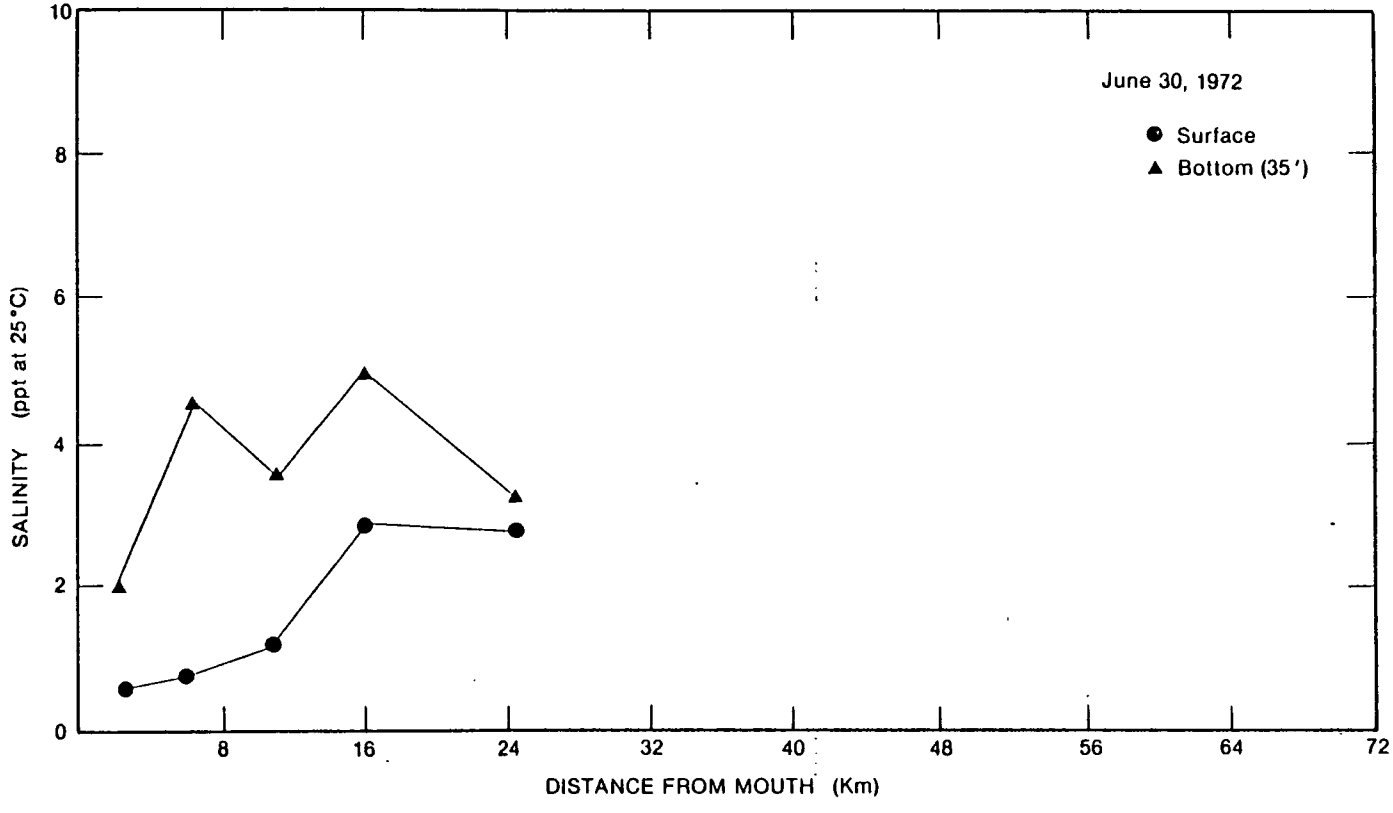

Figure 3.3-2. Salinity profile for the Chester River, June 30, 1972.

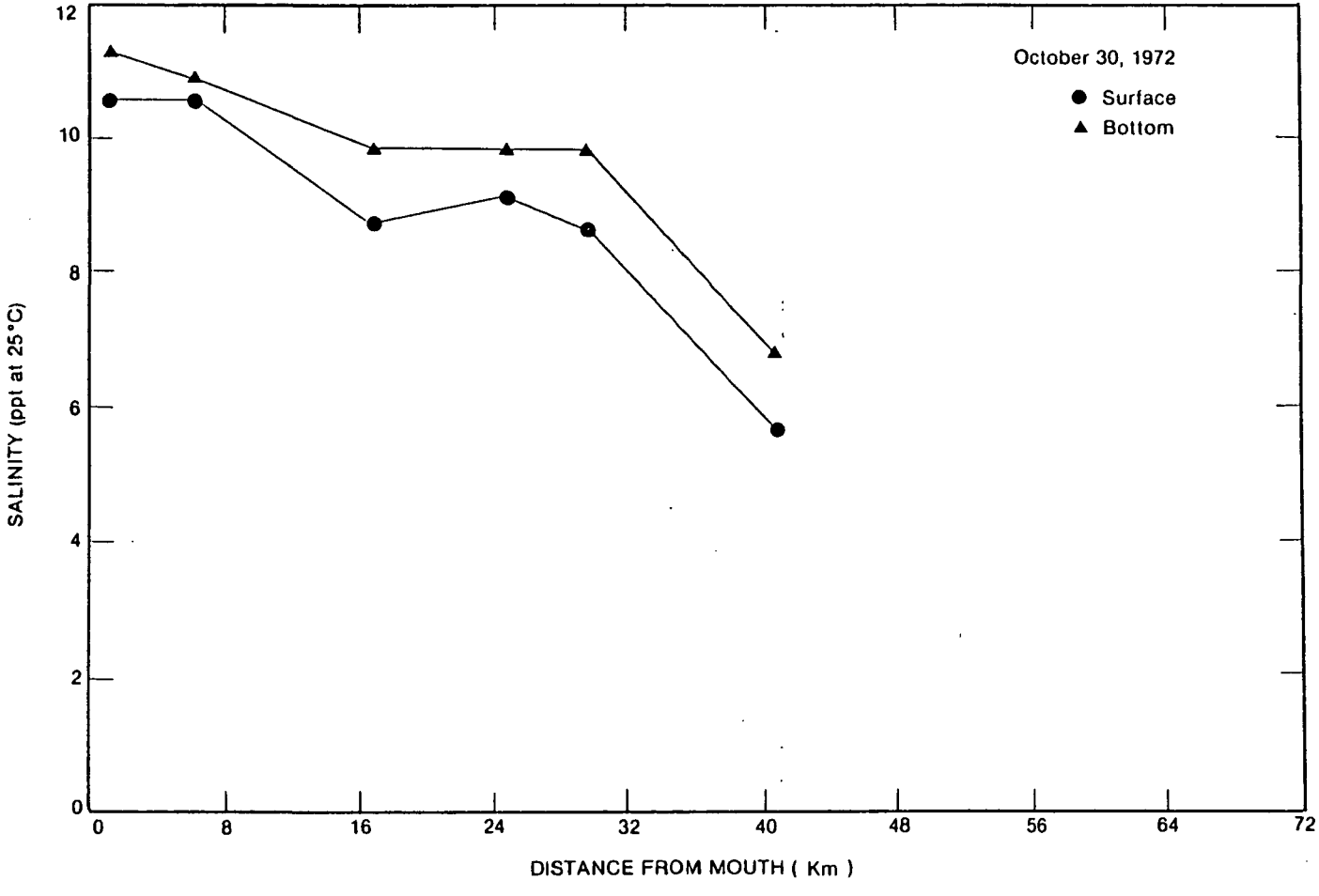

Figure 3.3-3. Salinity profile for the Chester River, October 30, 1972.

Vertically averaged salinity profiles for the high and low flow scenarios are shown in Figure 3.3-4. For convenience in applying the methods and to provide for smoothness of the data, second degree polynomials were fit to the salinity data. These are shown also in Figure 3.3-4. The equations and their corresponding correlation coefficients are given in the upper right-hand corner. These equations represent regressions of salinity (ppt) on river miles from the mouth of the estuary (1 mi = 1.61 km). Because of the averaging used to arrive at these profiles the low flow profile should be indicative of that occurring when Unicorn Branch is flowing at approximately 0.39 m^3 sec^{-1}. the high flow profile represents salinities corresponding to a flow of about 1.98 m^3 sec^{-1} in Unicorn Branch. The $7Q_{10}$ low flow at Unicorn Branch used for estuarine water quality computations is 0.12 m^3 sec^{-1} and the high flow rate used is 2.78 m^3 sec^{-1}. Therefore these salinity profiles are reasonably representative of actual salinities at those flows.

Historical temperature data are shown in Table 3.3-2 for different locations in the estuary. There is a pronounced seasonal variation in water temperature with temperatures seeming to increase slightly in the landward direction, regardless of season. Only slight temperature variations are observed over depth.

Table 3.3-3 shows dissolved oxygen data for the same dates and locations as for temperature. Sags are most noticeable during the summer-autumn low flow periods. The numbers in parentheses are the standard deviation of the parameter over readings taken at varying depths. High standard deviations indicate a trend towards stratification while low standard deviations indicate a well-mixed system. Higher deviations seem to occur most often in the warmer months.

Data for fecal and total coliform bacteria were not available for this system even though high levels of these indicator organisms

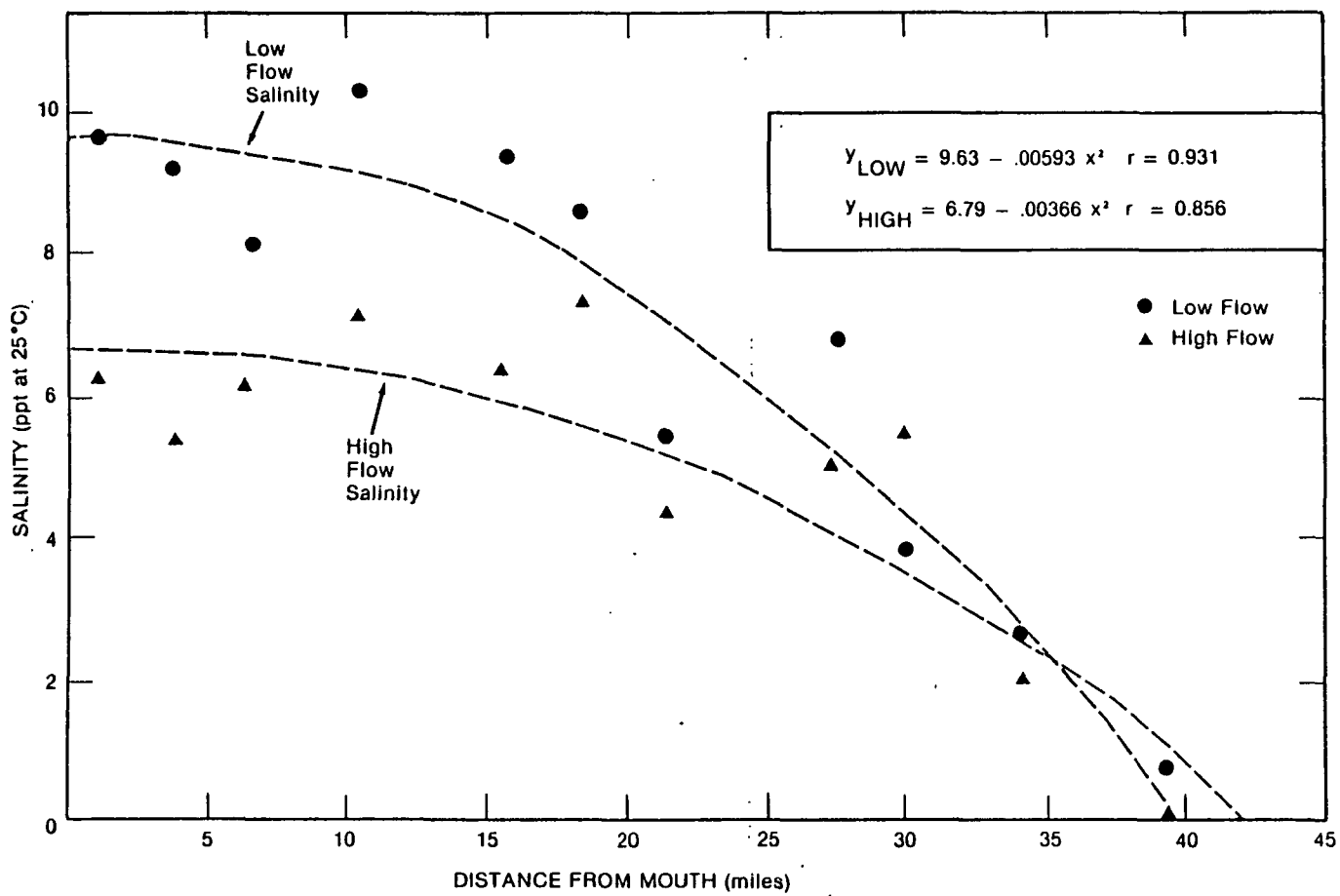

Figure 3.3-4. High and low flow vertically averaged salinities in the Chester River Estuary.

TABLE 3.3-2. VERTICALLY AVERAGE TEMPERATURES FOR THE CHESTER RIVER (°C)

RIVER KILOMETER		DATE [a]									
		720301	700312	700402	720522	700604	720619	720630	720822	700904	721030
1.6	(Love Pt. Light)	3.1	3.05	5.85	15.6	21.05	21.5	19.45	23.7	24.95	13.85
6.1		-	-	-	16.0	-	21.3	20.0	23.85	-	13.65
10.8		3.2	-	-	15.6	-	21.7	21.9	23.7	-	13.35
14.6	(Long Pt.)	3.2	3.73	5.33	15.65	20.63	21.85	23.4	24.5	25.1	13.0
24.5	(Boxes Pt.)	3.35	3.93	6.0	18.6	21.93	23.25	24.05	24.1	25.27	13.0
29.6	(Nichols Pt.)	-	4.45	6.25	17.7	22.8	23.25	-	24.5	25.25	13.25
34.6		-	-	-	19.2	-	23.7	-	24.5	-	-
43.4	(Melton Pt.)	-	4.8	6.73	19.35	23.6	23.25	-	25.0	25.75	13.5
48.3	(Chestertown)	-	5.65	7.35	19.5	24.6	-	-	25.3	25.6	-
54.7	(Possum Pt.)	-	6.55	7.8	-	25.05	-	-	-	25.25	-
62.4	(Crumpton Buoy)	-	8.1	6.5	-	25.0	-	-	-	25.1	-

a) Dates are given as year/month/day

TABLE 3.3-3. VERTICALLY AVERAGED DO CONCENTRATIONS (mg ℓ^{-1}) FOR THE CHESTER RIVER[a)]

RIVER KILOMETER		DATE									
		720301	700312	700402	720522	700604	720619	720630	720822	700904	721030
1.6	(Love Pt.)	12.9(.85)	11.7(.38)	8.8(.71)	6.4(3.9)	7.0(1.77)	6.2(1.8)	7.7(.71)	4.6(4.9)	7.0(.56)	8.7(.71)
6.1		-	-	-	6.2(4.6)	-	6.1(1.8)	6.4(2.5)	6.1(4.2)	-	9.1(.14)
10.8		12.9(.85)	-	-	5.0(4.5)	-	7.0(.78)	6.9(1.7)	4.8(4.2)	-	8.3(.21)
14.6	(Long Pt.)	12.9(.99)	11.8(.06)	9.6(2.4)	5.5(4.9)	5.2(2.9)	6.2(1.5)	6.7(2.5)	6.5(6.1)	3.4(2.6)	8.6(.28)
24.5	(Boxes Pt.)	13.0(.67)	11.5(.06)	9.6(1.6)	8.8(0)	6.9(.53)	7.7(2.5)	7.0(1.1)	5.1(4.4)	4.7(2.2)	8.3(.14)
29.6	(Nichols Pt.)	-	11.2(.07)	10.3(42)	6.1(3.2)	6.3(.99)	6.8(1.8)	-	5.0(4.4)	6.4(0)	7.8(.49)
34.6		-	-	-	7.4(.85)	-	6.3(1.6)	-	5.9(1.8)	-	-
43.4	(Melton Pt.)	-	10.8(.12)	9.7(.21)	7.6(.56)	6.5(.15)	5.9(1.3)	-	7.6(2.2)	6.0(.28)	9.5(.99)
48.3	(Chestertown)	-	10.2(.14)	9.6(.42	8.0(.71)	5.6(.67)	-	-	8.1(.99)	6.2(1.1)	-
54.7	(Possum Pt.)	-	10.3(.07)	9.3(0)	-	5.8(.07)	-	-	-	6.3(.42)	-
62.4	(Crumpton Buoy)	-	10.8(0)	-	-	6.4(0)	-	-	-	6.3(0)	-

a) Numbers in parentheses are standard deviations over depth.

have resulted in closure of many shellfish harvesting waters in the estuary.

Nutrient data were available for three dates from the 1970 investigations on the river. Chlorophyll-a measurements were also made during those studies. These data are shown in Table 3.3-4. The parenthetic values are again standard deviations over depth. Chlorophyll-a was sampled at the one-foot depth only.

Generally, total nitrogen profiles indicate relatively constant levels of nitrogen over the length of the estuary while phosphorus levels increase in the upstream direction. There is also an increase in chlorophyll-a production from the mouth to the head of the estuary. Chlorophyll-a levels as of 1970 in the Chester River have generally been in the region characterizing eutrophy (>8 $\mu g\ \ell^{-1}$) but not at levels at which algal blooms are considered a problem (>50 $\mu g\ \ell^{-1}$).

3.3.3 Point Source Load Estimates

Temperature, BOD_5, dissolved oxygen, flow, fecal and total coliform bacteria, total phosphorus, and nitrate and nitrite nitrogen data were available for most of the sewage treatment plants in the Chester River basin. All parameters, except temperature, were averaged over all available data to determine average plant effluent characteristics. The temperature of the discharge was taken as the average of those data taken only during the month in which low flow typically occurred. Effluent data for major municipal sewage treatment facilities and industrial dischargers are given in Table 3.3-5.

Loads to the estuary for low flow periods were calculated in the following way. The flows of the discharge and the receiving stream

TABLE 3.3-4. PLANT NUTRIENT AND CHLOROPHYLL-a LEVELS IN THE CHESTER RIVER

VERTICALLY AVERAGED TOTAL NITROGEN[a] (as N) (mg ℓ^{-1})

	700312	700402	700604	700904
Love Pt. (MOUTH)	.93 (.06)	1.32 (.06)	1.00 (.32)	-
Long Pt.	.73 (.12)	1.05 (.21)	1.20 (.15)	-
Boxes Pt.	.85 (.06)	.84 (.08)	.63 (.04)	-
Nichols Pt.	.77 (0)	1.05 (.01)	.57 (.11)	-
Melton Pt.	.89 (.11)	1.09 (.15)	.31 (.02)	-
Chestertown	1.55 (.03)	1.41 (0)	.46 (.06)	-
Possum Pt.	2.04 (.03)	1.58 (0)	.53 (.03)	-
Crumpton Buoy	1.57 (0)	1.21 (0)	.89 (0)	-

VERTICALLY AVERAGED TOTAL PO_4 (as PO_4) (mg ℓ^{-1})

	700312	700402	700604	700904
Love Pt. (MOUTH)	.10 (.02)	.14 (.06)	.11 (.01)	-
Long Pt.	.07 (.02)	.10 (.01)	.17 (.15)	-
Boxes Pt.	.11 (.02)	.10 (.01)	.14 (.01)	-
Nichols Pt.	.09 (0)	.14 (.02)	.12 (.04)	-
Melton Pt.	.17 (.02)	.20 (.04)	.26 (.01)	-
Chestertown	.38 (.05)	.32 (.09)	.36 (.02)	-
Possum Pt.	.47 (.10)	.51 (0)	.31 (.01)	-
Crumpton Buoy	.39 (0)	.63 (0)	.32 (0)	-

CHLOROPHYLL-a (µg ℓ^{-1})

	700312	700402	700604	700904
Love Pt. (MOUTH)	9.0	15.0	22.5	13.5
Long Pt.	10.5	1.5	24.0	19.5
Boxes Pt.	7.5	7.5	29.3	7.5
Nichols Pt.	7.5	7.5	20.3	8.3
Melton Pt.	9.8	1.5	30.0	15.0
Chestertown	11.3	6.0	32.3	24.8
Possum Pt.	16.5	9.0	22.5	52.5
Crumpton Buoy	29.3	10.5	20.5	111.0

a) The numbers in parantheses are the standard deviations over depth.

TABLE 3.3-5. EFFLUENT CHARACTERISTICS FOR MUNICIPAL STPs AND INDUSTRIAL DISCHARGES IN THE CHESTER RIVER BASIN

Municipal STP's	(m^3 sec^{-1})	Temperature (°C)	BOD_5 (mg ℓ^{-1})	DO (mg ℓ^{-1})	Fecal Coliform (MPN/100 ml)	Total Coliform (MPN/100 ml)	Total P (mg ℓ^{-1})	PO_4 (mg ℓ^{-1})	NO_2 + NO_3 (mg ℓ^{-1})	NH_3 (mg ℓ^{-1})	TKN (mg ℓ^{-1})	Suspended Solids (mg ℓ^{-1})
Eastern Correctional Camp	.014	23e	23	7.4	3	11	6	-	.5	-	-	26
Chestertown	.84	23e	22	7.6	10	197	6e	-	.22	-	-	103
Rock Hall	.34	23e	24	7.8	7	21	6e	-	-	-	-	58
Centreville	.43	23e	7	7.2	12	105	6e	-	-	-	-	10
Queenstown	.10	23e	53	7.0	214	1,196	6e	-	-	-	-	56
Suddlersville	.06	23e	18	7.5	65	848	6.2	6.0	.54	6.6	14.0	35
Millington	.05	23e	63	7.1	105	1,018	3.4	-	-	-	-	39
Industries												
Campbell's Soup Company	.21	17	24	3e	8.4	-	-	-	-	-	-	32
Tenneco Chemicals	.05	30e	46	5.2	-	-	-	-	-	-	-	-

(e) estimated

were added to yield a total flow. The temperature, BOD_5, dissolved oxygen, fecal and total coliform bacteria loads were computed as flow weighted averages. The values of BOD and total coliforms for the natural waters were taken from background iso-pollutant maps in McElroy et al. (1976). Background fecal coliform bacterial counts were assumed to be zero.

As an example showing how to calculate instream pollutant levels below a sewage treatment plant, total coliform bacterial data from the Suddlersville Sewage Treatment Plant on Red Lion Branch is used. The flow from the plant is 0.002 m^3 sec^{-1} and the nautral $7Q_{10}$ flow is 0.15 m^3 sec^{-1} for a combined flow of 0.152 m^3 sec^{-1} cfs. The resultant total coliform count is

$$TC = \frac{0.002\ (848) + 0.15\ (300)}{0.152} = 306 \text{ MPN/100 ml}$$

where 848 and 300 are the total coliform counts of the plant effluent data and the natural background count, from McElroy, et al. (1976), respectively.

Loads calculated in this way for low flow analysis are shown for the municipal sewage treatment plants and major industrial discharges to the Chester River in Table 3.3-6.

3.3.4 Estuarine Classification

Geometrically the Chester appears marginal for application to the screening calculations. Four creeks provide about one-third of the fresh water flow at the head of the estuary with the other two-thirds resulting from fairly well longitudinally distributed

TABLE 3.3-6. LOW FLOW LOADS TO THE CHESTER RIVER FROM MUNICIPAL AND INDUSTRIAL POINT SOURCES (PER TIDAL CYCLE)

Source	Volume of Water (m^3)	$CBOD_u$ (Kg)	$NBOD_u$ [a] (Kg)	Total Coliforms MPN x 10^{-9}	Fecal Coliforms MPN x 10^{-8}
Queenstown STP	126	9.8	9.4	1.5	2.7
Rock Hall STP and Grays Inn Creek	2,200	17.8	39.3	5.4	.31
Centreville STP and Corsica River	9,646	18.4	37.5	27.9	.65
Eastern Correctional Camp STP and Southeast Creek	10,384	16.0	1.2	31.0	.0005
Chestertown STP and Radcliff Creek	2,958	37.0	96.9	7.8	1.1
Tenneco Chemicals, Campbell's Soup and Morgan Creek	8,116	25.1	32.9	24.3	0
Suddlersville STP and Red Lion Branch	6,776	12.0	4.8	20.7	4.9
Millington STP, Mills Branch, Cypress Branch, Andover Branch, Unicorn Branch, Sewell Branch	32,806	54.0	4.7	78.7	.66
Langford Creek	10,366	15.2	0	31.1	0
Reed Creek	3,160	4.6	0	9.5	0

[a] estimated

tributaries further seaward. This violates the assumption of only one dominant inflow. No major side embayments exist on the Chester, however.

Both classification methods (flow ratio method and stratification-circulation method) were used in attempting to classify the Chester River estuary. The flow ratio was calculated under low and high flow conditions. The estimation of these flows has already been described. The estuary tidal prism used in the flow ratio method was calculated in the following way.

Transects were drawn normal to the flow at convenient locations on the USGS topographic maps. Bathymetric cross-sectional profiles were then constructed. Depths given on the maps are for mean low water. A mean tidal range is also given. By assuming that only depth and not the width of the channel changes under tidal fluctuations, a mean high water cross sectional area can be estimated. Using the length between transects the MLT (mean low tide) and MHT (mean high tide) volumes of the estuary are calculated. The tidal prism is the difference of these two values. For the Chester River the tidal prism volume is approximately 8.46×10^7 m^3.

River flow volumes over the tidal cycle are computed as

$$V = KQ_r t$$

where

V = volume of fresh water inflow per tidal cycle (m^3)

Q_r = fresh water flow rate (m^3 sec^{-1})

t = period of the tidal cycle (hr)

K = a units correction (3600 sec hr^{-1})

For the Chester River the tidal period is ∿12.4 hours. This was determined from co-spectral density plots for February tides (State of

Maryland, 1972). Q_r is taken to be the sum of all the fresh water inflows in the basin. Use of these values gives a flow ratio of 9.6×10^{-4} for low flow and 2.9×10^{-2} for high flow. This indicates that the Chester River is a well mixed estuary under both conditions (FR <0.1; see Section 6.3.5 of the screening manual).

The Stratification-Circulation (or Hansen-Rattray) method gives a different result. Using data obtained in the Chester River study (State of Maryland, 1972) the stratification and circulation parameters were computed for both the high and low flow conditions at Love Point Light. ΔS in the stratification parameter was computed using August and September (low flow) salinity data and salinity after the passage of Hurricane Agnes (high flow). The time averaged August and September surface salinity was 9.6 ppt and the average bottom salinity was 9.85 giving ΔS of 0.25. The average of these two values gives S_o, the cross-section mean salinity of 9.7 ppt. Similarly, for high flow ΔS is equal to 3.3 and S_o = 2.03. Using these values gives values of the stratification parameter ($\Delta S/S_o$) of 0.025 for low flow and 1.64 for high flow. U_f, the mean fresh water velocity, was calculated for these two cases by dividing the high and low flow rates by the mean tidal cross-sectional area at the river mouth (Love Point Light). The flow rates (from Table 3.3-1) are 1.88 $m^3\ sec^{-1}$ (low flow) and 56.8 $m^3\ sec^{-1}$ (high flow). The mean tidal cross section is 62296 m^2 at Love Point. A mean fresh water velocity (U_f) is computed for each condition of 3.0×10^{-5} $m\ sec^{-1}$ (low flow) and 9.1×10^{-4} $m\ sec^{-1}$ (high flow). U_s, the tidally averaged surface velocity, was determined by measurement (State of Maryland, 1972) to be less than 0.01 knots or approximately 0.004 m sec^{-1}. This measurement was taken during a period of intermediate inflow in the tributaries and as such represents a "median" value of this parameter, being neither representative of the high or low flow conditions. However, it is used as the value of U_s for both sets of conditions since it represents the only available measurement. This gives values for the circulation parameter (U_s/U_f) of 133 and 4.4 for low and high flow, respectively.

Plotting the above values on a stratification-circulation diagram shows that the mouth of the Chester falls into categories 2a and 2b, indicating a partially mixed estuary. This result is corroborated by the Chester River Study (State of Maryland, 1972). They report that Chesapeake Bay and its major tributaries belong to the partially mixed type estuary and cite Pritchard (1967). A value of U_s was not available for the upper portion of the estuary and calculations could not be made for this section of the river.

3.3.5 Flushing Calculations

The tidal prism, modified tidal prism and fraction of fresh water methods were used to calculate flushing times for the Chester River and several of its major tributary estuaries. Flushing times calculated for the Chester River by each of the three above methods are given in Table 3.3-7. A comprehensive example of the flushing time calculation is given in the Patuxent River section. The tidal prism method does not take flow into account and only one value is shown for it. For the other two methods, high and low flow flushing times are given. Additionally, the fraction of fresh water method was performed using a 2 ppt and a 1 ppt segmentation scheme to demonstrate the sensitivity of the method.

Although the river flow rate is used explicitly in the modified tidal prism method, the flushing times seem to be fairly insensitive to flow, the method yielding times of approximately equal magnitude while the river flow varied by a factor of 30. This indicates that the Chester River is flushed primarily by tidal action and not by advective flow.

The fraction of fresh water method on the other hand seems extremely sensitive to flow condition, giving greatly different flushing times of ∿380 days and ∿13 days for low and high low, respectively.

TABLE 3.3-7. FLUSHING TIMES FOR THE CHESTER RIVER BY THREE METHODS

Method		Flushing Time (days) High Flow	Low Flow
Tidal Prism		5.3	5.3
Modified Tidal Prism		143.	134.
Fraction of Fresh Water	(1 ppt) [a]	13.6	381
	(2 ppt)	12.7	382

[a] The estuary was segmented using first a 1 ppt salinity difference per segment and then a 2 ppt salinity difference per segment.

The results are somewhat afield from those obtained using the modified tidal prism method possibly because the salinity profiles used were not measured at the same flow rates used in the modified tidal prism method. Even if this were the case, salinity profiles are heavily influenced by antecedent flow conditions in estuaries with long residence times. The high flow flushing times are approximations since this estuary likely stratifies at high flows, invalidating the assumption of a well mixed system.

The fraction of fresh water method shows little improvement when a one-part-per-thousand segmentation scheme is used instead of two parts per thousand. The 1 ppt segmentation requires only a nominal additional effort above that required using 2 ppt.

Flushing times were also computed for several of the major tidal tributaries to the river for high and low flow scenarios using both the tidal prism and modified tidal prism methods. The results are given in Table 3.3-8. The low flow flushing times show a generally increasing trend with the MLT volume of the estuary with the modified tidal prism values being consistently higher than those computed by the tidal prism method.

Because of the relative ease of applying the tidal prism method as opposed to the modified method, it would be desirable to use the former if possible in a screening procedure. However, it is known that this method underestimates the true flushing time considerably (Officer, 1976). For this reason, ratios of the two methods were computed and are also shown in Table 3.3-8. For the high flow regime the ratio of the values produced by the two methods are consistently around 4.0 for the tributary estuaries. However for the entire river this ratio is 22:1. For the low flow regime, the ratios are variable and seem related to the MLT volume of the estuary. Figure 3.3-5 shows an empirical relationship between flushing time ratio

TABLE 3.3-8. FLUSHING TIMES FOR THE CHESTER RIVER AND SELECTED TRIBUTARIES

River/Creek	MLT Volume (m^3)	Flushing Time (days) Tidal Prism Method	Modified Tidal Prism Method High	Modified Tidal Prism Method Low	Ratio MTP/TP Method High	Ratio MTP/TP Method Low
Langford Creek						
(East Fork)	2.07×10^7	4.3	16.7	69	3.9	16.0
(West Fork)	1.76×10^7	5.0	17.7	59	3.5	11.8
Corsica River	1.19×10^7	2.2	9.8	18.1	4.5	8.2
Gray's Inn Creek	3.68×10^6	3.8	15.0	26.4	3.9	6.9
Chester River	7.39×10^8	6.4	140.1	136.4	21.9	21.3

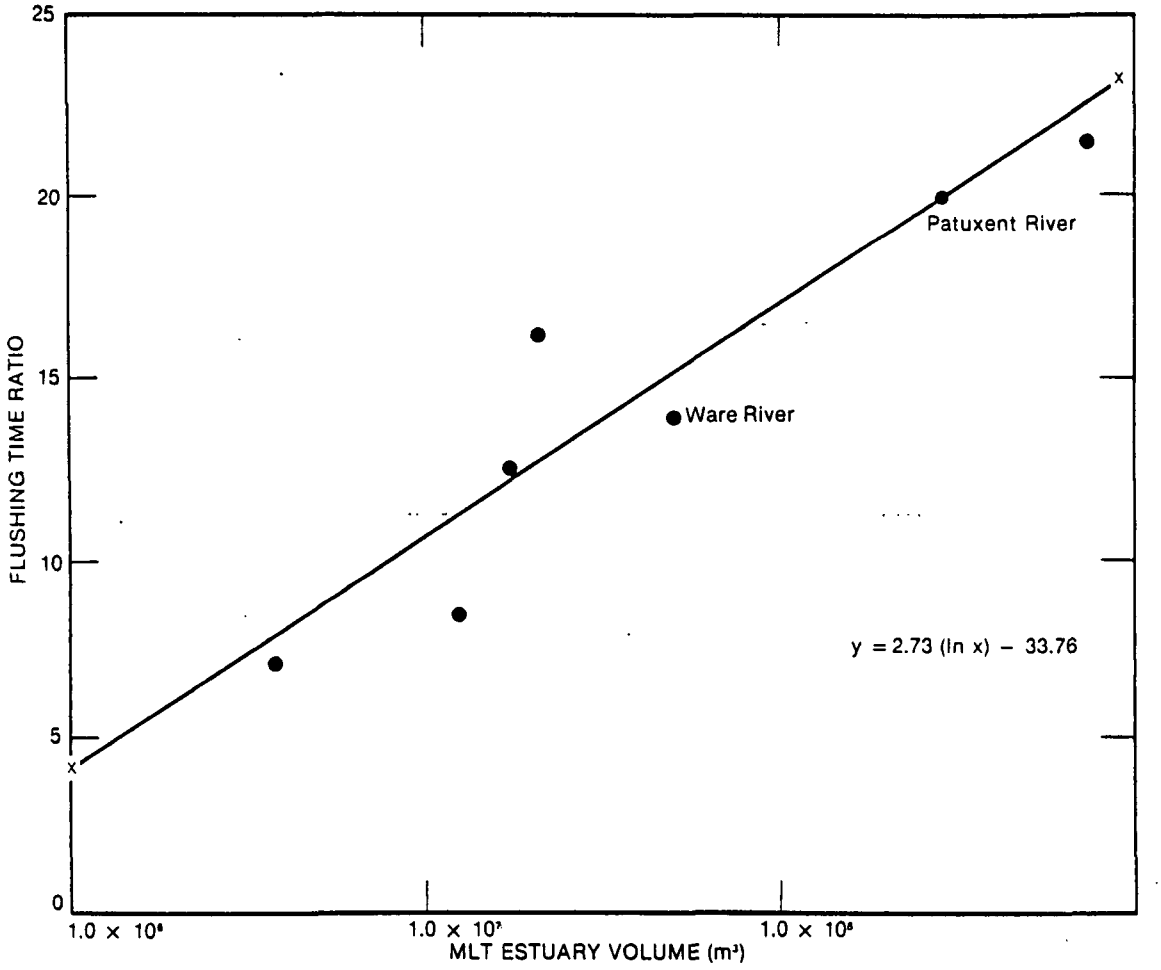

Figure 3.3-5. Empirical relationship between the ratio of modified tidal prism and tidal prism methods and mean low tide estuary volume.

and MLT volume. Also plotted on the figure are points calculated for the Ware and Patuxent Rivers. The agreement between the relationship developed on the Chester River and applied to two other estuaries tributary to the Chesapeake Bay is good.

3.3.6 Pollutant Distribution

Pollutant distributions in the Chester River are analyzed under both high and low sets of flow conditions. The low flow scenario considers the direct discharges of point sources into the estuary and streams flowing into the estuary. The high flow scenario considers primarily nonpoint source discharges into the system. For the purposes of this analysis, nonpoint loadings distributed along the length of the river are treated as discrete point loadings into each of several segments into which the river has been separated.

3.3.6.1 Low Flow

Figure 3.3-6 shows a schematic of the Chester River with the major point source discharges. The loads from these dischargers have been listed in Table 3.3-6. The first step in performing the pollutant distribution calculations is to determine which of the 30 modified tidal prism segments receives the discharge. Having done this, the initial concentration in the segment of discharge (C_d) can be calculated for the appropriate segments by dividing the load from the point source (Kg tidal cycle^{-1}) by the hypothetical fresh water volume passing through the segment during a tidal cycle. This is expressed as:

$$C_d = \frac{W}{R} f_d$$

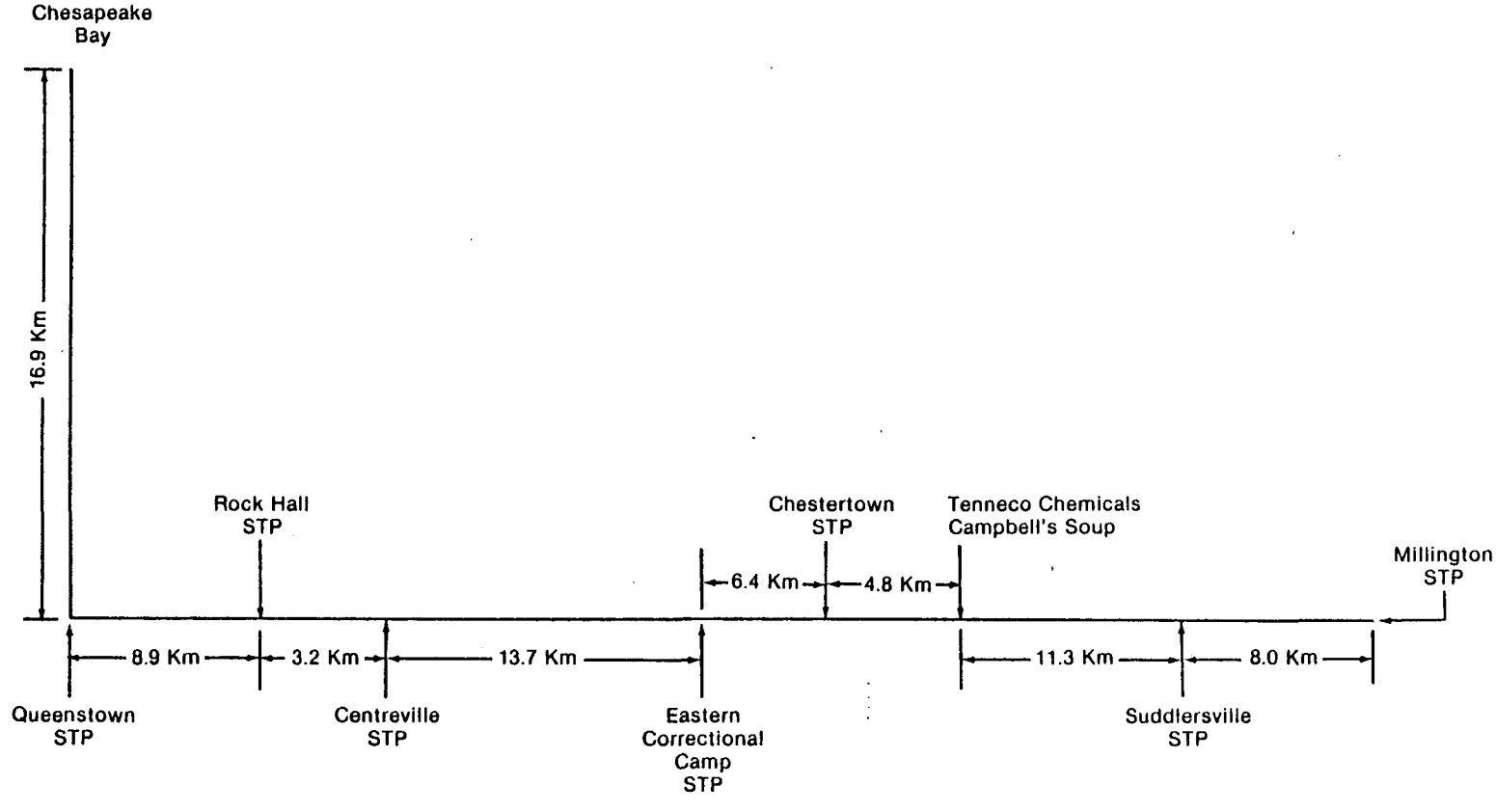

Figure 3.3-6. Schematic of Chester River and point sources (not to scale).

where C_d = the initial concentration in the segment of discharge ($Kg\ m^{-3}$)

W = mass of pollutant per tidal cycle from the point source (Kg)

R = Volume of river inflow per tidal cycle (m^3)

f_d = fraction of fresh water in the segment of discharge (unitless)

Total coliform bacteria concentrations and ultimate NBOD plus CBOD concentrations were calculated for the Chester River. The results are shown in Table 3.3-9. Each initial concentration shown is due solely to a single point source. From the calculated concentrations it can be concluded that these point sources have little impact on the water quality of the main stem of the Chester River, although they quite possibly may be degrading quality in tributary estuaries into which they discharge before entering the main river. Because these concentrations are so low, the technique of estimating their longitudinal distribution (which is essentially to superpose individual concentration profiles) is not demonstrated here but is discussed in the Patuxent River section.

3.3.6.2 High Flow

The Chester River basin was divided into sub-basins, and nonpoint loads under "average" high flow conditions were estimated for each sub-basin. In the following calculations, a delivery ratio of 0.1 was used for all the nonpoint loadings (Midwest Research Institute, 1979). Since the effects of point sources were judged to be of minor importance in the previous section, their contributions to the total loads were not considered for the high flow analysis. The parameters analyzed under this scenario were BOD_5, total nitrogen, total phosphorus, and suspended sediment. All parameters were treated as conservative materials with the exception of BOD_5.

TABLE 3.3-9. CALCULATED INITIAL CONCENTRATIONS IN THE CHESTER RIVER FOR TWO WATER QUALITY PARAMETERS

Point Source /Segment	Total Coliform Bacteria (MPN/100 ml)	$(NBOD \text{ plus } CBOD)_u$ $(mg\ \ell^{-1})$
Queenstown STP/22	0.11	1.37×10^{-2}
Rock Hall STP/18	0.90	9.50×10^{-2}
Centreville STP/16	5.9	1.19×10^{-1}
Eastern Correctional Camp STP/11	16.7	9.20×10^{-2}
Chestertown STP/9	6.0	1.03
Campbell's Soup Co. and Tenneco Chemical Co./8	20.6	4.92×10^{-1}
Suddlersville STP/3	23.7	1.92×10^{-1}
Millington STP/0	93.8	7.00×10^{-1}

There are two cases to consider in the treatment of nonpoint sources. First, there are sub-basin loads which enter as a point source to the estuary via the tributaries. Also, there are distributed loads from sub-basins adjacent to the estuary. Tributary inflows are easily assigned to one of the 23 segments delineated by the modified tidal prism method. Usually, distributed inflow loads from adjacent sub-basins have units of ML^{-1} (mass per unit length). In this case a portion of the total load assigned to each segment is calculated by multiplying the load per unit length by segment length. For instance, if the loading rate from an area adjacent to the estuary is 3 Kg/Km of estuary length and the area adjoins three 1 Km segment, the loading into each is 3 Kg for a total of 9 Kg in all three segments. Initial concentrations are computed for each high flow segment just as in the low flow case.

Once the initial concentrations for each segment are determined, they are distributed in the estuary in the upstream direction as the salinity gradient and downestuary as the fraction of fresh water. This is most easily accomplished by setting up a coefficient matix for the system. This matrix, called the distribution matrix, is made up of coefficients f_i/f_d for segments downstream of the discharge segment (below the main diagonal of the matrix) and S_i/S_d upstream of the discharge segment (above the main diagonal) with coefficients of unity along the matrix diagonal. The f_i are fractions of fresh water in the i^{th} segment, and the d subscript denotes the discharge segment. The same subscripts apply to the salinities (S). Table 3.3-10 shows the high flow distribution coefficient matrix for the Chester River.

Conservative pollutant distribution in the estuary is determined as follows. First, the following terms are defined:

C_{dm} = initial concentration of a pollutant that is discharged into segment m

p = number of pollutant dischargers into the estuary

TABLE 3.3-10. CHESTER RIVER CONSERVATIVE POLLUTANT DISTRIBUTION COEFFICIENT MATRIX (HIGH FLOW)

SEGMENT NUMBER	SEGMENT NUMBER																								
	0	1	2	3	4	5	6	7	8	9	10	11	12	13	14	15	16	17	18	19	20	21	22	23
0	1	0	0	0	0	0	0	0	0	0	0	0	0	0	0	0	0	0	0	0	0	0	0	0
1	.82	1	.54	.39	.31	.27	.23	.21	.21	.21	.20	.20	.19	.19	.18	.18	.18	.18	.18	.18	.18	.18	.18	.18
2	.67	.82	1	.71	.58	.49	.42	.39	.39	.38	.37	.36	.35	.34	.34	.33	.33	.33	.33	.33	.32	.32	.32	.32
3	.54	.66	.80	1	.82	.69	.58	.55	.54	.53	.52	.51	.50	.48	.48	.47	.47	.46	.46	.46	.46	.46	.46	.46
4	.44	.54	.66	.81	1	.84	.72	.68	.67	.66	.64	.62	.61	.59	.58	.58	.58	.57	.57	.57	.56	.56	.56	.56
5	.34	.41	.51	.63	.77	1	.85	.80	.79	.76	.76	.73	.73	.70	.69	.68	.68	.67	.67	.67	.66	.66	.66	.66
6	.22	.27	.33	.41	.50	.65	1	.95	.93	.91	.90	.87	.85	.83	.81	.80	.80	.79	.79	.79	.78	.78	.78	.78
7	.18	.22	.27	.33	.41	.53	.82	1	.98	.97	.95	.92	.90	.87	.86	.85	.85	.84	.84	.84	.82	.82	.82	.82
8	.16	.19	.24	.36	.36	.47	.73	.89	1	.98	.97	.93	.92	.89	.88	.86	.86	.85	.85	.85	.84	.84	.84	.84
9	.15	.18	.22	.28	.34	.44	.68	.83	.94	1	.98	.95	.93	.91	.89	.88	.88	.86	.86	.86	.85	.85	.85	.85
10	.13	.16	.19	.24	.30	.38	.59	.72	.81	.87	1	.97	.95	.92	.91	.89	.89	.88	.88	.88	.87	.87	.87	.87
11	.10	.12	.15	.18	.23	.29	.45	.56	.62	.67	.77	1	.98	.95	.94	.92	.92	.91	.91	.91	.90	.90	.90	.90
12	.09	.11	.13	.17	.20	.26	.41	.50	.56	.60	.69	.90	1	.97	.95	.94	.94	.93	.93	.93	.91	.91	.91	.91
13	.06	.07	.09	.11	.14	.18	.27	.33	.38	.40	.46	.60	.67	1	.98	.97	.97	.96	.96	.96	.94	.94	.94	.94
14	.04	.05	.06	.07	.09	.12	.18	.22	.25	.27	.31	.40	.44	.67	1	.98	.98	.97	.97	.97	.96	.96	.96	.96
15	.03	.04	.04	.06	.07	.09	.14	.17	.19	.20	.23	.30	.33	.50	.75	1	1	.99	.99	.99	.97	.97	.97	.97
16	.03	.04	.04	.06	.07	.09	.14	.17	.19	.20	.23	.30	.33	.50	.75	1	1	.99	.99	.99	.97	.97	.97	.97
17	.01	.01	.01	.02	.02	.03	.04	.06	.06	.07	.08	.10	.11	.17	.25	.33	.33	1	1	1	.98	.98	.98	.98
18	.01	.01	.01	.02	.02	.03	.04	.06	.06	.07	.08	.10	.11	.17	.25	.33	.33	1	1	1	.98	.98	.98	.98
19	.01	.01	.01	.02	.02	.03	.04	.06	.06	.07	.08	.10	.11	.17	.25	.33	.33	1	1	1	.98	.98	.98	.98
20	0	0	0	0	0	0	0	0	0	0	0	0	0	0	0	0	0	0	0	0	1	1	1	1
21	0	0	0	0	0	0	0	0	0	0	0	0	0	0	0	0	0	0	0	0	0	1	1	1
22	0	0	0	0	0	0	0	0	0	0	0	0	0	0	0	0	0	0	0	0	0	0	1	1
23	0	0	0	0	0	0	0	0	0	0	0	0	0	0	0	0	0	0	0	0	0	0	0	1

K_{ij} = element in the distribution matrix found in row i and column j (i, j = 0, 1, 2, . . . , n)

n = number of segments into which the estuary is divided.

The pollutant concentration in segment i due to the single discharge into segment m, C'_i, is given as:

$$C'_i = K_{im} C_{dm}$$

Then the actual concentration in segment i, C_i, is the sum of the contributions from all the dischargers, namely:

$$C_i = \sum_p K_{im} C_{dm}$$

This procedure is repeated for all segments i = 0, 1,2, . . . n.

The Patuxent River section contains a comprehensive example of this calculation for a conservative pollutant.

Nonconservative pollutant distribution must take into account the decay of the substance as well as dilution as it moves away from the segment of discharge. Officer (1976) and Dyer (1973) develop the algorithm for nonconservative substances within the constructs of the tidal prism method only for the case in which the exchange ratios (r_i) for each segment are equal. The case for which the r_i are not equal is approximated by the following expressions:

$$C_i = C_d \frac{f_i}{f_d} \prod_{i=d}^{d+a} B_i$$

in the downstream direction and

$$C_i = C_d \frac{S_i}{S_d} \prod_{i=d}^{d-a} B_i$$

in the upstream direction

where C_i = the concentration of nonconservative pollutant in segment "i"

f_i = fraction of fresh water in segment "i"

f_d = fraction of fresh water in the segment of discharge

C_d = the initial concentration in the segment of discharge, assuming the pollutant acts conservatively

B_i = the decay term $\left(\frac{r_i}{1 - (1 - r_i)\, e^{-k}}\right)$

S_i = the salinity in segment "i"

S_d = the salinity in the segment of discharge

a = an index telling how many segments up or down the estuary from the segment of discharge that segment "i" is located

r_i = tidal exchange coefficient ($1/T_i$, where T_i is the segment flushing time) and

k = nonconservative constituent decay rate (tidal cycles^{-1}).

For the segment of discharge the expressions reduce to

$$C_i = C_d\, B_i \qquad (i = d)$$

Table 3.3-11 shows calculated pollutant distributions for the Chester River. BOD_5 distributions were computed using a high and a low decay rate (.05 and .41 per tidal cycle). Decay coefficients were

TABLE 3.3-11. HIGH FLOW POLLUTANT DISTRIBUTIONS IN THE CHESTER RIVER ESTUARY

Segment	Distance of Landward End from Mouth	BOD_5 (Low Decay) ($mg\ell^{-1}$)	BOD_5 (High Decay) ($mg\ell^{-1}$)	Total Nitrogen ($mg\ell^{-1}$)	Total Phosphorus ($mg\ell^{-1}$)	Suspended Sediment ($mg\ell^{-1}$)
0	71.1	4.98	3.54	2.68	0.35	791
1	62.7	5.40	2.80	3.20	0.43	949
2	56.8	5.03	2.07	3.21	0.42	951
3	51.2	4.09	1.36	2.97	0.40	879
4	45.6	3.41	0.81	2.62	0.34	784
5	39.8	2.41	0.30	2.12	0.28	637
6	32.4	1.32	0.08	1.52	0.22	455
7	29.6	0.70	0.02	1.32	0.17	393
8	27.9	0.52	0.03	1.22	0.15	366
9	26.5	0.43	0.04	1.13	0.14	342
10	24.6	0.24	0.02	0.97	0.14	298
11	22.4	0.13	0.01	0.77	0.11	234
12	20.0	0.09	~0	0.70	0.10	207
13	17.4	0.04	0	0.46	0.06	139
14	14.6	0.01	0	0.28	0.02	96
15	12.5	~0	0	0.22	0.02	72
16	10.6	~0	0	0.22	0.02	72
17	9.16	~0	0	0.07	0	22
18	7.61	~0	0	0.07	0	22
19	6.16	~0	0	0.07	0	22
20	4.64	0	0	~0	0	0
21	3.34	0	0	0	0	0
22	2.11	0	0	0	0	0
23	0.91	0	0	0	0	0
AVERAGE	-	0.13	0.03	0.27	.028	84.2

not adjusted longitudinally for temperature based on the uniformity of historical temperature observations in the estuary. At the bottom of the table, volumetrically weighted average concentrations for the entire estuary are shown.

The table shows that the pollutant distributions almost without exception monotonically decrease towards the mouth of the river. This occurs primarily because the method assumes that the tidal prism of the most seaward segment is replaced entirely by background waters with no pollutant after each tidal cycle, which may not really be the case.

Figure 3.3-7 shows vertically averaged total nitrogen profiles for the river. Three of the profiles are observed and were measured for substantially lower fresh water inflow rates than was used in calculation of the predicted profile. There are a number of possible reasons for the discrepancies between the observed and predicted profiles. The high values at the upper end of the estuary may be due to the use of a delivery ratio that is too large. The perturbation of predicted values by changes in the delivery ratio is approximately linear for conservative parameters. Therefore, halving the pollutant load would result in reduction of instream concentrations by a factor of two, etc. Second, the methodology assumes that the pollutant is continuously entering the estuary at a constant rate. During high flow events, both the quantity of water and pollutant entering the estuary vary. Thus, an error is introduced into the calculations by making the constant inflow assumption, although it is difficult to determine how this error quantitatively affects the magnitude of the concentrations in each segment. In reality, when the loadings abruptly stop, dispersion tends to cause a flattening of the longitudinal gradient over time as the high loads in the upper estuary are flushed towards the mouth. In such a case the resultant distribution would more closely resemble the observed profiles.

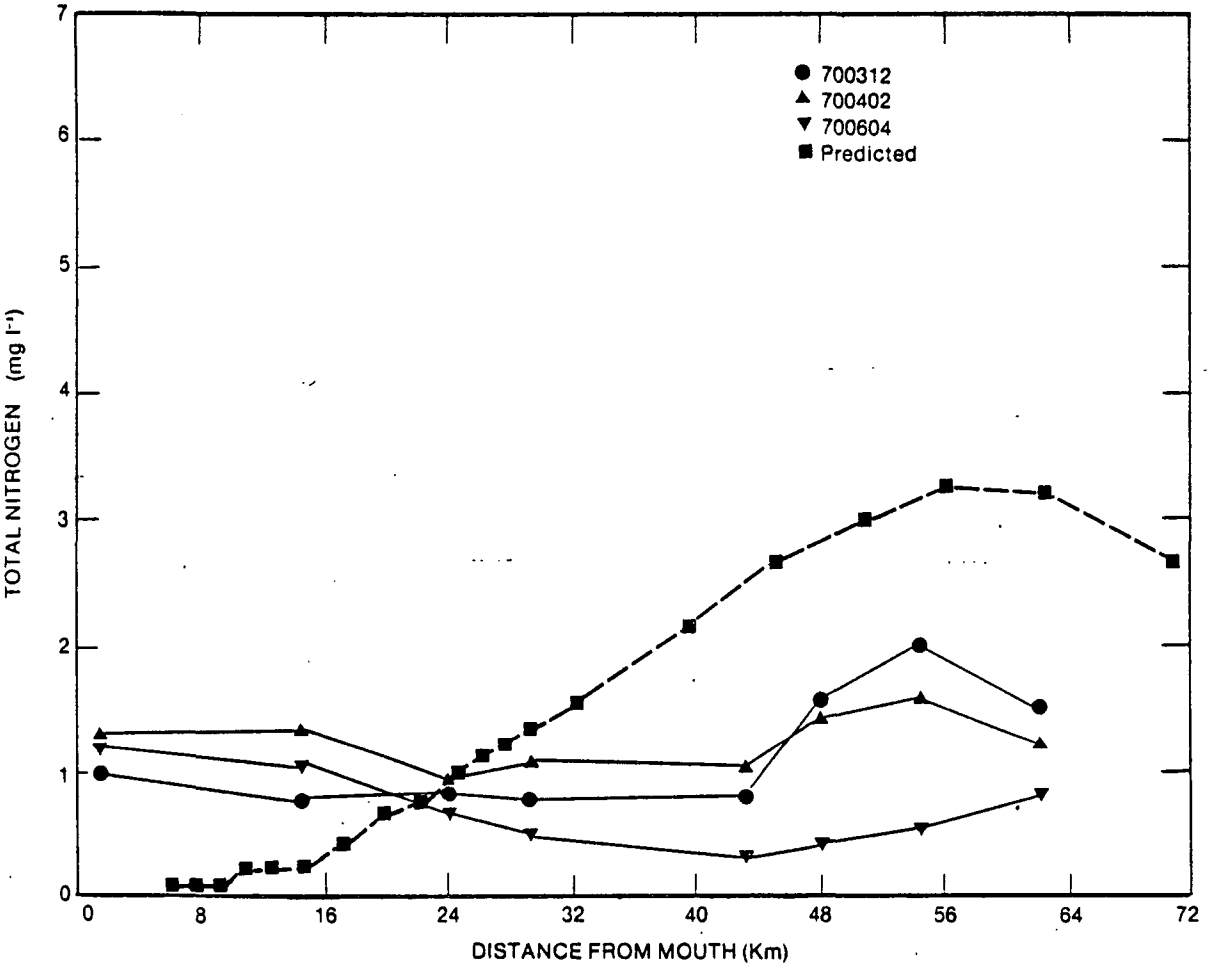

Figure 3.3-7. Observed and predicted total nitrogen profiles in the Chester River Estuary.

The prediction of pollutant levels in the lower estuary is further complicated by tidal exchanges between Kent Narrows and Eastern Bay caused by phase differences. Several seafood packing plants operate in this area and contribute both BOD and nutrients to the system. Description of this exchange within the constructs of the methodology presented here is not possible. Therefore, this exchange has not been accounted for and is a source of error in the predicted profiles.

Since the total storm load is assumed to enter the estuary in a tidal cycle, this is equivalent to saying that in succeeding cycles loads of equal magnitude enter the estuary. Therefore, the concentrations given in Table 3.3-11 are necessarily upper limit values. Lower limit concentrations may be found by assuming that the storm load is equally distributed over each tidal cycle during the length of time base of the inflow hydrograph. To estimate initial concentrations for this case the pollutant load must first be divided by the time base (in hours) of the inflow hydrograph and multiplied by the number of hours in a tidal cycle. The resultant load is then divided by the hypothetical flow rate (per tidal cycle) through the receiving segment as is normally done to arrive at the initial concentration. Alternatively, dispersion equations may be used if the user wishes to treat the event as a single event discharge.

3.3.7 Eutrophication

Using the volumetrically averaged predicted nitrogen and phosphorus concentrations from Table 3.3-11, N:P ratios are computed for the river. The ratio of total nitrogen (as N) to total phosphorus (as P) is 0.27:0.028 or 9.64:1. This falls into the region where either nitrogen or phosphorus may be limiting. To compare the predicted N:P ratio with observed data, the ratio of total soluble inorganic nitrogen (TSIN = NH_3 + NO_2 + NO_3 (as N) to total orthophosphorus (PO_4 as P)

was used. (Total phosphorus data were not available.) Observed ratios for the three available dates of March 12, April 2, and June 4, 1970 were computed as 12.6, 11.7, and 4.52 respectively. These values in general support the calculated conclusion of either nitrogen or phosphorus limitation.although it appears from the 1970 data the phos-phosphorus was limiting early in the calendar year while nitrogen was limiting during the summer months. Not only can the limiting nutrient vary seasonally, but it may well change from nitrogen to phosphorus in the less saline portions of the estuary (Porcella and Bishop, 1974).

Correlation coefficients computed for chlorophyll-a observations on selected observed water quality parameters are shown in Table 3.3-12. They show that chlorophyll-a concentrations are strongly correlated with surface nitrite and nitrate nitrogen and total nitrogen early in the year. This dependence diminishes as time progresses. However dependence on phosphorus concentration remains strong throughout the spring and summer. There is also a tendency for algal growth to occur in the less saline waters as indicated by the correlation of chlorophyll-a on salinity. Chlorophyll -a is also correlated negatively with Secchi depth which indicates possible light limitation in the estuary.

To investigate this latter phenomenon a two-parameter light pene=tration model was fit to Secchi depth vs. chlorophyll-a found in Table 3.3-4. The model formulation is

$$D_s = \frac{-\ln (0.1)}{\alpha + \beta\ (\text{Chl-}a)}$$

where

D_s = Secchi depth, meters

Chl-a = chlorophyll-a concentration in $\mu g\ \ell^{-1}$

$\ln (0.1)$ = a constant relating Secchi depth at disappearance to light penetration in seawater

TABLE 3.3-12. CORRELATIONS FOR CHLOROPHYLL-a ON SELECTED WATER QUALITY PARAMETERS IN THE CHESTER RIVER

	DATE [a]		
Parameter	700312	700402	700604
Surface $NO_2 + NO_3$	+.90	+.50	-.15
Surface Total PO_4	+.76	+.36	+.62
Surface Total N	+.65	+.23	-.38
Secchi Depth	-.64	-.47	-.44
Surface Salinity	-.87	-.38	-.25

[a] year/month/day

α = background extinction coefficient

β = coefficient of incremental extinction due to the algal concentration

The regression produced values of 3.6 for α and 0.069 for β. The incremental extinction coefficient falls outside the typical range for algae (.015-.022) (Megard, 1979) and the background extinction is also quite high. At typical Chl-a concentrations in the estuary the magnitude of α (3.6) is three to five times greater than that of $\beta \cdot$Chl-a. This indicates possible light limitations due to some constituent other than algae, perhaps suspended sediment or detritus. No suspended sediment data were available concurrent with Chl-a measurements to validate this hypothesis.

The depth of the photic zone has been defined as the depth to which 1% of surface illumination penetrates (Lorenzen, 1972). Using average Chl-a concentrations in the light model and substituting ln (0.01) for ln (0.1) gives an average photic zone depth for the estuary of approximately one meter. This value is appreciably less than the mixing depth (assuming that the estuary is fully mixed) indicating that algal production is light limited.

3.4 DEMONSTRATION EXAMPLE: THE PATUXENT RIVER

The Patuxent River system affords a good opportunity to use both the river and stream methodology and the estuarine methodology in a single system. A complicating feature of this system is a section of river which is tidally influenced but has no salinity gradient (i.e., it consists entirely of fresh water). This introduces a situation which is not covered by the river methodology and is only briefly addressed in the estuary methodology through application of advection-dispersion equations. A major tributary to the system, Western Branch, enters the Patuxent in this section.

Parameters analyzed in the low flow assessments of the previous systems (temperature, dissolved oxgyen, BOD, and fecal coliforms) are also investigated for this system. High flow assessments for the Patuxent include total phosphorus and total nitrogen. High flow analyses were not performed in the riverine portion of the system.

3.4.1 Data Collection

Quadrangle maps (7½ minute series) were obtained from the U.S. Geological Survey as were flow data and stage-discharge curves at various locations. Flow data for approximately 10 years were used in the analysis. The most recent available stage-discharge curves were utilized to determine flow depths.

The user is cautioned here that use of 10 years of low flow data to estimate the $7Q_{10}$ will almost always give a biased estimate of this statistic. The $7Q_{10}$, like any other statistic, has some distribution around its mean value. Necessary sample sizes for estimating the mean can be determined by the Law of Large Numbers (Haan, 1977).

Some water quality data were provided by the Maryland Department of Natural Resources (DNR). Among the quality data available from the Maryland DNR were:

- Salinity profiles at several flow regimes and times of year
- Dissolved oxygen and BOD
- Total chlorophyll-*a* and phaeophytin-*a*
- Phosphorus (total whole, total filtered, orthophosphorus)
- Ammonia nitrogen, nitrate nitrogen, total Kjeldahl nitrogen (whole and filtered), and
- Fecal coliforms.

Copious data were also available from the STORET system at locations in the estuary and in the tidal fresh water and the riverine portions of the system.

Effluent data for municipal point sources were provided both by the Maryland DNR and individuals in the various municipalities within the basin. Industrial sources were judged to be insignificant contributors for the parameters analyzed. The Maryland DNR has compiled a list of all point source discharges in the basin. They are shown in Table 3.4-1.

3.4.2 Data Reduction and Supplementation

Gaging stations in the nontidal fresh water portion of the Patuxent used for the stream analysis were located at Laurel, Savage, and Bowie, Maryland. Sufficient data were not available at either the Savage or Bowie stations to estimate the $7Q_{10}$ low flows. For the Savage location an upstream station at Guilford was used and the $7Q_{10}$ flow estimate there was extrapolated to Savage by areal weighting. The $7Q_{10}$ at Bowie was also estimated by areal weighting.

Gaging stations as well as the major point sources in the basin were located on the 7½ minute series maps. Distances and elevation changes between these gages and point sources were measured and average slopes were computed and recorded. Depths and velocities were determined at each gage for the $7Q_{10}$ flows using stage-discharge curves and the continuity equation.

For the estuarine portion of the system, transects were drawn at convenient locations normal to the flow and cross sections were measured. Lengths between the transects were recorded and the MHT and MLT volumes of the estuary were calculated. Transects were taken at the locations shown in Table 3.4-2. Mean high tide (MHT) cross sections were calculated

TABLE 3.4-1. ACTIVE DISCHARGERS IN THE PATUXENT RIVER BASIN

Publicly Owned Treatment Plant	Private	Industrial Wastes
Lower Patuxent		
	Academy Natural Sciences of Philadelphia	Asher, B.F. Sand & Gravel
	Evergreen Park, STP	Denton, Warren & Co., Inc.
	Natural Resources Institute	Lore, J.C. & Sons
	Village Center, The	Patuxent River Oyster Co.
		Pepco, Chalk Point
		Trossback Brothers
Middle Patuxent		
Marlton Temporary STP	Boone's Mobile Estates	Annapolis Sand & Gravel Co.
	Croom Vocational H.S.	Calvert Meats, Inc.
	Edgemeade of Maryland	Davidsonville Sand & Gravel
	First Md. Utilities, STP	First Maryland Utilities
	Lyons Creek Mobile Home Pk.	Pepco Flyash - Brandywine
	Md. Manor Mobile Homes	
	Northern School, STP	
	Patuxent Mobile Home Estates	
	Patuxent River 4-H Center	
	Southern Senior H.S.	
	Tucker's Restaurant	
	Wayson's Mobile Court	
Western Branch		
Western Branch STP	Andrews Field Motel	
	Pointer Ridge Lagoon	
Upper Patuxent		
Bowie State College	Bowie Race Course	Bio-county Aggregate Corp.
Bowie City of, STP	City of Capitals, STP	Bowie Water Filtration Plant
Horsepen Branch, STP		Electro-Therm, Inc.
Maryland City, STP		
Parkway, STP		
Little Patuxent		
Maryland House of Corrections	John Hopkins University	Arctec, Inc.
Patuxent, STP	Parkway Manor Motel	Barton, Alan E., Inc.
Savage, STP		Bercon Parkaging, Inc.
		Columbia Park
		Contee Sand & Gravel
		Crofton Meadows Water Treatment Plant
		Crofton Water Treatment Plant

TABLE 3.4-2. ESTUARINE CROSS SECTIONS IN THE PATUXENT RIVER

Location	Distance From Mouth (km)	MLT Cross Section (m^2)	MHT Cross Section (m^2)
Peterson's Point	14.5	15,205	16,233
Broome's Island	18.9	8,152	8,836
Prison Point	26.6	12,028	13,299
Trent Hall Point	32.3	5,643	6,305
Rt. 231 Bridge	36.7	4,060	4,543
Potts Point	42.4	2,843	3,017
Milltown Landing	51.89	1,417	1,591
Hall Creek	59.0	1,282	1,816

assuming that the banks of the estuary are vertical and using the mean tidal range given on the USGS topographic maps.

3.4.3 Fresh Non-Tidal Waters

The free flowing fresh waters of the Patuxent extend to approximately Hardesty, Maryland, 89 km above the mouth. Above this point, along the Patuxent to the Rocky Gorge Reservoir Dam (41 km) and along the Little Patuxent to Savage (70 km), river methodologies were applied. The Patuxent was divided into seven reaches and the Little Patuxent was divided into seven reaches for the low flow analysis. Reach segmentation was based on the locations of important sewage treatment plant effluent discharges. These reaches are schematically shown in Figure 3.4-1. The accompanying hydraulic data for each reach are shown in Table 3.4-3. The characteristic depth shown is the hydraulic depth of the stream. A range of velocities for each reach is also shown in the table. The lower of the two velocities is that derived by continuity ($Q = AV$), and the upper value was derived from the Manning equation using a roughness coefficient (n) of 0.08. This coefficient was evaluated using the hydraulic data of Tsivoglou and Wallace (1972). It falls into the category of "sluggish river reaches, rather weedy with very deep pools" (Schwab et al., 1966). Tsivoglou and Wallace (1972) describe the stream as "a typical coastal plains stream characterized by alternating small pools and riffles."

The Patuxent and Little Patuxent Rivers in this portion of the basin flow through a region adjoined by marshy areas. The $7Q_{10}$ outflow at the Bowie gage is greater than the sum of the inflows at the Savage and Laurel gage and the sewage treatment plant inflows. The difference in these is assumed to come from the swampy areas adjacent to the river. This flow was distributed incrementally by proportioning it to the length of the reach. The last column of Table 3.4-3 gives these incremental natural flows. For the most part the numbers in this table are estimates only, interpolated from hydraulic data at the gaging stations.

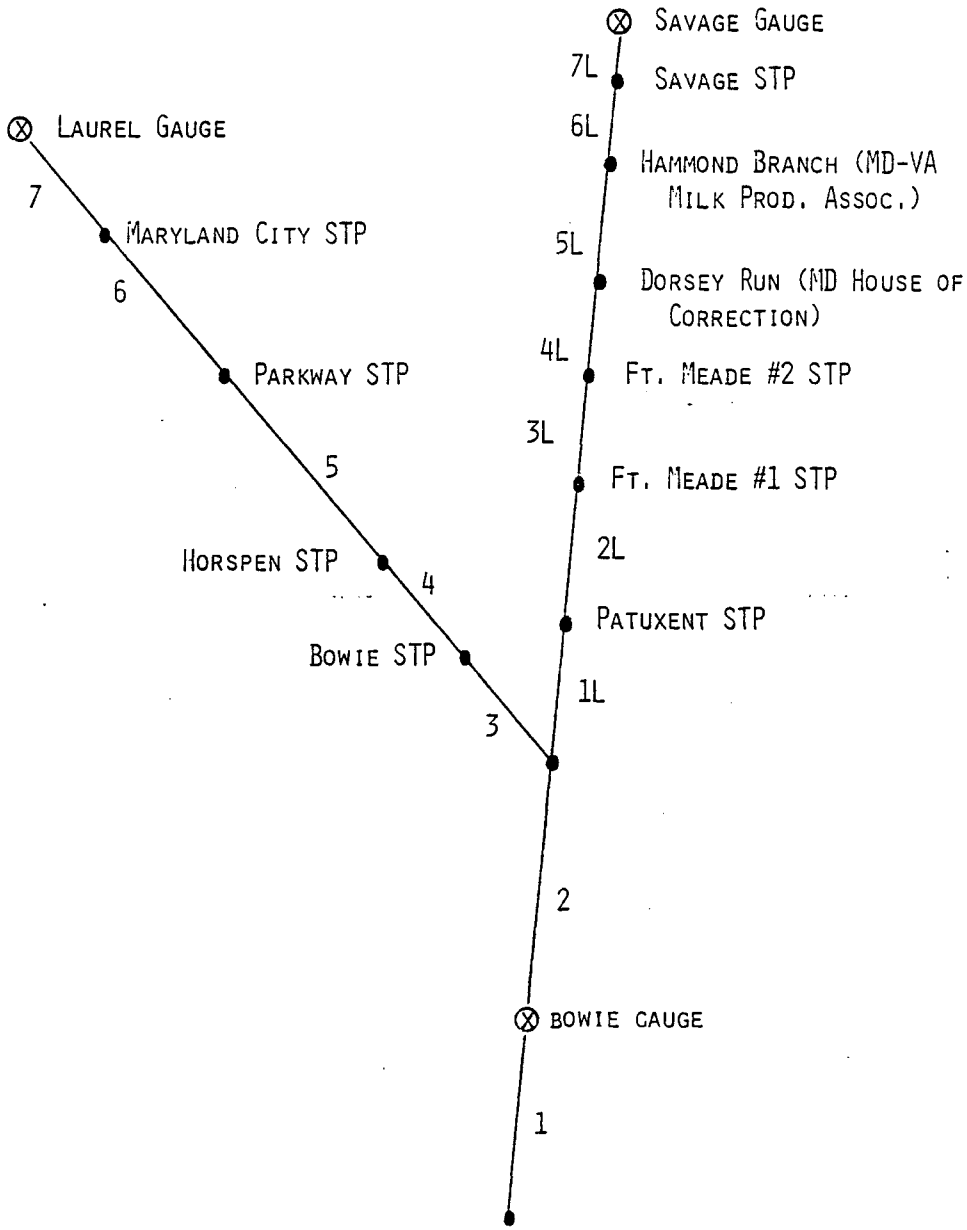

Figure 3.4-1. Reach segmentation schematic for the Patuxent River.

TABLE 3.4-3. PATUXENT RIVER HYDRAULIC DATA FOR FREE FLOWING WATERS (LOW FLOW)

Patuxent Reach #	Descriptor at Upstream End of Reach	Characteristic Depth (m)	Cross Section (m^2)	Flow ($m^3\ sec^{-1}$)	Slope ($m\ km^{-1}$)	Velocity ($m\ sec^{-1}$)	Reach Length (km)a)	Natural Water Incremental Inflow Downstream ($m^3\ sec^{-1}$)
1	Bowie Gauge	0.70	16.3	1.81	0.20	.11 -.14	7.61	0.032
2	Confl w/Little Patuxent	0.25	7.8	0.640	0.91	0.082-.15	5.02	0.022
3	Bowie STP	0.22	7.2	0.558	1.00	0.076-.15	3.04	0.013
4	Horsepen STP	0.22	6.8	0.532	0.68	0.79 -.12	2.27	0.010
5	Parkway STP	0.16	2.3	0.278	1.27	.12	13.28	0.057
6	Maryland City STP	0.15	2.2	0.235	1.34	.11 -.13	4.55	0.019
7	Laurel Gauge	0.15	2.2	0.212	2.29	.098-.17	5.33	0.023
							41.10	
Little Patuxent								
1L	Patuxent STP	0.384	10.3	0.985	0.87	.094-.20	3.52	0.015
2L	Fort Meade #1	0.421	9.6	0.898	1.19	.094-.24	7.64	0.033
3L	Fort Meade #2	0.460	8.7	0.813	1.57	.094-.30	7.79	0.033
4L	Confl w/Dorsey Run	0.475	8.5	0.773	0.83	0.091-.22	2.90	0.012
5L	Confl w/Hammond Branch	0.497	8.0	0.748	0.53	0.094-.18	4.57	0.020
6L	Savage STP	0.506	7.9	0.374	0.76	0.049-.22	1.61	0.0068
7L	Savage Gauge	0.509	7.8	0.371	4.36	0.046-.53	0.76	0.0031
							28.79	0.297
							69.89	

a) For reference, the Bowie gauge is 98 km from the mouth. The mouth is defined as the transect connecting Drum Point with Fishing Point.

3.4.3.1 Temperature Profiles

Temperature profiles for the system were developed using the equilibrium temperature (T_e) approach (Section 4.4.4, p. 205 of the screening manual). Data used to calculate T_e for the Patuxent are as follows:

$$u = 14.5 \text{ km hr}^{-1} \text{ (9 mi hr}^{-1}\text{)}$$

$$H_{sn} = 14500 \text{ BTU m}^{-2} \text{ day}^{-1} \text{ (1350 BTU ft}^{-2} \text{ day}^{-1}$$

$$T_a = 21.1°C \text{ (70°F)}$$

$$\text{Relative Humidity} = 72\%$$

$$\text{Cloud cover fraction} = 0.5$$

These values represent average conditions for the month of September. Observed annual low flows typically occurred in this month. The computed T_e for the Patuxent basin is 20.2°C.

Temperature profiles were calculated using equation IV-36, section 4.4.5, p. 217 of the screening manual. Two cases were used to evaluate temperature profiles. The difference in the two cases involved assumptions concerning the natural incremental inflow temperature. This inflow can be assumed to be at the temperature of the ground water (when the inflow is primarily from subsurface sources) or at the equilibrium temperature (when the inflow is primarily from standing marsh water). Incoming flow at Laurel and Savage from the headwaters was assumed to be at the equilibrium temperature. Calculations show that the river essentially does not deviate from the equilibrium temperature except in reach #5 when the incremental inflow temperature is assumed to be that of subsurface water (10°C).

3.4.3.2 Estimation of Reaeration and Deoxygenation Coefficients

Deoxygenation rates for each reach were calculated using the Bosko equation,

$$k_d = k_1 + n(V/D)$$

with a mean k_1 of 0.45 (see Zison et al., 1978). No differentiation was made between NBOD and CBOD deoxygenation.

Pheiffer et al., (1976) studied BOD decay rates in the Patuxent River below the Parkway Sewage Treatment Plant (reach #5). CBOD decay rates were determined to be 0.61 day^{-1} in 1973 and 0.30 day^{-1} in 1975 (all coefficients are base e). The difference between these two rates was attributed to more efficient CBOD removal at the Parkway plant caused by upgrading in the interim. For NBOD, rates changed from 0.76 day^{-1} in 1973 to 0.48 day^{-1} in 1975. The mean deoxygenation rate calculated from Bosko is 0.56 day^{-1} which is greater than both the current NBOD and CBOD decay rates for this reach, but less than the rates determined before the upgrading of the treatment facility.

Reaeration rates were determined by each of three methods, Tsivoglou-Wallace, O'Connor, and Owens. Table 3.4-4 shows both the deoxygenation rates and reaeration rates computed by these three methods. The table values are for temperatures of 20°C with the exception of the Tsivoglou-Wallace rates which are at 25°C. Tsivoglou and Wallace (1972) used the gas-tracer method to evaluate reaeration in the Patuxent. Flows at that time were similar to the $7Q_{10}$ flows used in this investigation. Their value for the reaeration rate in reach #5 was 3.3 day^{-1} (base e) at 25°C. The rate predicted by their equation using interpolated hydraulic data is 2.31 day^{-1} at 25°C. The O'Connor and Owens formulations for this reach give values an order of magnitude higher (20.9 day^{-1} and 37.2 day^{-1} respectively).

TABLE 3.4-4. DEOXYGENATION AND REAERATION RATES FOR THE PATUXENT RIVER FREE FLOWING WATERS

Reach #	Mean Deoxygenation Rate (day^{-1} base e @20°C)	Reaeration Rates (day^{-1} base e)		
		Tsivoglou-Wallace (@25°C)	O'Connor (@20°C)	Owens (@20°C)
Patuxent				
1	0.47	0.38	2.37	2.54
2	0.52	1.61	10.5	15.9
3	0.53	1.71	12.4	19.5
4	0.52	1.03	12.2	19.0
5	0.56	2.31	20.9	37.2
6	0.57	2.45	22.8	41.4
7	0.68	4.65	25.4	47.7
Little Patuxent				
1L	0.51	1.93	6.25	8.49
2L	0.51	3.09	5.95	8.07
3L	0.56	4.69	5.56	7.47
4L	0.50	1.98	4.73	6.04
5L	0.48	1.11	4.16	5.12
6L	0.49	1.56	4.00	4.88
7L	0.67	19.11	5.79	8.02

3.4.3.3 BOD Mass Balance

Equation IV-7, section 4.2.4, p. 152, of the screening manual was used to perform all BOD mass balance calculations for the Patuxent River. Three cases were used to demonstrate BOD routing. In the first, BOD_5 profiles were developed to determine closeness to observed BOD_5 data. The second case used BOD_5 plant effluent data converted to $CBOD_u$ together with estimated $NBOD_u$ values for all plants based on the type of treatment that they employ (U.S. Army Corps of Engineers, 1977). Lastly, $NBOD_u$ and $CBOD_u$ were routed using $NBOD_u$ values as determined using the Kjeldahl nitrogen values from plant effluent data. Municipal treatment plant effluent data are shown in Table 3.4-5. The headwaters above Savage and Laurel and the incremental inflow waters were assumed to have background BOD_5 values of 1.0 mg ℓ^{-1}.

The results of these calculations are shown in Table 3.4-6. The range given shows the upstream to downstream variation within each reach. The cases in which NBOD are determined, one with the total Kjeldahl nitrogen data for the treatment plants and one assuming a treatment type for the treatment facility (see Appendix A), are shown for comparative purposes. Without actual data to rely on, the user would likely estimate BOD loads with a percent reduction based on the type of treatment that the facility employs. Using this approach, the predicted instream ultimate BOD concentrations in this example are often two to three times higher than the profiles predicted using observed loading data. No observed ultimate BOD data were available for comparison with either of these profiles.

Using routed treatment plant BOD_5 data, the predicted BOD_5 values in reach #5 range from 1.80 to 1.19. The observed BOD_5 data (retrieved from STORET) for September in that reach have a mean of 4.9 ± 2.8 which puts the calculated values below the low end of the one standard deviation range. One plausible explanation for this discrepancy is that

TABLE 3.4-5. MAJOR SEWAGE TREATMENT PLANT EFFLUENT DATA IN THE PATUXENT RIVER SYSTEM[a)]

Plant	Flow ($m^3\ sec^{-1}$)	Temperature (°C)	BOD_5 ($mg\ \ell^{-1}$)	Dissolved Oxygen ($mg\ \ell^{-1}$)	NH_3 ($mg\ \ell^{-1}$)	Total Kjeldahl Nitrogen ($mg\ \ell^{-1}$)	Total Phosphorus ($mg\ \ell^{-1}$)	Fecal/Total Coliforms (MPN/100 mℓ)
Western Branch	.40	19.1	3.6	9.2	5.2	8.8	5.7	12147/-
Savage	.37	18.5	13.6	8.9	9.0	14.7	8.7	4/84
Bowie	.07	23.8	23.1	10.0	18.2	25.0	9.4	2/26
Patuxent	.15	20.5	41.1	8.6	10.8	16.7	6.7	1847/126552
Parkway	.20	24.4	2.2	8.0	4.6	7.7	3.8	7/242
MD-VA Milk Producers Assn.	.01	20.7	23.3	4.9	817.6	23.8	28.3	39/2732
Maryland House of Correction	.03	23.8	5.4	7.9	0.60	2.3	3.2	4/9
Maryland City	.02	22.2	16.3	5.5	16.6	22.3	9.4	723/13200
Horsepen	.02	18.7	5.7	9.8	7.5	9.8	4.3	2/1204
Ft. Meade #1	.05	21.3	22.4	6.9	9.0	12.2	6.8	177/1005
Ft. Meade #2	.05	20.9	28.0	7.9	8.2	12.9	6.8	6/116

a) All values are averages of composite samples except dissolved oxygen (grab sample).

TABLE 3.4-6. BOD MASS BALANCE FOR THE FREE FLOWING WATERS OF THE PATUXENT RIVER

Reach #	$CBOD_5$	(CBOD + NBOD)u (NBOD Determined by Estimation)	(CBOD + NBOD)u (NBOD Determined from Plant TKN)
1	4.44 - 3.03	31.1 - 21.1	19.9 - 13.5
2	5.11 - 4.44	35.8 - 31.1	22.9 - 19.9
3	3.50 - 2.79	47.7 - 37.7	26.6 - 21.0
4	1.30 - 1.12	42.1 - 34.9	14.1 - 11.8
5	1.80 - 1.19	64.9 - 39.9	20.9 - 12.9
6	2.10 - 1.57	13.5 - 9.8	11.9 - 8.7
7	1.0 - 0.68	1.47- 1.0	1.47- 1.0
1L	7.80 - 6.41	42.5 - 34.8	29.3 - 24.0
2L	4.50 - 2.81	35.6 - 22.0	21.3 - 13.2
3L	5.30 - 3.14	48.3 - 28.4	28.4 - 16.7
4L	5.00 - 4.15	50.0 - 41.3	29.3 - 24.3
5L	6.60 - 4.99	63.0 - 47.3	39.1 - 29.4
6L	7.20 - 6.43	69.1 - 62.0	43.4 - 39.0
7L	1.0 - 0.87	1.47- 1.29	1.47- 1.29

while the BOD_5 test of plant effluent represents primarily carbonaceous demand, samples taken from streams may contain the effects of some nitrogenous deoxygenation. This should be small, however, since the travel time through the riverine system is short. It is also probable that the small incremental inflows from the marshy areas have concentrations greater than the 1.0 mg ℓ^{-1} assumed in this exercise. The user is warned, however, against drawing such conclusions based on only a point observation in the system.

Figure 3.4-2 shows observed and predicted BOD_5 concentrations in the Patuxent River from below Rocky Gorge Dam to just below the confluence of the Patuxent and Little Patuxent rivers (approximately km 130 to km 100). The observed data were measured on September 26, 1978 by the Maryland Department of Natural Resources. The flow in reach #3 was 0.71 m^3 sec^{-1}. The comparison between predicted and observed results is quite good. However, the background BOD_5 assumption of 1.0 mg ℓ^{-1} seems too low as evidenced by the discrepancy in the upper reaches where this assumption has greatest effect.

The background condition is damped out after a substantial source of BOD enters the system. The large spike at river km 104 is due to the inflow of the Little Patuxent River whose quality is more degraded than that of the Patuxent.

3.4.3.4 Dissolved Oxygen Profiles

A dissolved oxygen mass balance for the Patuxent River was performed using both Tsivoglou-Wallace and O'Connor reaeration rates. The O'Connor formulation was developed on rivers having depths of 0.3 to 9 meters and consequently produces reaeration rates lower than the Owens equation which was developed on faster, shallower streams. Because the O'Connor method yielded dissolved oxygen concentrations greater than those observed instream, and close to saturation, profiles using the Owens

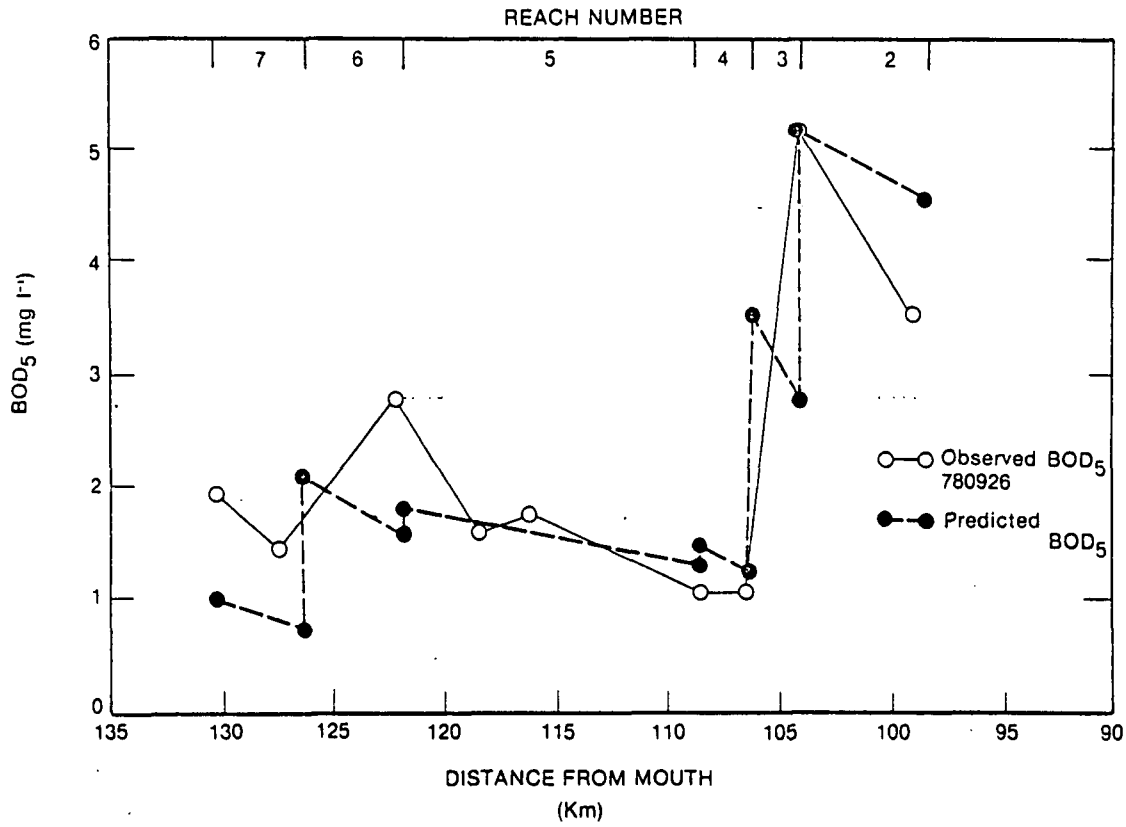

Figure 3.4-2. Observed and predicted BOD_5 in the Patuxent River.

method for reaeration were not calculated. Ultimate BOD from the case in which $NBOD_u$ was estimated from plant total Kjeldahl nitrogen data was used to perform all dissolved oxygen calculations. Temperature profiles showed that 20°C was a good approximation of temperature throughout the system. The corresponding dissolved oxygen saturation is 9.2 mg ℓ^{-1}. NBOD and CBOD decay rates were not differentiated so equation IV-18 (Streeter-Phelps), section 4.3.6, p. 170 of the screening manual was used.

One complicating factor in this calculation is the presence of the Rocky Gorge Reservoir just upstream from the Laurel gage. If stratification occurs in the lake and hypolimnion water is released into the Patuxent, very low initial values of dissolved oxygen might be observed at Laurel. On the other hand, turbulent flow releases might drive waters with initially low dissolved oxygen to near saturation. (See section 4.3.4 of the screening manual, Effect of Dams on Reaeration.) Dissolved oxygen profiles were computed using both assumptions. For the first case, the initial dissolved oxygen level at the Laurel gage was assumed to be at saturation. For the latter, the boundary dissolved oxygen value was selected to be 5.0 mg ℓ^{-1}. Table 3.4-7 shows computed dissolved oxygen profiles for the Patuxent and Little Patuxent Rivers using the assumption that waters released from Rocky Gorge Reservoir were at saturation. Again, the ranges represent the longitudinal variation within each reach. Average observed dissolved oxygen levels at Duvall Bridge (in reach #5) for the month of September were 6.5 ± 0.52 mg ℓ^{-1}. From this point observation, it appears that perhaps the Tsivoglou-Wallace rates are better indicators of actual reaeration rates. However, Figure 3.4-3 shows that this may not be the case. This figure illustrates an observed dissolved oxygen profile taken on 26 September, 1978 at a flow rate not greatly different from that used in the analysis. Predicted profiles were computed using the assumption that release waters from Rocky Gorge were at 5 mg ℓ^{-1} dissolved oxygen. The observed data validate this assumption. Although they are not plotted, predicted dissolved

TABLE 3.4-7. DISSOLVED OXYGEN PROFILES IN THE PATUXENT RIVER FOR TWO REAERATION RATES

Reach #	Dissolved Oxygen (mg ℓ^{-1}) O'Connor	Tsivoglou-Wallace
1	8.3 - 6.4	2.7 - 0.0
2	8.2 - 8.3	3.4 - 2.7
3	8.7 - 8.2	5.0 - 3.4
4	8.9 - 8.7	5.9 - 5.0
5	9.0 - 8.9	7.5 - 5.9
6	9.2 - 9.0	9.1 - 7.5
7	9.2 - 9.2	9.2 - 9.1
1L	7.6 - 7.1	5.8 - 4.0
2L	6.7 - 7.6	5.4 - 5.8
3L	5.5 - 6.7	1.8 - 5.4
4L	5.5 - 6.0	2.0 - 1.8
5L	7.0 - 5.5	6.6 - 2.0
6L	9.2 - 7.0	9.2 - 6.6
7L	9.2 - 9.2	9.2 - 9.2

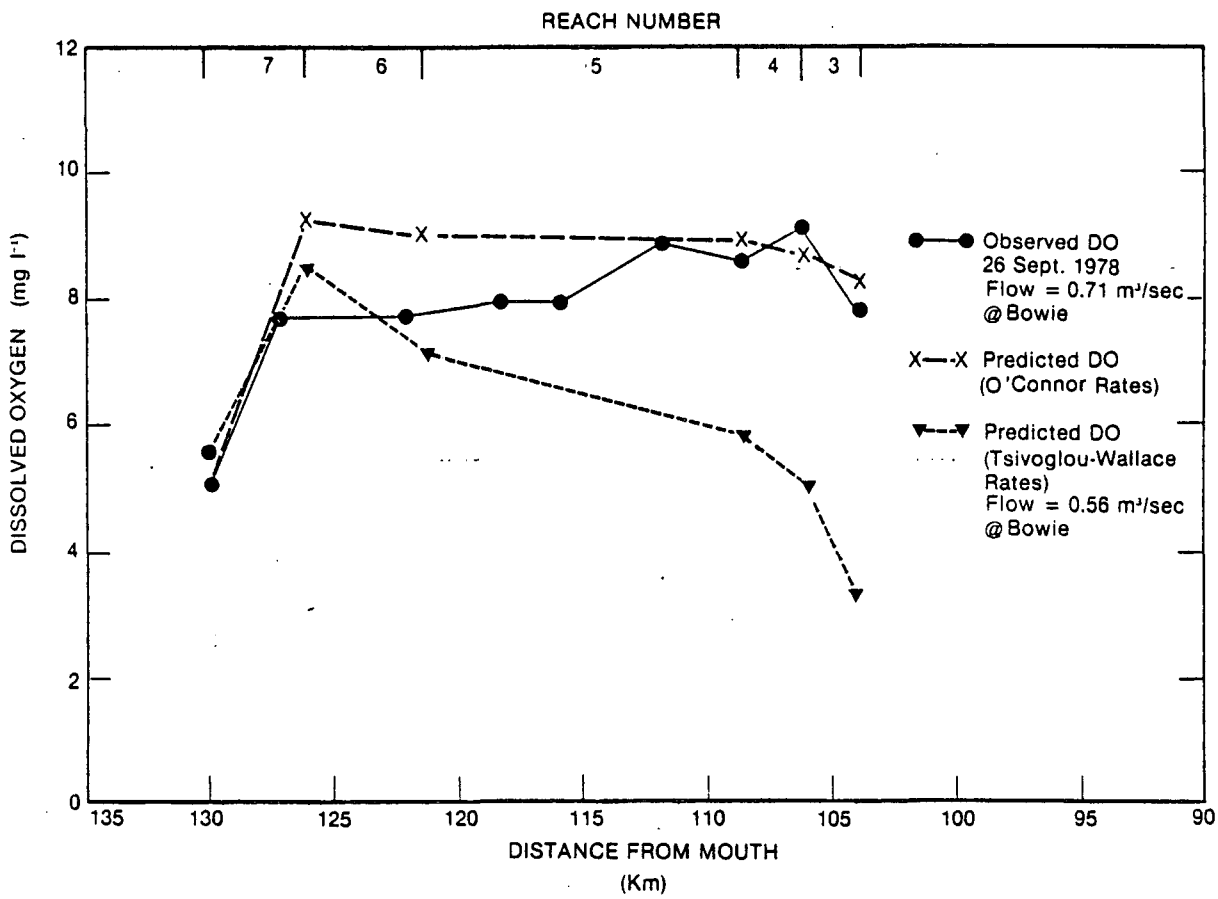

Figure 3.4-3. Observed versus predicted dissolved oxygen profiles for the Patuxent River.

oxygen values for reaches #1 and #2 are essentially the same as those values shown in Table 3.4-7 for reaches #1 and #2. The plot also shows that the Tsivoglou-Wallace formulation yields reaeration rates that appear to be too low because the predicted dissolved oxygen profile is considerably below the observed profile. However, this is indirect evidence since there may be other causes for the discrepancy, such as inaccurate BOD data.

For the purposes of selecting between alternatives, the use of lower reaeration may be more appropriate. For instance, if the planner has to choose between reach A or B as a possible site for a sewage treatment facility, the use of very high predicted reaeration rates which maintain dissolved oxygen at or near saturation may make A and B appear equally attractive. The use of lower reaeration rates may show that one reach is less desirable than the other.

The use of 9.2 or 5.0 mg ℓ^{-1} for background conditions at the upstream end of reach #7 made essentially no difference when using O'Connor rates since the predicted dissolved oxygen was driven to saturation in both cases. Using Tsivoglou-Wallace rates, the difference in predicted dissolved oxygen levels was about 1 mg ℓ^{-1} at the end of reach #7, about 0.3 mg ℓ^{-1} at the downstream end of reach #6 and negligible thereafter. Selection of the boundary dissolved oxygen value will tend to be more important when boundary flows are large compared to incoming flows from waste sources in the system.

Critical travel times and critical dissolved oxygen deficits were also computed for several of the waste treatment plants using the $7Q_{10}$ low flow for the Patuxent. Equations IV-22 and IV-24 (section 4.3.7, pp. 175-176) in the screening manual were used in this evaluation. Alternatively, Tables IV-10 and IV-11 in the same section can be used for this purpose. Table 3.4-8 shows critical travel times and critical deficits calculated by the equations. If T_c (time of travel to critical deficit) is undefined or zero, then the answer

TABLE 3.4-8. CRITICAL TRAVEL TIMES, DISTANCES AND DISSOLVED OXYGEN DEFICITS FOR SOME PATUXENT STPs AT THE $7Q_{10}$ LOW FLOW

STP Name/ Reach Number	Travel Time (days)		Distance to Deficit (km)		Critical Deficit (mg ℓ^{-1})	
	O	T-W	O	T-W	O	T-W [a]
Savage/6L	0.59	1.15	6.9	13.4	4.00	8.6
Ft. Meade #2/ 3L	0.00 [b]	0.00	0.0	0.0	3.70	7.4
Ft. Meade #1/ 2L	0.00	0.00	0.0	0.84	3.60	3.8
Patuxent/1L	0.00	0.73	0.0	9.0	3.40	5.9
Maryland City/ 6	0.15	0.81	1.50	8.4	0.27	1.9
Parkway/5	0.00	0.70	0.0	7.2	1.70	3.8
Horsepen/4	0.00	0.93	0.0	7.9	3.30	4.9
Bowie/3	0.00	0.71	0.0	6.8	4.20	6.3

a) O - O'Connor reaeration rates
T-W - Tsivoglou-Wallace reaeration rates.

b) A zero entry indicates that the deficit occurs at the STP outfall.

obtained from Equation IV-24 for D_c (the critical deficit) is not valid. In such cases D_c occurs at the location of the waste water discharge and can be determined by calculating a flow weighted average dissolved oxygen deficit using the upstream deficit and the deficit in the incoming waste water.

In general, Tables IV-10 and IV-11 are simpler to use than Equations IV-22 and IV-24. As an example, for the stretch of the river below the Parkway Sewage Treatment Plant, the user first calculates D_o/L_o (L_o is the instream BOD concentration just below the sewage treatment plant, and D_o is the initial deficit) and k_a/k_L (the reaeration constant over the deoxygenation constant for the reach). The results are:

$$\frac{D_o}{L_o} = \frac{1.7 \text{ mg } \ell^{-1}}{20.9 \text{ mg } \ell^{-1}} = .08$$

and

$$\frac{k_a}{k_L} = \frac{2.07 \text{ day}^{-1}}{.056 \text{ day}^{-1}} = 3.696 \sim 3.7$$

L_o is taken from the calculated BOD concentrations in Table 3.4-6 for reach #5. D_o is calculated from the dissolved oxygen concentration in Table 3.4-7 for reach #5, using Tsivoglou-Wallace reaeration rates and a saturation concentration of 9.2 mg ℓ^{-1}. The rate constants k_a and k_L are for reach #5 also. The reaeration constant k_a is computed from the Tsivoglou-Wallace formulation adjusted to 20°C to be consistent with the temperature base of the deoxygenation rate:

$$k_a = 2.31 \ (1.022)^{(-5)} = 2.07$$

Using these values as the abscissa and ordinate in Table IV-10 of the screening manual, the value for D_o/L_o is found to be 0.18. When this

is multiplied by L_o (20.9), D_c is found to be 3.8 mg ℓ^{-1}. This is identical to the value found in Table 3.4-8 obtained using Equation IV-24 of the screening manual.

3.4.3.5 Total Coliform Routing

Total coliform bacteria levels in the free flowing portion of the Patuxent River system were computed using average plant effluent concentrations from Table 3.4-5. As was previously discussed in the Sandusky River example, coliform bacteria loadings can be quite variable depending on the reliability of the chlorination process at each sewage treatment plant. The predicted concentrations could vary several orders of magnitude under an identical set of flow conditions. Calculations showed that the likely problem areas with respect to bacterial concentrations at low flow would be downstream from the Patuxent sewage treatment facility where the calculated concentrations reached 16,477 MPN/100 ml. Initial concentrations of 1317 and 562 MPN/100 ml were predicted instream at the outfalls of the Maryland City and Parkway sewage treatment plant facilities. The high predicted value at the Patuxent sewage treatment plant kept the concentrations of total coliforms in the 7600 to 3600 MPN/100 ml range from the confluence of the Patuxent and Little Patuxent to the end of the free flowing portion of the river at Hardesty.

A background value of 300 MPN/100 ml (McElroy et al., 1976) was used in the mass balance equation (case 2) for total coliforms. (See section 4.6.2, p. 237, of the screening manual.)

The State of Maryland standards for fecal coliforms are 200 MPN/100 ml for Class I waters and 70 MPN/100 ml for Class II waters. The Patuxent River Class I waters extend from source to 63 kilometers above the mouth of the estuary. Below this point the waters are categorized as Class II. Sampling on 26 September 1978 indicated violations of Class I standards at ten locations with concentrations as high as

4000 MPN/100 ml. No violations occurred in Class II waters on this date.

3.4.4 Estuarine Waters

The Patuxent River estuary is an excellent choice for demonstration of the estuarine methods because of its geometry and drainage characteristics. It has no major side embayments, and the assumption of one fresh water inflow at the head of the estuary is very nearly met. Flow ratio calculations using a tidal prism volume of 3.51×10^7 m^3 and estimated flows at the head of the estuary of 2.3×10^4 m^3 and 3.58×10^6 m^3 yield flow ratios of 0.004 and 0.103 for the low and high flows cases investigated here. These values indicate that the estuary is well mixed for both flow rates. However, historical data indicate that the Patuxent River estuary is partially stratified at high flows. Unfortunately, sufficient velocity data were not available to check the classification of the estuary using the stratification-circulation method.

The estuarine waters of the Patuxent extend from Hall Creek to Sheridan Point, a distance of approximately 46.6 km. Above these waters is a 37.5 km segment of fresh tidally influenced waters and below are embayment waters which are essentially of the same salinity and quality as the Chesapeake Bay.

3.4.4.1 Flushing Times

Flushing times for the Patuxent River estuary were calculated by each of the tidal prism, modified tidal prism, and fraction of fresh water methods. Both high and low river flow volumes per tidal cycle at the Bowie gage were extrapolated to the location identified as the beginning of the estuary (Hall Creek) by areal proportioning. These volumes were estimated to be 1.42×10^5 m^3 for the low flow conditions

($7Q_{10}$) and 3.6 x 10^6 m^3 for high flow conditions. The volume of tidally influenced fresh water immediately upstream of the first modified tidal prism segment was assumed not to influence the flushing characteristics of segments down the estuary.

The results of the flushing calculations are as follows:

- The tidal prism method gives a flushing time of 6.1 days for both scenarios.
- The modified tidal prism method gives flushing times of 119 days for low flow and 36 days for the high flow case.
- The fraction of fresh water method gives flushing times of 203 days and 14.3 days for the low and high flow scenarios, respectively.

As an example, the calculations for flushing times using the modified tidal prism method to estimate flushing times in the Patuxent River under high flow conditions are summarized in Table 3.4-9. The "0" segment begins when Hall Creek enters the Patuxent River.

The analysis shows the modified tidal prism method when applied to the Patuxent River is more sensitive to flow rate changes than it is for the Chester River, even though the flow rates are comparable for the two systems. The drainage basins of the two estuaries are shaped quite differently, and the Patuxent more nearly meets the "single inflow at the estuary head" assumption than does the Chester. The Patuxent drainage basin is also more than twice as large but the volume of the Chester estuary is greater. It can be concluded that flow rate changes of approximately equal magnitude have less impact on the larger estuary's flushing times.

The fraction of fresh water method produced flushing time estimates that closely approximated those attained by the modified tidal prism method. This was not the case for the Chester River. Some allowance

TABLE 3.4-9. CALCULATION OF FLUSHING TIMES FOR HIGH FLOWS CONDITIONS IN THE PATUXENT RIVER USING THE MODIFIED TIDAL PRISM METHOD

Segment	Segment Length	P_i (m^3)	V_i (m^3)	$T_i = \frac{P_i + V_i}{P_i}$ (tidal cycles)
0	15.4	3.6×10^6	3.0×10^7	9.3
1	9.6	5.7×10^6	3.4×10^7	7.0
2	5.9	4.1×10^6	4.0×10^7	10.7
3	3.9	5.8×10^6	4.4×10^7	8.6
4	4.1	5.0×10^6	4.9×10^7	10.8
5	3.9	4.8×10^6	5.4×10^7	12.3
6	3.8	4.6×10^6	5.9×10^7	13.8
				T_f = 72.5 tidal cycles or ∿ 36 days

must be made for the fact that salinity data used in the fraction of fresh water method were not always measured at the exact flow rates used in the modified tidal prism method analysis.

3.4.4.2 Pollutant Distribution

3.4.4.2.1 Low Flow

A significant problem in estimating pollutant loads into the head of the Patuxent estuary is the long reach of tidally influenced fresh water between the free flowing waters and the estuary head (defined by the location where salinity gradient begins). In this reach, the distribution of pollutants cannot be determined by the estuarine methods due to the lack of a salinity gradient. Neither can it be treated with the river methods because of the unsteady flow induced by tidal action and the attendant increased dispersive effects. In effect, it exhibits both river and estuary characteristics.

Since pollutants entering the estuary from the river must pass through the fresh water tidal reach, a method must be devised to route pollutants through the reach. Conservative pollutants loads to the estuary can be determined by a simple mass balance. For non-conservative pollutants, decay must be taken into account. This was done as follows. The reach containing the tidal fresh waters was divided into two segments, that above the confluence of Western Branch with the Patuxent and that portion below this confluence to the head of the estuary. A parabolic shape was assumed for the channel at Bowie where the closest reliable hydraulic information existed in the upstream direction. Using this assumption the cross sectional area was calculated, knowing the top width and flow depth at the low flow rate. (For a parabola, the cross section is two-thirds of the product of the top width and maximum flow depth.) The estuary at Hall Creek is also roughly parabolic in shape. The flow in the river just above the confluence of Western Branch was determined by linearly interpolating between the net fresh water flows at Bowie and Hall Creek. Net velocities at each of

the three locations (Bowie, confluence of Western Branch and confluence of Hall Creek) were estimated by dividing calculated flows by the respective cross sectional areas. The cross section at Hall Creek was taken to be the average cross section between high and low tide. Tidal variation at Bowie was assumed to be zero. From these net velocities, the excursion time for a plug was determined for each of the two segments. The excursion times under the conditions of the $7Q_{10}$ low flow were 60 days from Bowie to the confluence of Western Branch and 64 days from the mouth of Western Branch to the confluence of Hall Creek with the Patuxent River. Because the excursion times are so much longer than the period for which flow was averaged, the use of this flow and these excursion times to estimate pollutant decay and subsequent loadings to the estuary is unrealistic. A more reasonable method for calculating a "normal" load to the estuary is demonstrated below using BOD as an example.

Consider Figure 3.4-4, which shows the relative frequency of the seven-day moving average of mean daily flows of the Patuxent River at Laurel, Maryland. If it is assumed that the frequency of seven-day moving average flows at the head of the estuary has the same probability mass function (pmf) as those occurring at Laurel, then the expected seven-day average flow at the head of the estuary can be found by scaling the class width of the histogram and finding the expected value of the rescaled pmf. The expected value is given by

$$E(x) = \sum_i \bar{x}_i f(x)_i$$

where $\bar{x}_i$ = designates the midpoint of the class interval, and

$f(x)_i$ = is the relative frequency in class "i".

The class interval is rescaled by areal proportioning using drainage area above each location which makes the new class interval

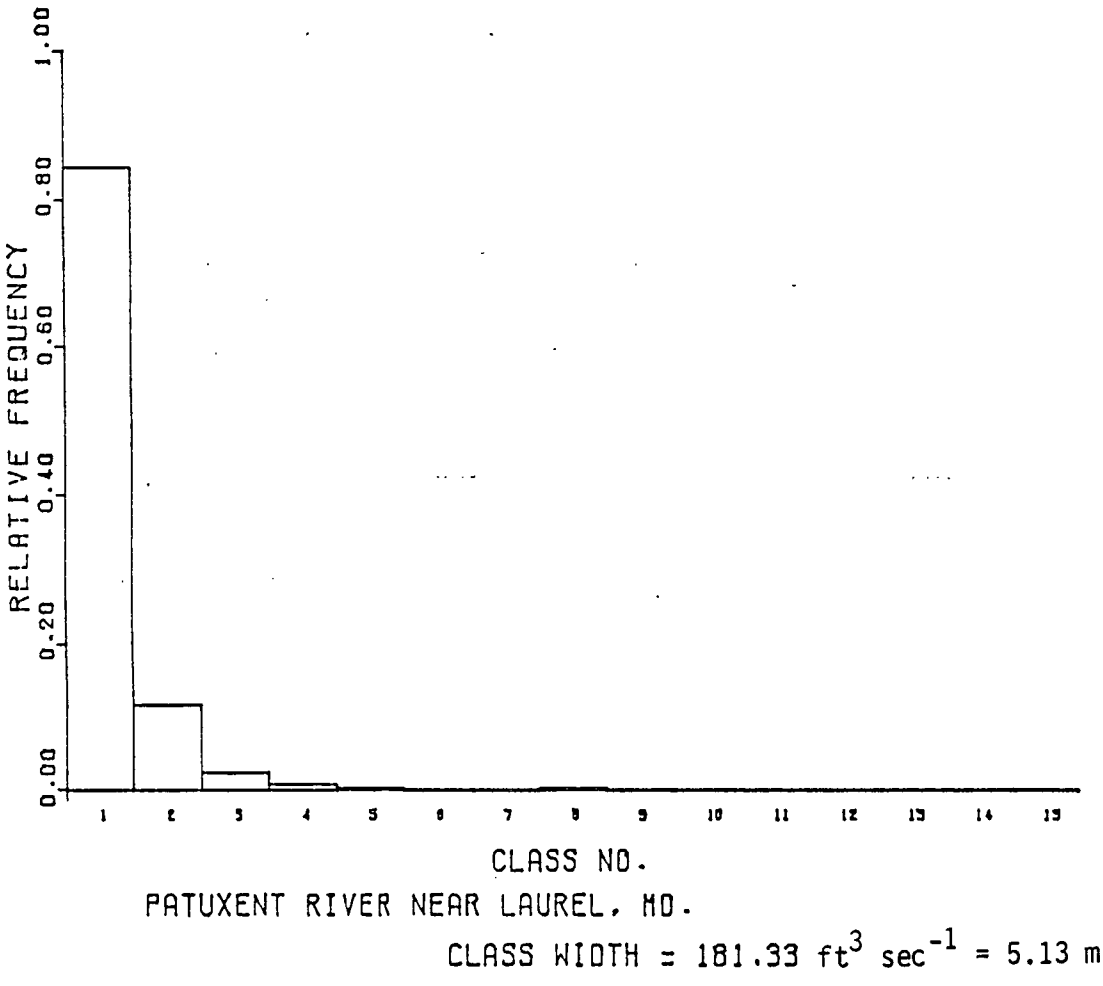

Figure 3.4-4. Frequency histogram of 7-day moving average flows.

$$182 \frac{ft^3}{Sec} \times \frac{620\ mi^2}{132\ mi^2} = 855\ ft^3/sec$$

where 620 mi^2 = the drainage area above the Hall Creek transect, and

132 mi^2 = the area above the Laurel gage.

The expected value of flow is 573 ft^3/sec or 16.23 m^3/sec. Using this flow and dividing by the average of the Bowie and the Hall Creek cross sections (775 m^2) gives an estimate of the average velocity in the tidal fresh water section of 0.021 m sec^{-1}. Using this velocity and the length of the section givens the "expected excursion time of 20.7 days. Using a first order decay rate of 0.1/day and a travel time of 20.7 days gives an ultimate biochemical oxygen demand of 4 mgl^{-1} at the head of the estuary. This, in a sense, is the flow averaged concentration of BOD_u that will occur at that location. This value is substantially greater than the value predicted using the $7Q_{10}$ flow but not large enough to adversely impact dissolved oxygen levels in the estuary.

Concentrations of total nitrogen and total phosphorus were estimated at the head of the estuary for the $7Q_{10}$ low flow condition. These predicted concentrations are solely the result of treatment plant effluent discharges in the upper basin. Because total nitrogen and total phosphorus are treated conservatively, they are distributed as the fraction of fresh water in the estuary. Figures 3.4-5 and 3.4-6 compare predicted total nitrogen and total phosphorus to observed data collected by the Maryland Department of Natural Resources on 27 September 1979. On this date, the flow at the Bowie gage was 0.71 $m^3\ sec^{-1}$. The $7Q_{10}$ flow used in the analysis was 0.53 $m^3\ sec^{-1}$.

The most obvious disparity between predicted and observed values is the decrease in total nitrogen and total phosphorus concentrations upstream of the observed location of the dilution gradient. This dilution

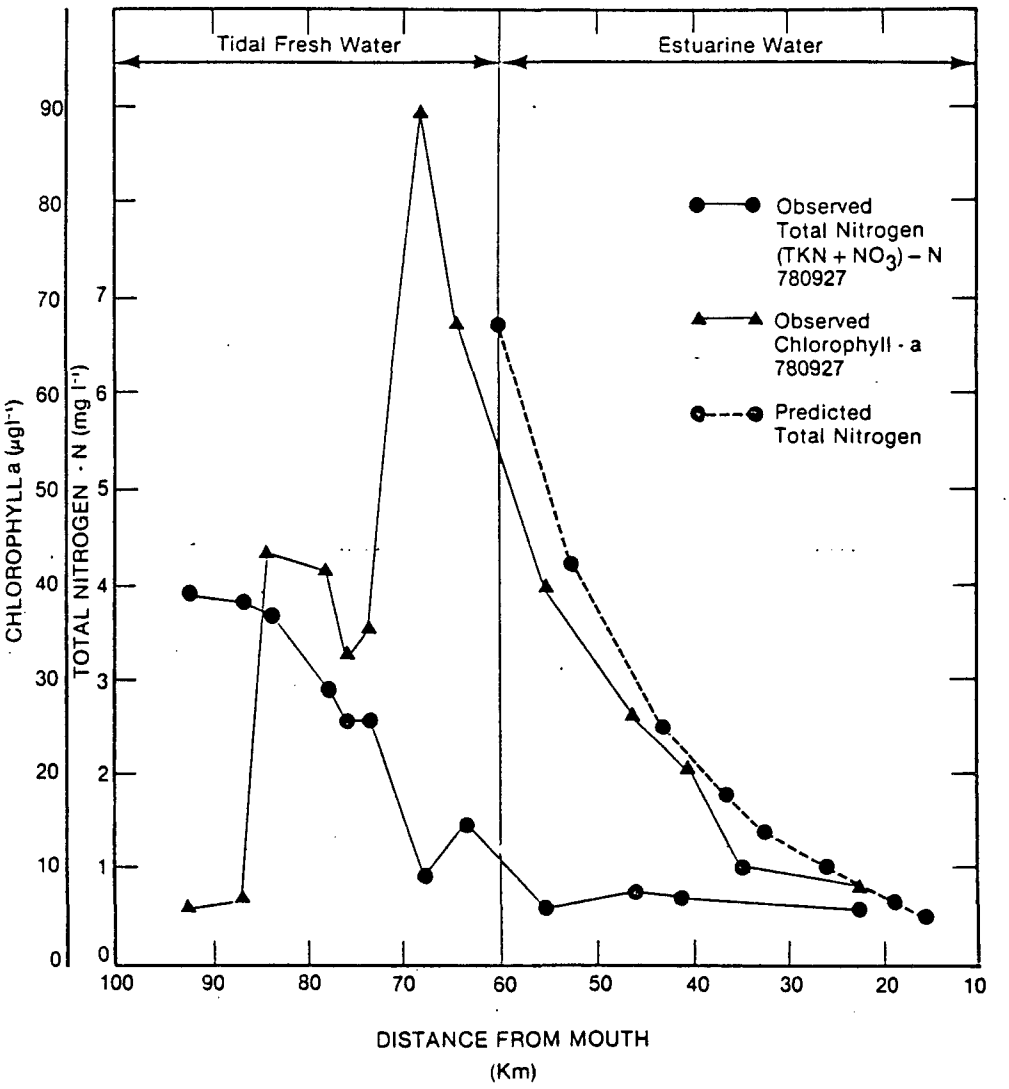

Figure 3.4-5. Predicted and observed total nitrogen and observed chlorophyll-a in the Patuxent River, September 27, 1978.

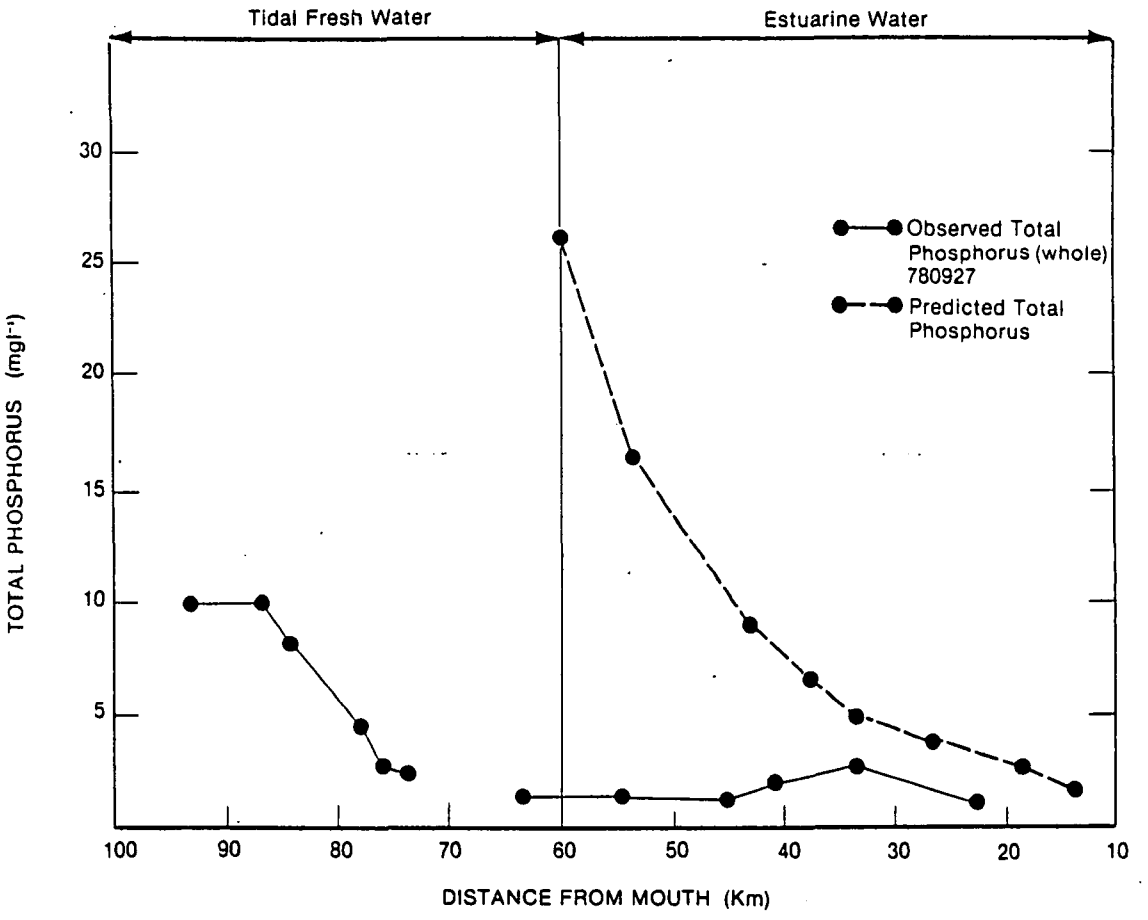

Figure 3.4-6. Predicted and observed total phosphorus in the Patuxent River, September 27, 1978.

should occur where salt water begins to intrude on the fresh water outflow from the watershed. This indicates that total nitrogen and phosphorus are not acting conservatively as the fraction of fresh water method assumes. The reason for this behavior may be copious algal production at the interface of the tidal fresh and estuarine waters as evidenced by elevated chlorophyll-a concentrations there. (See Figure 3.4-5.) Nitrate nitrogen decreases rapidly in this zone but total Kjeldahl nitrogen (whole sample) increases only slightly. As a result total nitrogen (shown here as TKN (whole) + NO_3 as N) decreases drastically. Macrophyte uptake or phytoplankton utilization followed by settling may account for the overall total nitrogen reduction in the waters. Total phosphorus likewise decreases in this segment of the river.

The zone in which this action occurs probably corresponds to the null zone described by Officer (1976) as the zone at which riverine type flow occurs up the estuary and estuarine or density gradient flow occurs down the estuary. This zone is also the area of longest particle residence time and, consequently, the zone in which the phytoplankton crop and turbidity usually achieve their maximums.

In Figure 3.4-7 the peak chlorophyll-a concentration has moved downstream approximately 14 km in comparison with the September study. This chlorophyll-a data was taken earlier in the summer (July 19, 1978) at a higher upstream flow rate. Areally extrapolated fresh water flow at the Hall Creek transect was 11.84 m^3 sec^{-1} versus 4.17 m^3 sec^{-1} at the same location on September 26, 1978. Predicted total nitrogen levels are much closer to observed values for this date. Total nitrogen behaves more conservatively and consequently the fraction of fresh water method yields better estimates. The same is true for the total phosphorus predictions in Figure 3.4-8.

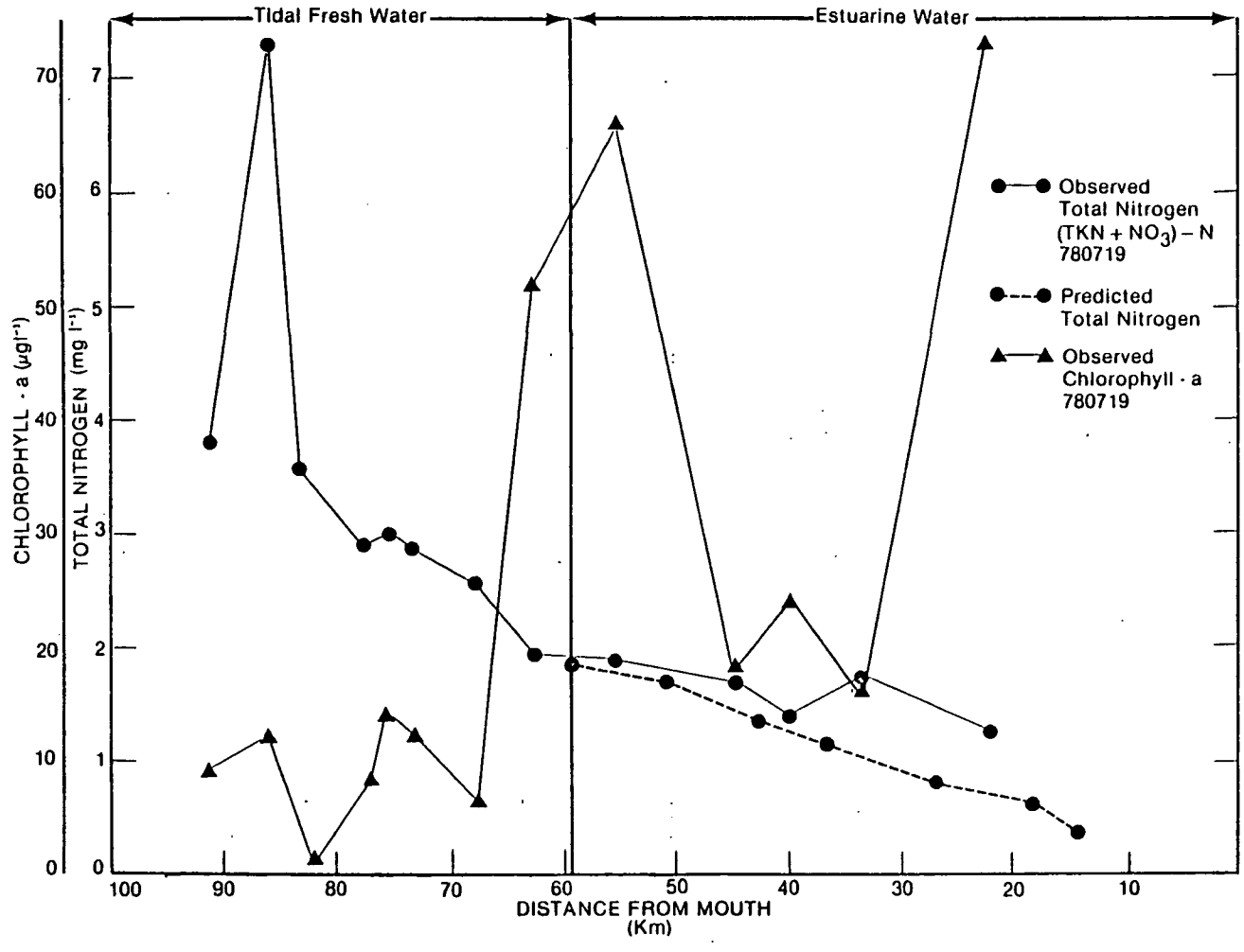

Figure 3.4-7. Observed and predicted total nitrogen and observed chlorophyll-a in the Patuxent River, July 19, 1978.

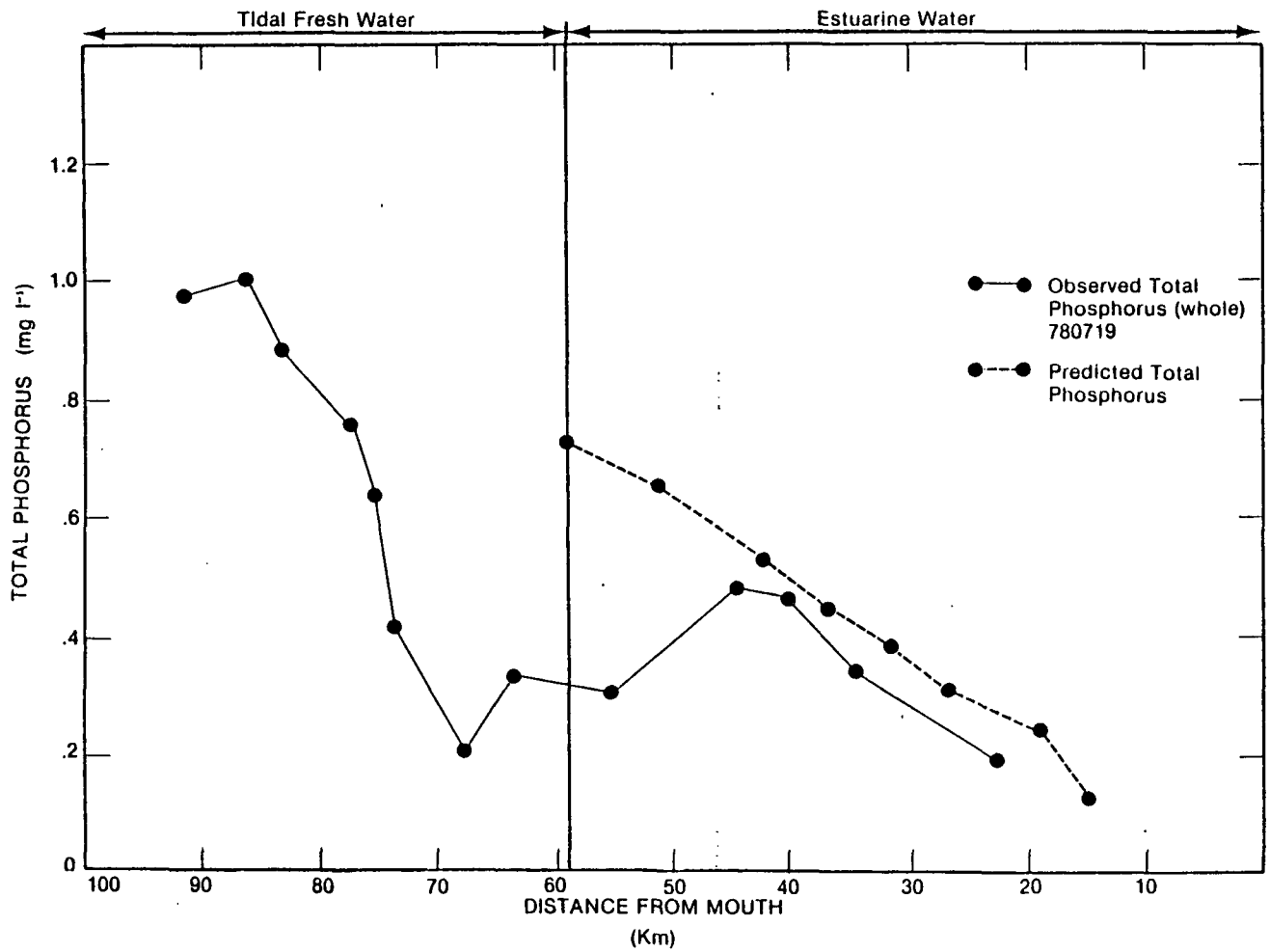

Figure 3.4-8. Observed and predicted total phosphorus in the Patuxent River, 19 July 1978.

3.4.4.2.2 High Flow

There were essentially no observed water quality data available at a flow rate comparable to that used in the Patuxent River high flow analysis. Therefore, high flow analyses were only done for total nitrogen and total phosphorus in order to draw conclusions concerning eutrophication. (See section 3.4.4.3.)

The total nitrogen and total phosphorus loads provided by the Midwest Research Institute's nonpoint source calculator were divided into two groups:

- Loads entering the estuary with the upstream river flow, and
- Loads entering the estuary laterally from adjacent land areas.

The former were distributed according to the fraction of fresh water in each high flow modified tidal prism segment. The latter were distributed through use of the distribution coefficient matrix. The nonpoint loads due to lateral inflows were provided as a single value. This value was proportioned to each modified tidal prism segment by dividing the length of the segment by the total length of the estuary. Resultant loads were assumed to be discrete point loads entering at the center of each segment.

The Patuxent River estuary under the high flow scenario was divided into seven segments. The segment characteristics and the related information needed to perform the analysis are given in Table 3.4-10. The hypothetical flow rate through the segment is the riverine flow per tidal cycle divided by the fraction of fresh water in the segment (Officer, 1976). The approximate net fresh water flow rate past Hall Creek is 83 m^3 sec^{-1} for this segmentation scheme or 3.6×10^6 m^3 per tidal cycle. Salinity data for high flow was obtained

TABLE 3.4-10. CHARACTERISTIC DATA FOR THE PATUXENT RIVER ESTUARY AT HIGH FLOW

Segment	Length (km)	Hypothetical Flow Through Segment (m^3 tidal $cycle^{-1}$)	Salinity (ppt)	Fraction of Fresh Water (-)
0	15.4	4.32×10^6	1.6	0.83
1	9.6	5.78×10^6	3.6	0.62
2	5.9	6.52×10^6	4.3	0.55
3	3.9	1.24×10^7	6.7	0.29
4	4.1	1.63×10^7	7.4	0.22
5	3.9	1.79×10^7	7.6	0.18
Total	46.6	8.3×10^7	$S_b = 9.5$	

from STORET and was measured at a flow rate of only 15.9 m^3 sec^{-1} at the same location. Thus, concentrations predicted will be lower than what would be predicted if coincidental salinity and flow data were available.

The distribution coefficient matrix, necessary for treatment of lateral loads, was constructed from the salinity and fraction of fresh water data in Table 3.4-10 and is shown in Table 3.4-11. As in the Chester River example, the entries in the upper right hand corner are computed by dividing the salinity in the i^{th} segment by the salinity in the segment of discharge. For example, entry $C_{2,4}$ = 0.58 is calculated by dividing the salinity in segment 2 by the salinity in segment 4 (4.3/7.4 = 0.58). Similarly, the entries in the lower left hand corner are determined by ratios of fraction of fresh water.

Total nitrogen is used to provide a comprehensive example. The load carried into the estuary in the riverine flow is 1.18 x 10^5 kg-N. This is distributed by the fraction of fresh water divided by the river flow rate per tidal cycle to give a concentration and is shown as Column 2, Table 3.4-12. Column 3 is the fraction of the total length of the estuary that is attributed to each segment. This column multiplied by the total lateral load into the estuary (4.22 x 10^4 kg) and divided by the hypothetical flow rate in each segment gives the initial concentration due to lateral loads in each segment (Column 4). These loads are multiplied by the diagonal entries of unity on the distribution coefficient matrix. These are then multiplied by the coefficients in each column to obtain the concentration distribution in the estuary (Columns 5). These entries are summed for each row over all columns and added to the river borne loads in each segment (Column 2) to give Column 6, the total steady state concentration in each segment in mg ℓ^{-1}. The average concentration in the estuary also shown in Table 3.4-11 is found by computing a flow weighted average concentration using each segment.

TABLE 3.4-11. DISTRIBUTION COEFFICIENT MATRIX FOR THE PATUXENT RIVER HIGH FLOW

		Segment Number						
		0	1	2	3	4	5	6
Segment Number	0	1	0.44	0.37	0.24	0.22	0.21	0.21
	1	0.75	1	0.84	0.54	0.49	0.47	0.46
	2	0.66	0.39	1	0.64	0.58	0.57	0.55
	3	0.35	0.47	0.53	1	0.91	0.88	0.86
	4	0.27	0.35	0.40	0.76	1	0.97	0.95
	5	0.24	0.32	0.36	0.69	0.91	1	0.97
	6	0.22	0.29	0.33	0.62	0.82	0.90	1

TABLE 3.4-12. TOTAL NITROGEN CALCULATION IN THE PATUXENT RIVER ESTUARY FOR HIGH FLOW

(1) Segment	(2) Contribution from Riverine Flow (mg ℓ^{-1})	(3)	(4)	(5) 0	1	2	3	4	5	6	(6) Total Concentration (mg ℓ^{-1})
0	27.2	0.33	3.2	3.2	0.7	0.3	0.1	0.1	0.0	0.0	31.6
1	20.3	0.21	1.5	2.4	1.5	0.7	0.1	0.1	0.1	0.1	25.3
2	18.0	0.13	0.83	2.1	1.3	0.83	0.2	0.1	0.1	0.1	22.7
3	9.5	0.08	0.27	1.1	0.7	0.4	0.27	0.2	0.2	0.1	12.5
4	7.2	0.09	0.23	0.9	6.5	0.3	0.2	0.23	0.2	0.2	9.7
5	6.6	0.08	0.19	0.8	0.5	0.3	0.2	0.2	0.19	0.2	7.8
6	5.9	0.08	0.17	0.7	0.4	0.3	0.2	0.2	0.2	0.17	7.1
										AVERAGE	12.0

Results of the calculations for total nitrogen and total phosphorus are shown in Table 3.4-13. The upper limit numbers assume that all of the storm nonpoint source loads enter during a tidal cycle and remain at that steady-state loading rate during succeeding tidal cycles. The lower limit concentrations assume that the storm loads enter the estuary equally distributed over the seven-day high flow period. This is equivalent to assuming that the total storm load is introduced into the estuary approximately every 14 tidal cycles. The true concentration should lie between these limiting values.

The impact of urban nonpoint source runoff contributions from the towns of Laurel, Bowie, and Columbia on total nitrogen and total phosphorus concentrations in the Patuxent River estuary was also determined. As in the Sandusky analysis, the urban loads were supplied on an annual basis. Therefore, two cases were investigated. The first assumed that urban nonpoint source runoff entered the river system distributed evenly throughout the year. This amounted to loads of 406 kg of total N and 194 kg of total P being supplied to the stream in the high flow runoff event. The alternative assumption was that all of the total annual load was washed off by a single high flow event. Under this assumption loads to the estuary were 21182 kg of total N and 10091 kg of total P per event. These quantities were added to the riverine load and distributed by the fraction of fresh water method in the estuary. The resultant concentrations are given in Table 3.4-14 for the case that all the annual urban load is released in a single high flow event. The addition of urban total N and total P loads under the other assumption had no impact on estuarine water quality.

Comparison of the mean estuarine concentrations indicates that even for this "worst case" assumption the urban nonpoint source loads have only a small effect on water quality in the estuary. The mean total nitrogen concentration increased 12% which the total phosphorus mean concentration increased by 36%. The N:P ratio using only

TABLE 3.4-13. UPPER AND LOWER LIMIT TOTAL NITROGEN AND TOTAL PHOSPHORUS CONCENTRATIONS IN THE PATUXENT RIVER DUE TO NON-URBAN NPS LOADING

Segment	Upper Limit Total N (mg ℓ^{-1})	Lower Limit Total N (mg ℓ^{-1})	Upper Limit Total P (mg ℓ^{-1})	Lower Limit Total P (mg ℓ^{-1})
0	31.6	2.26	7.1	0.51
1	25.3	1.81	5.4	0.39
2	22.7	1.62	4.8	0.34
3	12.5	0.89	2.5	0.18
4	9.7	0.69	1.9	0.14
5	7.8	0.56	1.6	0.11
6	7.1	0.51	1.4	0.10
Average Estuary Concentration	12.0	0.88	2.5	.18

TABLE 3.4-14. UPPER LIMIT TOTAL NITROGEN AND PHOSPHORUS CONCENTRATIONS IN THE PATUXENT RIVER DUE TO URBAN AND NON-URBAN NPS LOADS

Segment	Total N (mg ℓ^{-1})	Total P (mg ℓ^{-1})
0	36.5	9.4
1	28.9	7.1
2	25.9	6.3
3	14.2	3.3
4	11.0	2.5
5	9.0	2.2
6	8.1	1.9
Average Estuary Concentration	14.1	3.4

non-urban loads (based on predicted values) were 4.8:1. The same ratio computed using both urban and non-urban loads decreased to 4.15:1.

3.4.4.3 Estuarine Eutrophication

The ratios just presented would tend to indicate that as urbanization of the watershed continues, algal growth may become more nitrogen limited. Accompanying this trend is also a seasonal trend in the N:P ratio. Figure 3.4-9 shows N:P ratios for a three-year period from May 1978 to November 1970 taken near the PEPCO Chalk Point Power Plant. The periodic trend is that higher N:P ratios occur in the spring corresponding to periods of high runoff and consequently high nonpoint source loadings. The lower N:P ratios occur during the typical low flow autumn period. Based on predicted total nitrogen and phosphorus for the dates 26 September 1978 and 19 July 1978, this ratio would be 2.60. Therefore, the predicted N and P reflect this seasonal periodicity, low N:P ratios during low flow with higher N:P ratios occurring during high flows.

N:P ratios were computed from the Maryland DNR data for the low flow dates mentioned above. The ratios were calculated for several locations in the estuary and averaged to give values of 5.85 and 4.79, respectively. These values are roughly twice the predicted N:P ratio but are still in the region that one could conclude that algal growth is nitrogen limited. Longitudinal variation in the N:P ratios showed no particular trend.

3.5 DEMONSTRATION EXAMPLE: THE WARE RIVER

The Ware River is the smallest of the watershed-river systems used to demonstrate Midwest Research Institute's nonpoint source calculator and Tetra Tech's non-designated 208 screening methodology. Because of its small size, a unique feature exists here not found in the other systems.

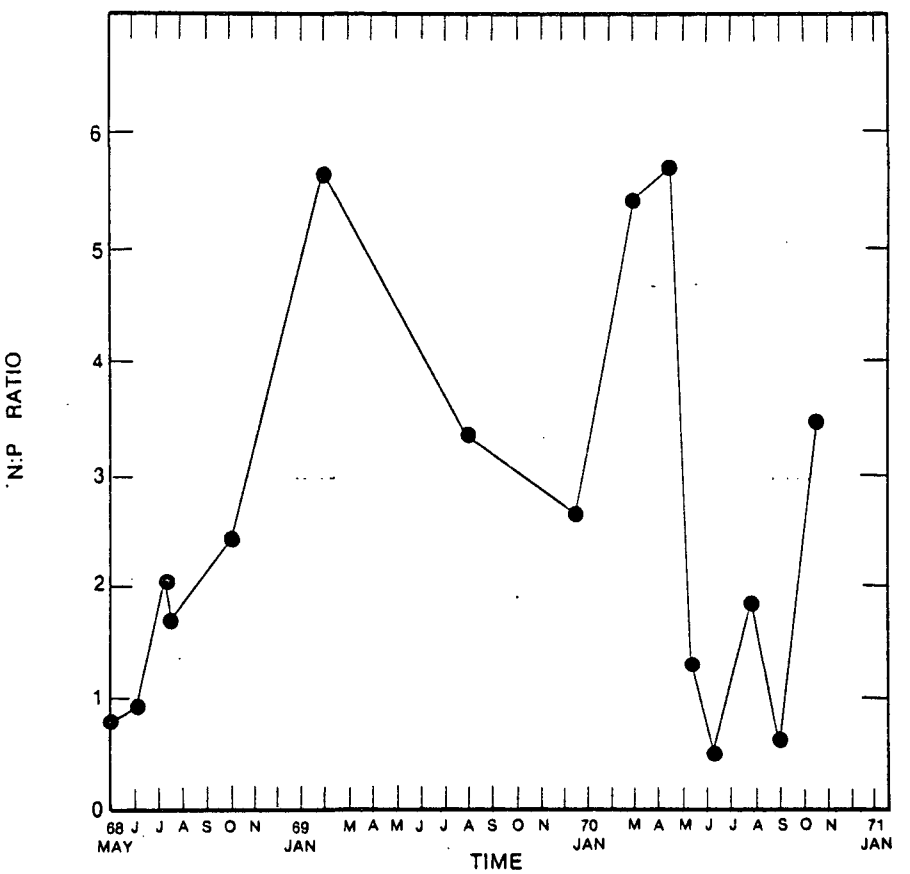

Figure 3.4-9. Seasonal trend of the N:P ratio in the Patuxent River.

The Ware River is composed of several creeks that drain through marshy land into an estuary that is tributary to the Chesapeake Bay. (See Figure 3.1-4.) During high flows the salinity gradient exists only in the main estuary. However, during dry periods, the salinity gradient moves up into the tidal portions of the tributary creeks, and the salinity in the main estuary becomes essentially that of the Chesapeake Bay. This situation affords the opportunity to apply the estuarine methods to a very small estuary ($V_{MLT} \simeq 4.66 \times 10^4$ m^3).

3.5.1 Data Collection

The USGS provided 7½ minute series topographic maps, as well as flow data and stage-discharge curves for the one existing gage in the basin, Beaver Dam Swamp near Ark, Virginia. Ten years of flow data were used to estimate the $7Q_{10}$ flow for low flow analysis.

Water quality data were available from the EPA STORET system, although they were of marginal value for this demonstration. Of greater use were data being collected in a monitoring program conducted by the Virginia Institute of Marine Sciences. Additionally, the Tidewater Regional Office of the Virginia Water Control Board provided some useful data in the form of two documents relating the results of two special water quality studies carried out in Fox Mill Run (a tributary to the Ware River) during 1977.

3.5.2 Data Reduction and Supplementation

The available flow information at the USGS gage was used to evaluate $7Q_{10}$ flow. However, no salinity data in the estuary were available to coincide with this low flow (0.003 m^3 sec^{-1}). Therefore, a water quality analysis corresponding to $7Q_{10}$ flow conditions was not done for this estuary.

Bathymetric information and mean tidal ranges were obtained from USGS topographic maps of the basin. From this information, estuarine cross sections at various transects were determined at mean high and mean low tides. This information was subsequently used to evaluate estuarine flushing times and to determine the distribution of pollutants in the system. The data are shown in Table 3.5-1.

Some hydraulic data for the estuarine analysis of Fox Mill Run were given in the special studies report of the Water Control Board (Virginia Water Control Board, 1977). Using these data, together with information from topographic maps, this creek was hydraulically characterized from the outfall of the Gloucester Sewage Treatment Plant to its mouth. Where insufficient data existed, cross-sectional areas for the creek were determined by linear interpolation.

3.5.3 Estuarine Analysis of Fox Mill Run

The only permitted discharger in the Ware River basin is the Gloucester Sewage Treatment Plant, which is located on Fox Mill Run approximately 4.5 km upstream of the mouth of the creek. The tidal portion of the creek begins about 0.5 km downstream from the outfall.

On August 10 and 11, 1977, flow and water quality samples were taken from the plant effluent and at several stations in the creek, one of which was upstream of the outfall. These data were collected by the Tidewater Regional Office of the Virginia Water Control Board. The observed data were compared to concentrations predicted by the estuarine screening methods. The application and results are described below.

The quality of the plant effluent and the quality of the natural waters upstream of the outfall were tabulated. Table 3.5-2 shows these data. Using this information, flow-averaged concentrations of quality

TABLE 3.5-1. WARE RIVER ESTUARINE HYDRAULIC DATA

Location of Transect	Distance from Mouth (km)	MLT Cross Section (m^2)	MHT Cross Section (m^2)	Width (m)	Hydraulic Depth[a] (m)
Ware Neck Pt.	0.0	10,038	15,063	3,383	3.71
Windmill Pt.	4.0	4,129	5,289	1,585	2.97
Jarvis Pt.	7.3	2,192	3,017	1,128	2.31
Horse	8.9	878	1,279	549	1.97
Hall	10.4	325	637	427	1.12
Confluence of Beaver Dam Swamp and Fox Mill Run	11.1	362	942	792	0.67

[a] Computed from the tidally averaged cross-sectional area.

TABLE 3.5-2. SEWAGE TREATMENT EFFLUENT AND NATURAL WATER QUALITY IN FOX MILL RUN AUGUST 10-11, 1977

	Gloucester STP Effluent	Fox Mill Run (Upstream of Effluent Outfall)
Flow (m^3 sec^{-1})	0.006	.024
Temperature (^oC)	30.0	29.5
$CBOD_u$ (mg ℓ^{-1})	45.3	6.3[a]
$NBOD_u$ (mg ℓ^{-1})	66.3[c] (119)[b]	1.83[c]
Total N (mg ℓ^{-1}) as N	19.9[d]	0.46[d]
Total P (mg ℓ^{-1}) as P	10.0	0.10
Total Suspended Solids (mg ℓ^{-1})	27.6	4.5
$NO_2 + NO_3$ (mg ℓ^{-1}) as N	5.4	0.06

[a]Value reported is BOD_{30} with suppressed nitrification.

[b]Estimated by type of treatment facility.

[c]Derived from total Kjeldahl nitrogen data.

[d]Sum of TKN, NO_2 and NO_3 (as N)

parameters were calculated and used as inputs to the head of the tidal portion of the Fox Mill Run estuary.

Modified tidal prism segmentation was used to determine the distribution of both conservative and nonconservative substances in this small estuary. The tidal portion of Fox Mill Run was described by a series of four estuarine segments with a fresh water inflow at its head of 1.32×10^3 m^3 per tidal cycle. Table 3.5-3 shows the data required to perform the estuarine analyses for Fox Mill Run. The distances given are measured from the mouth of the creek to the center of each segment. Salinities were interpolated from observed salinity profiles of August 10-11, 1977 and represent the average profile over several tidal cycles. Fractions of fresh water values were computed, using a background salinity of 20 ppt (Lippson, 1973). Exchange ratios (r_i) were computed as the inverse of the flushing times for each individual segment. (Flushing times produced by the modified tidal prism method and the fraction of fresh water method compared very favorably, being 5.2 tidal cycles and 5.3 tidal cycles, respectively.) Two sets of B_i (decay correction terms) were computed for the estuary using the above exchange ratios. One set was calculated using a high deoxygenation rate (0.8 day^{-1} at 20°C) and the other using a low rate (0.1 day^{-1} at 20°C). These rates were corrected for temperature. The average water temperature over the study period was 29.5°C with no appreciable longitudinal variation.

In Figure 3.5-1 the observed $CBOD_{30}$ with suppressed nitrification are plotted against three predicted $CBOD_u$ profiles. The two lower predicted profiles were computed using average plant effluent characteristics from January 1978 to December 1979. The upper predicted profile was computed using a $CBOD_u$ concentration of 74 mg ℓ^{-1} which represents the average of the effluent $CBOD_{30}$ measured on 10 and 11 August 1979.

The figure leads to two important conclusions. First, the difference in decay coefficients between the lower two curves to greater

TABLE 3.5-3. DATA FOR ESTUARINE ANALYSIS OF FOX MILL RUN BY MODIFIED TIDAL PRISM METHOD

Segment	Distance from Mouth (km)	S_i (ppt)	f_i (-)	r_i (tidal cycles $^{-1}$)	B_i (low decay)	B_i (high decay)
0	3.72	3.5	0.83	0.76	0.98	0.87
1	3.20	8.6	0.57	0.83	0.98	0.91
2	2.36	13.4	0.33	0.71	0.97	0.84
3	1.08	17.8	0.11	0.77	0.98	0.88

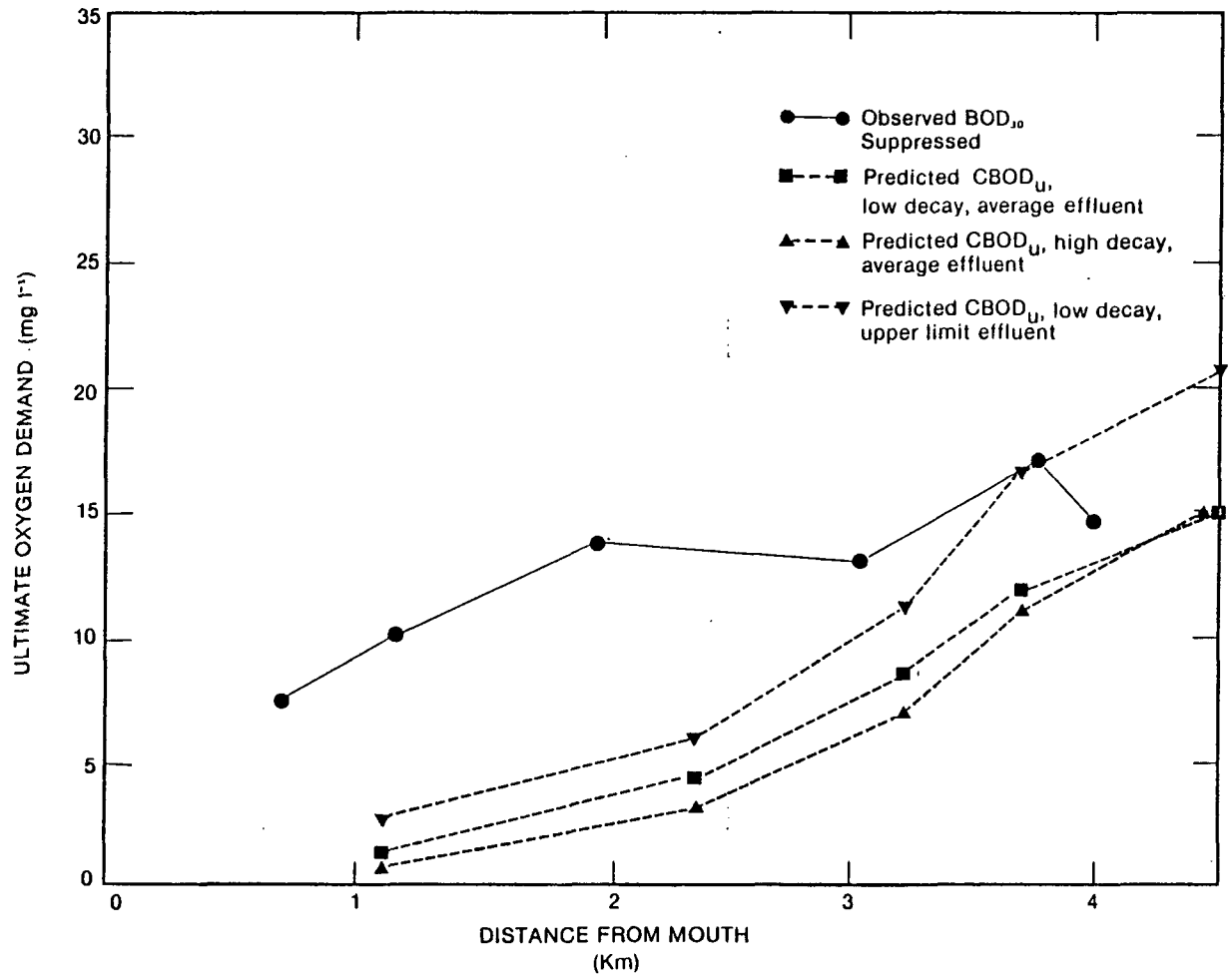

Figure 3.5-1. Predicted and observed $CBOD_u$ in Fox Mill Run.

than an order of magnitude, but the effects of decay compared to the effects of dilution even in this small estuary are minor. Second, it appears that the modified tidal prism method, using the method of Officer (1976) to decay the nonconservative pollutants, attenuates them too quickly. It is possible that another source of CBOD enters the stream between kilometers two and three causing the predicted and observed profiles to diverge. Contamination from replacement waters could partially explain the high observed values at the estuary mouth. However, the observed concentrations increase in the upestuary direction supporting the postulate that an unidentified source is contributing CBOD. In fact, a stream fed by a small pond does enter Fox Mill Run between kilometers two and three.

Treating total nitrogen as a conservative material, levels were predicted in the Fox Mill Run estuary using the fraction of fresh water method and the segmentation scheme in Table 3.5-3. Figure 3.5-2 shows the predicted distribution versus observed data. The observed data represent the sum of total Kjeldahl nitrogen and nitrite- and nitrate-nitrogen expressed as N. The two profiles compare favorably with the exception of the discrepancies at the head and mouth of the estuary. Because of the good reproduction of observed values everywhere else, the tendency is to believe that these deviations represent sampling errors.

Using the predicted concentrations in segment 3, the loads to the Ware River estuary can be calculated by multiplying these concentrations by the effective downestuary transport rate. The following low flow loads per tidal cycle result:

- Total nitrogen, 5.9 kg
- Total phosphorus, 2.7 kg and
- Ultimate oxygen demand, 51.8 to 45.4 kg. (The range is determined by the choice of decay coefficient for BOD.)

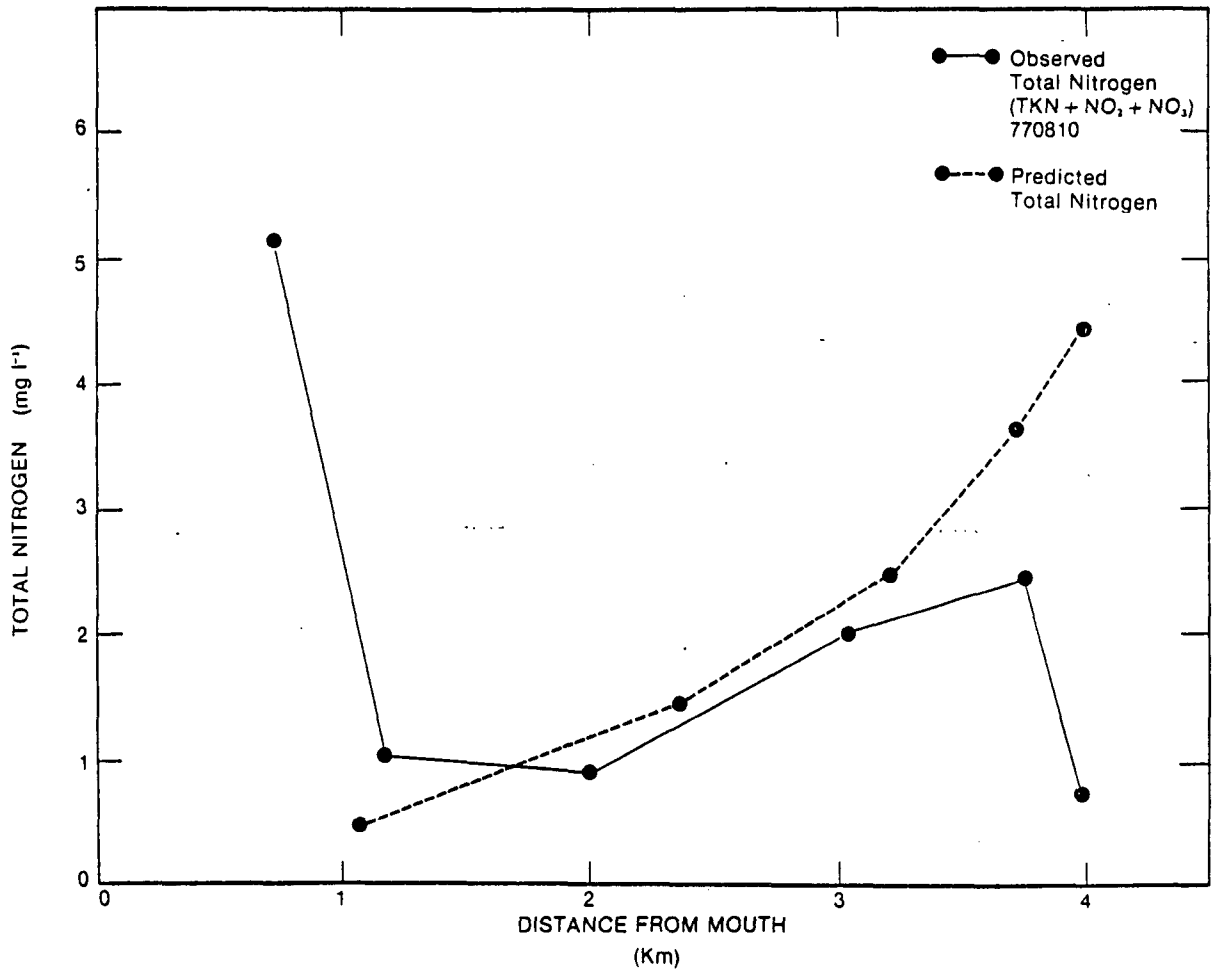

Figure 3.5-2. Predicted and observed total nitrogen in Fox Mill Run.

3.5.4 Ware River Estuary Flushing Times

Both the tidal prism and modified tidal prism methods were used to determine flushing times for the Ware River estuary. The flushing time produced by the tidal prism method was 4.3 tidal cycles. This result is insensitive to flow rate changes. Using the modified tidal prism method, flushing times of 58.2 and 39.3 tidal cycles were calculated for low and high flow conditions, respectively. It was shown in the Chester River example that the relationship between mean low tide volume and the ratio of low flow modified tidal prism to tidal prism flushing times for the Ware River was consistent with the results found in the Chester River. The small difference in these two flushing times indicates that advective flow has only minor impact on the flushing processes in the estuary.

3.5.5 Pollutant Distribution in the Ware River

A comparison of the loads of total nitrogen and total phosphorus calculated during low flow with those loads predicted during a typical high flow event using the nonpoint calculator shows that loadings occurring during low flows are almost negligible. For instance, Fox Mill Run contributes approximately 600 kg of total nitrogen and 80 kg of total phosphorus (assuming a delivery ratio of 0.1) to the Ware Estuary during an everage high flow event. This load can be assumed to enter the estuary in one tidal cycle. The calculated loads during low flow were only 5.9 and 2.7 kg of total nitrogen and total phosphorus per tidal cycle respectively. (See section 3.5.3.) Because the concentrations of total nitrogen and phosphorus during low flows were small compared to the high flow loads, they were not considered in this analysis. High flow analyses only were performed on the Ware River estuary for the sediment, total nitrogen, total phosphorus, and BOD_5 parameters. These analyses were performed assuming that the total "average" storm load enters the estuary on each tidal cycle giving upper limits for the constituent concentrations

in each estuarine segment. Loads were provided by the nonpoint source calculator. A delivery ratio of 0.1 was used in all subsequent calculations.

From Figure 3.5-3 it does not appear that the prediction of sediment distribution in the Ware estuary is particularly good. It has been pointed out previously that the distribution shown is an upper limit because of the assumptions that the nonpoint source loads are steady and continuous and that settling of the suspended material is negligible. It should be noted, however, that the large concentrations predicted in the upper estuary are associated with segments having small volumes. The volumetrically weighted mean sediment concentration (also shown in Figure 3.5-3) is not unreasonably greater than the oberved profile. The volumetric mean is actually calculated as a weighted average with the weights in each segment equal to the hypothetical flow rate (R/f_i) in each segment when R is the river flow (m^3 tidal $cycle^{-1}$) and f_i is the fraction of fresh water in the segment.

The total phosphorus distribution (Figure 3.5-4) closely resembles the observed total phosphorus profile throughout most of the estuary. The volume-weighted mean of 0.05 mg ℓ^{-1} is representative of actual total phosphorus concentrations in the estuary during and immediately following high flows.

Predictions for sediment and phosphorus were in general better than predictions for total nitrogen and BOD_5. Figure 3.5-5 shows total nitrogen (TKN + NO_2 + NO_3) and BOD_5 observed in the estuary at high water slack on May 15, 1979 three days after a major streamflow event. The volumetric mean of total N and BOD_5 (low decay) are also illustrated. The BOD_5 profile was computed using a decay rate of 0.1/day (20°C) adjusted to the mean water temperature of 23.1°C on that date. Although the prediction of the BOD_5 and total nitrogen distributions were poor, the mean estuarine concentration is reasonably predicted by the estuary screening techniques. The trend observed in the phosphorus, nitrogen,

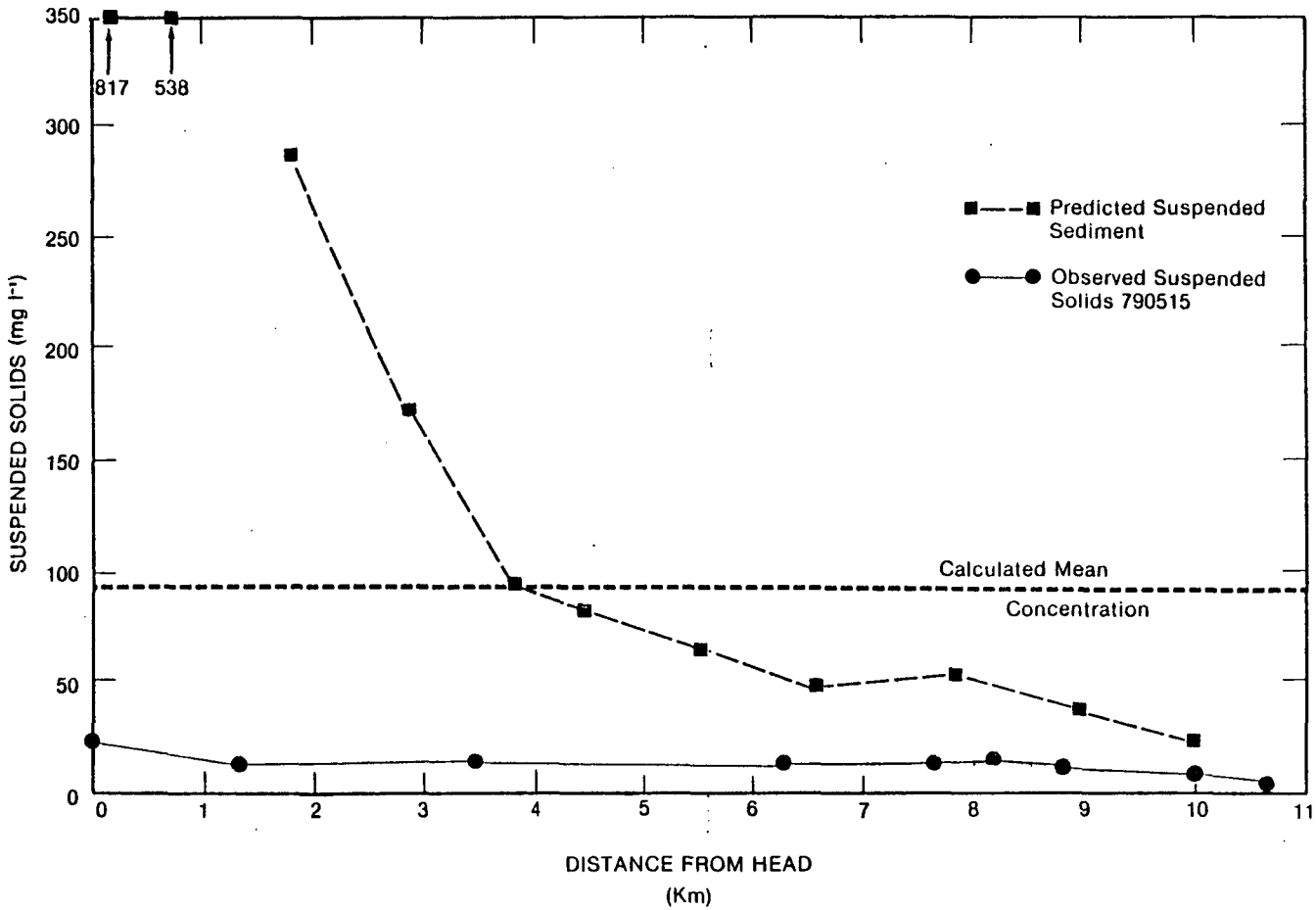

Figure 3.5-3. Suspended sediment distribution in the Ware River during high flow.

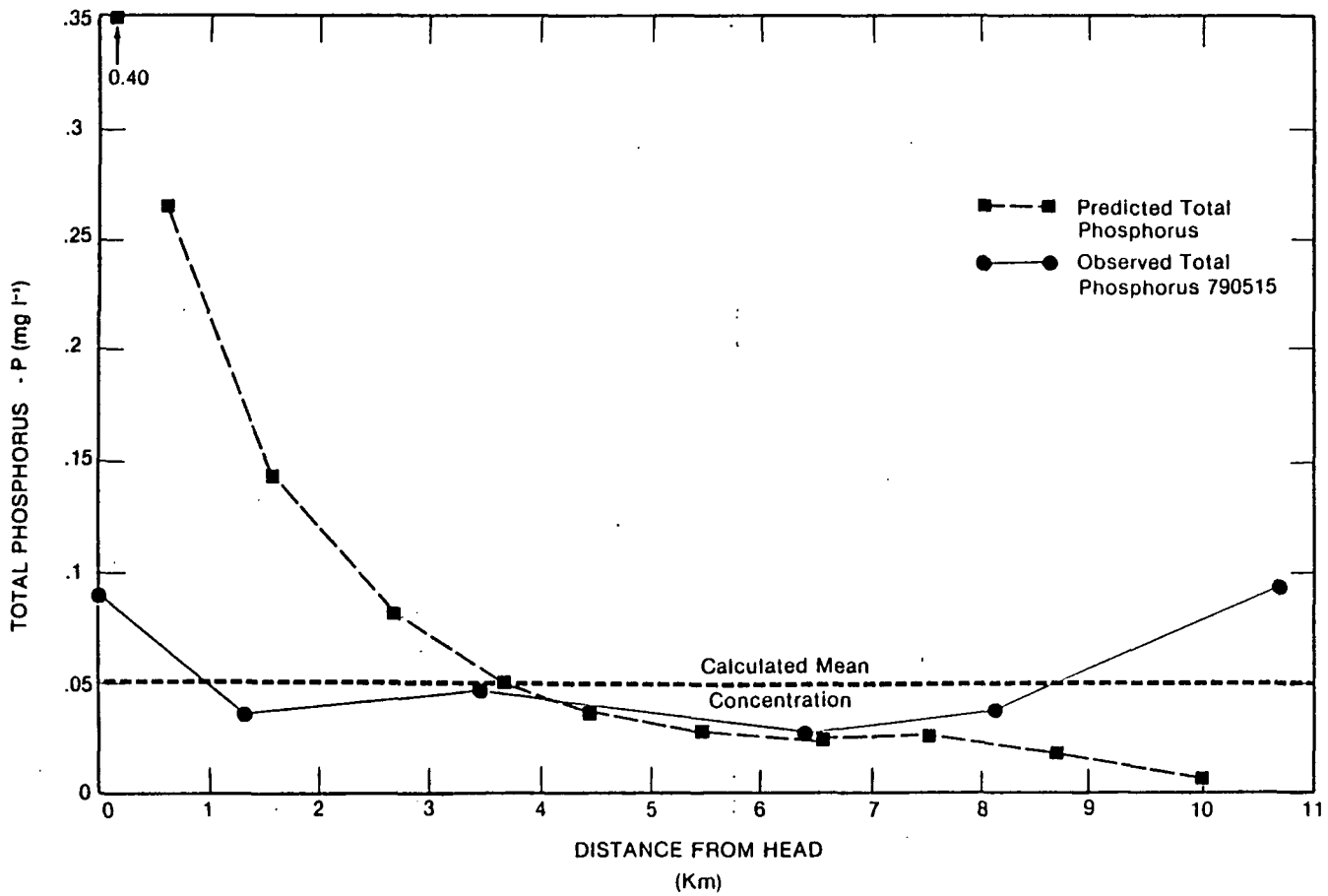

Figure 3.5-4. Total phosphorus distribution in the Ware River during high flow.

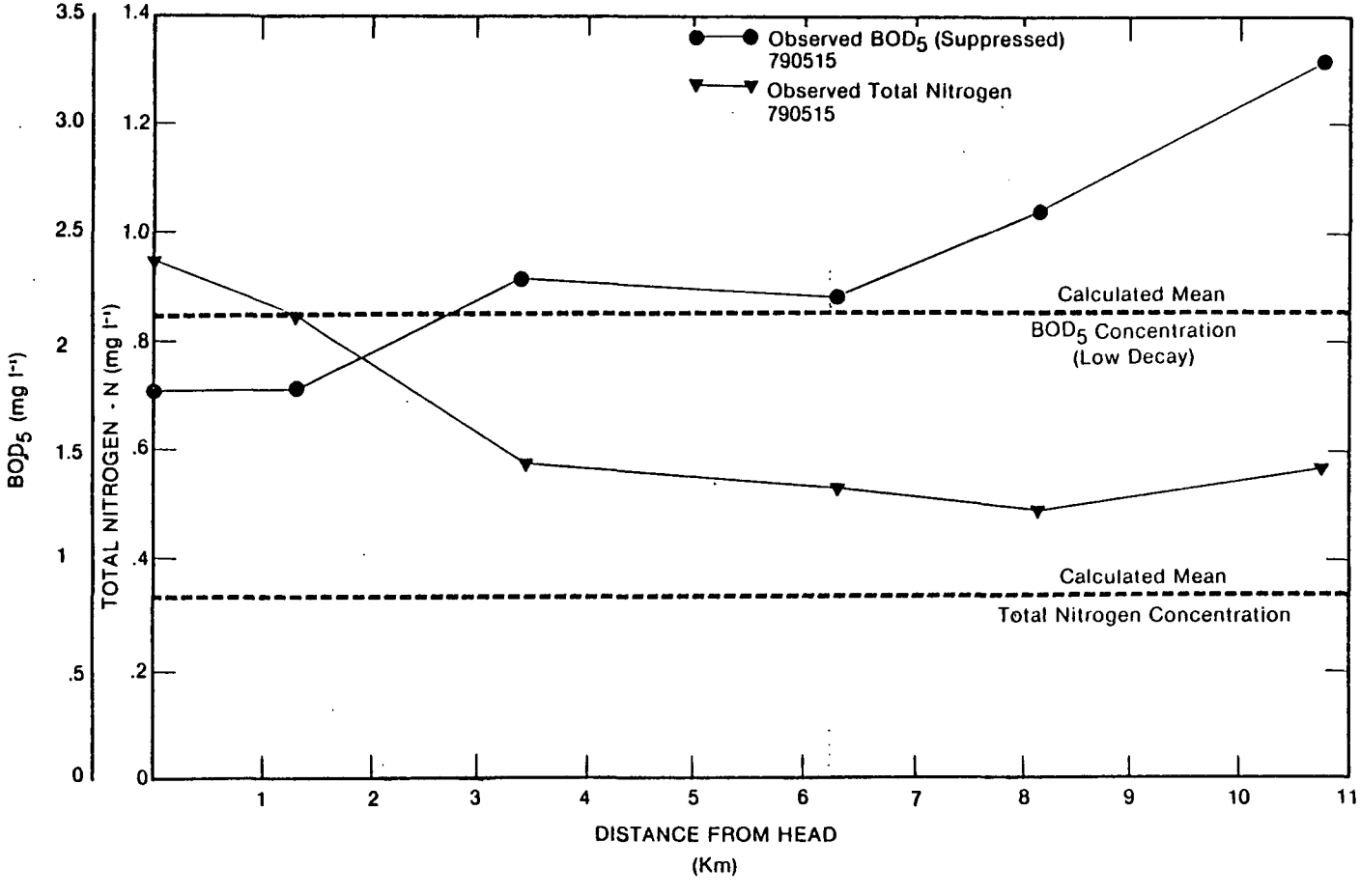

Figure 3.5-5. Observed and predicted total nitrogen and BOD_5 in the Ware River estuary during high flow.

and BOD profiles of an increase in these parameters at the mouth of the estuary is probably due to contamination from the Chesapeake Bay.

3.5.6 Eutrophication

3.5.6.1 Nutrient Limitation

Using observed slack water data collected at biweekly intervals from 11 April to 22 August, 1979, N:P ratios were computed for the Ware River estuary. Several dates were not used because total phosphorus was reported only as less than .10 mg ℓ^{-1}. When a "less than" value appeared infrequently in an otherwise usable data set the upper limit was used in computations. The N:P ratios using total nitrogen (TKN (whole) + NO_2 + NO_3) as N and total phosphorus (whole) as P were computed for the dates 11 April, 25 April, 9 May, 15 May, 26 July, 8 August and 22 August, 1979. The average N:P ratio for those dates was 10.2. The spring dates gave an average of 11.2, while the summer dates had a mean N:P ratio of 8.73. This indicates a slight seasonal influence in the ratio.

The N:P ratios based on predicted values of total nitrogen and total phosphorus for the high flow scenario was 6.8, which is lower than the observed ratios (recall the low mean total nitrogen predictions). This value might lead to the improper conclusion that nitrogen is limiting.

Based on the low flow loadings to the estuary from Fox Mill Run (5.9 kg - N and 2.7 kg - P per tidal cycle), the N:P ratio in the estuary is 2.2. Using total N and P concentrations of the natural waters (see Table 3.5-2), this ratio is 4.4. Thus, it appears that addition of sewage treatment plant effluent tends to shift the N:P ratio towards nitrogen limitation.

Based on the predicted high flow and low flow N:P ratios there is less seasonality evident in this basin than in the Patuxent. This is because point sources do not dominate water quality during the low flow periods as they do in the Patuxent.

3.5.6.2 Light Limitation

The two parameter light model

$$D_s = \frac{-1n\ (0.1)}{\alpha + \beta x}$$

where

D_s = the Secchi disc depth

α = background extinction coefficient

β = incremental extinction coefficient

x = a water quality constituent

was used to analyze the estuary for light limitation. Suspended solids and chlorophyll-a were used as independent variables. The least squares estimates of the incremental extinction coefficient, β, for both independent variables were found to be negative. The values are -0.008 and -0.056 for solids and chlorophyll-a, respectively. These estimates for β are meaningless since it is not expected that the water column transmits more light at higher concentrations of these parameters. Notice, however, that the coefficients are very close to zero. This is because large values of the independent variables are not found in the data set. Therefore, in this particular data set these variables do not occur in the light limitation range. The regression equation is essentially analyzing background noise; hence, the values are close to zero for the incremental extinction coefficient. This hypothesis is supported in a study done by Thompson et al., 1979. In their work, extinction coefficients were determined for light of different wavelengths in a turbid

coastal inlet. Values of extinction coefficients were determined for light of different wave lengths during the summer and winter season. These ranged from 2.03 for light of 630 mm wave length during the summer to a high of 4.42 for light with a 445 mm wavelength also during the summer season. The α coefficients for the Ware River are 3.5 for chlorophyll-a and 3.4 for suspended solids, and fall within the range reported by Thompson et al., 1979. Thompson et al., 1979 further report that particulates, as opposed to dissolved materials, dominate extinction. The property most highly correlated with extinction in the visible light region was particle cross-sectional area, indicating that turbidity may be a good choice for an independent variable in the light model.

Using 3.5 as the extinction coefficient and substituting -ln (0.01) for -ln (0.1) in the light parameter model, the depth of the euphotic zone is calculated to be 1.32 meters for the Ware River. Comparisons of this depth with the hydraulic depths in Table 3.5-1 show that the estuary is probably light limited for algal growth in all except the most landward portions.

3.6 DEMONSTRATION EXAMPLE: THE OCCOQUAN RESERVOIR

The Occoquan basin was used in this demonstration to test the impoundment section of the non-designated 208 screening manual. Because the Occoquan Reservoir is a public drinking water supply downstream from metropolitan areas (see Figure 3.1-5), large quantities of water quality data were available to compare to the screening method's outputs. This example follows the sequence of methods described in Chapter 5 of the screening manual with the exception of the discussion of water quality during high flow events.

3.6.1 Stratification

Using the screening manual, the first step in assessing impoundment water quality is to determine whether the impoundment thermally stratifies. This requires knowledge of local climate, impoundment geometry, and inflow rates. Using this information, thermal plots likely to reflect conditions in the prototype are selected from the screening manual (Appendix D).

For the thermal plots to realistically describe the thermal behavior of the prototype, the plots must be selected for a locale climatically similar to that of the area under study. Because the Occoquan Reservoir is within 32 kilometers of Washington, D.C., the Washington thermal plots should best reflect the climatic conditions of the Occoquan watershed.

The second criterion for selecting a set of thermal plots is the degree of wind stress on the reservoir. This is determined by evaluating the amount of protection from wind afforded the reservoir and estimating the intensity of the local winds. Table 3.6-1 contains the average annual wind speed frequency distribution for Washington, D.C. and Richmond, Virginia. The data suggest that winds in the Occoquan area are of moderate intensity.

Predicting the extent of shielding from the wind requires use of topographic maps. The reservoir is situated among hills that rise 25 meters or more above the lake surface within 200 meters of the shore. The relief provides little access for wind to the lake surface. The combination of shielding and moderate winds implies that low wind stress plots are appropriate.

The geometry of the reservoir is the third criterion used in the selection of thermal plots. Geometric data for the Occoquan Reservoir

TABLE 3.6-1. AVERAGE ANNUAL FREQUENCY OF WIND SPEED IN PERCENT[a)]

State	Station	Wind Speed Categories ($km\ hr^{-1}$) 0-5	6-12	13-20	21-29	30-39	40-50	51-61	62-74	75 and Over	Mean Speed ($km\ hr^{-1}$)
D.C.	Washington	11	26	35	22	5	1	*	*	*	15.6
VA	Richmond	14	37	36	11	1	*	*	*	*	12.6

*Under 1%

[a)] Source: U.S. Department of Commerce, 1968.

are summarized in Table 3.6-2. The volume, surface area, and maximum depth are all nearly midway between the parameter values used in the 40-foot and 75-foot maximum-depth plots. However, the mean depth is much closer to the mean depth of the 40-foot plot.

The mean depth represents the ratio of the volume of the impoundment to its surface area. Because the volume and surface area are proportional to the thermal capacity and heat transfer rates respectively, the mean depth should be useful in characterizing the thermal response of the impoundment. It follows that the 40-foot thermal profiles should match the temperatures in the Occoquan Reservoir more closely than the 75-foot profiles. However, it is desirable to use both plots in order to bracket the actual temperature.

Flow data provide the final information needed to determine which thermal plots should be used. Most of the inflow comes from two tributaries whose confluence form the upper end of the impoundment. The flows in these two creeks are listed in Table 3.6-3.

The hydraulic residence time can be estimated by using the expression:

$$\tau_w = \frac{V}{Q} = \frac{3.71 \times 10^7 \text{ m}^3}{20.09 \frac{\text{m}^3}{\text{sec}} \times 86400 \frac{\text{sec}}{\text{day}}} = 21.4 \text{ days}$$

Since the residence time is midway between the thermal plot parameter values of 10 and 30 days, both should be used to bracket the mean hydraulic residence time in the prototype. It should be noted that these flow estimates do not include runoff from the area immediately around the lake. However, the upstream Occoquan watershed is large enough to justify the assumption that the contribution of the immediate area is not significant.

The likelihood that the Occoquan Reservoir thermally stratifies can now be evaluated. For a hydraulic residence time of ten days, the thermal plots show that stratification is not likely for maximum depths of 40 or 75 feet. In the case of a 30-day hydraulic residence time,

TABLE 3.6-2. COMPARISON OF GEOMETRY OF OCCQUAN RESERVOIR TO PARAMETER VALUES USED TO GENERATE THERMAL PLOTS

Impoundment	Data Source	Maximum Depth (m)	Volume (m^3)	Surface Area (m^2)	Mean Depth (m)
Occoquan Reservoir	*a*		3.71×10^7	7.01×10^6	5.29
@ Occoquan Dam	*b*	17.1			
@ High Dam	*b*	7.92			
Mean		12.5			
40-foot Max. Depth Plots	*c*	12.2	1.74×10^7	3.08×10^6	5.6
75-foot Max. Depth Plots	*c*	22.9	1.14×10^8	1.08×10^7	10.6

a) Northern Virginia Planning District Commission: HSP Model Idealized Channel Geometry.

b) Maximum depths were taken from water quality profiles retrieved from EPA STORET System.

c) Screening Manual, Section 5.2.2.1, p. 279.

TABLE 3.6-3. MEAN MONTHLY INFLOWS TO OCCOQUAN RESERVOIR[a)]

Month	Occoquan River (m^3 sec^{-1})	Bull Run River[b)] (m^3 sec^{-1})	Total (m^3 sec^{-1})
January	18.24	10.26	28.50
February	23.35	12.41	35.76
March	14.91	7.92	22.83
April	17.02	11.03	28.05
May	10.66	5.44	16.10
June	15.40	13.12	28.52
July	4.35	2.48	6.83
August	2.99	1.52	4.51
September	9.35	6.45	15.8
October	3.55	2.90	6.45
November	10.47	6.32	16.79
December	19.32	11.63	30.95
Mean	12.47	7.62	20.09

[a)] Based on daily mean flow data for October, 1968 to September, 1976. Source: USGS Regional Office, Richmond, VA

[b)] Flow data for Bull Run River @ Clifton are estimated from another upstream gage by areal extrapolation.

the profiles suggest that the reservoir develops a thermal gradient between 1°C m^{-1} and 3 C°m^{-1} for either value of maximum impoundment depth. The 40-foot plots indicate stratification occurs from May to August (see Figure 3.6-1). However, the 75-foot plots predict that the impoundment will have a thermal gradient greater than 1°C m^{-1} only at depths greater than 17 meters. Since the Occoquan Reservoir is only 17.1 meters deep, this suggests that the impoundment does not stratify.

The mean hydraulic residence time can be computed using either the average annual flow rate or the flow rate just prior to stratification. In order to use the latter method, the flow rate during the months of March and April should be computed. The flow rate for this period, 25.4 m^3 sec^{-1}, reduces the hydraulic retention time to 17 days. Since the model predicts no stratification for a ten-day residence time, the judgment as to whether stratification occurs becomes difficult.

Because ten- and 30-day residence times do bracket both calculated residence times and because the 30-day plots predict stratification while the ten-day plots do not, it may be concluded that stratification is possible, but not certain. In borderline cases such as this, the reservoir will almost certainly stratify during some part of the summer.

The accuracy of predictions made using the impoundment screening methodology can be assessed by comparing them with available temperature depth data. Temperature profiles retrieved from the EPA STORET system are listed in Table 3.6-4. These profiles show that stratification occurs at both ends of the reservoir.

At the upper end of the reservoir (High Dam) the thermal gradient remained near 1°C m^{-1} between the surface and depths of 3.0 and 4.6 meters on the two dates shown. Below this region of gradually decreasing temperatures, the thermal gradient increased sharply to 3.3 and 2.9°C m^{-1} on the June and July dates respectively. These temperature profiles demonstrate that the distinctly stratified conditions predicted by the

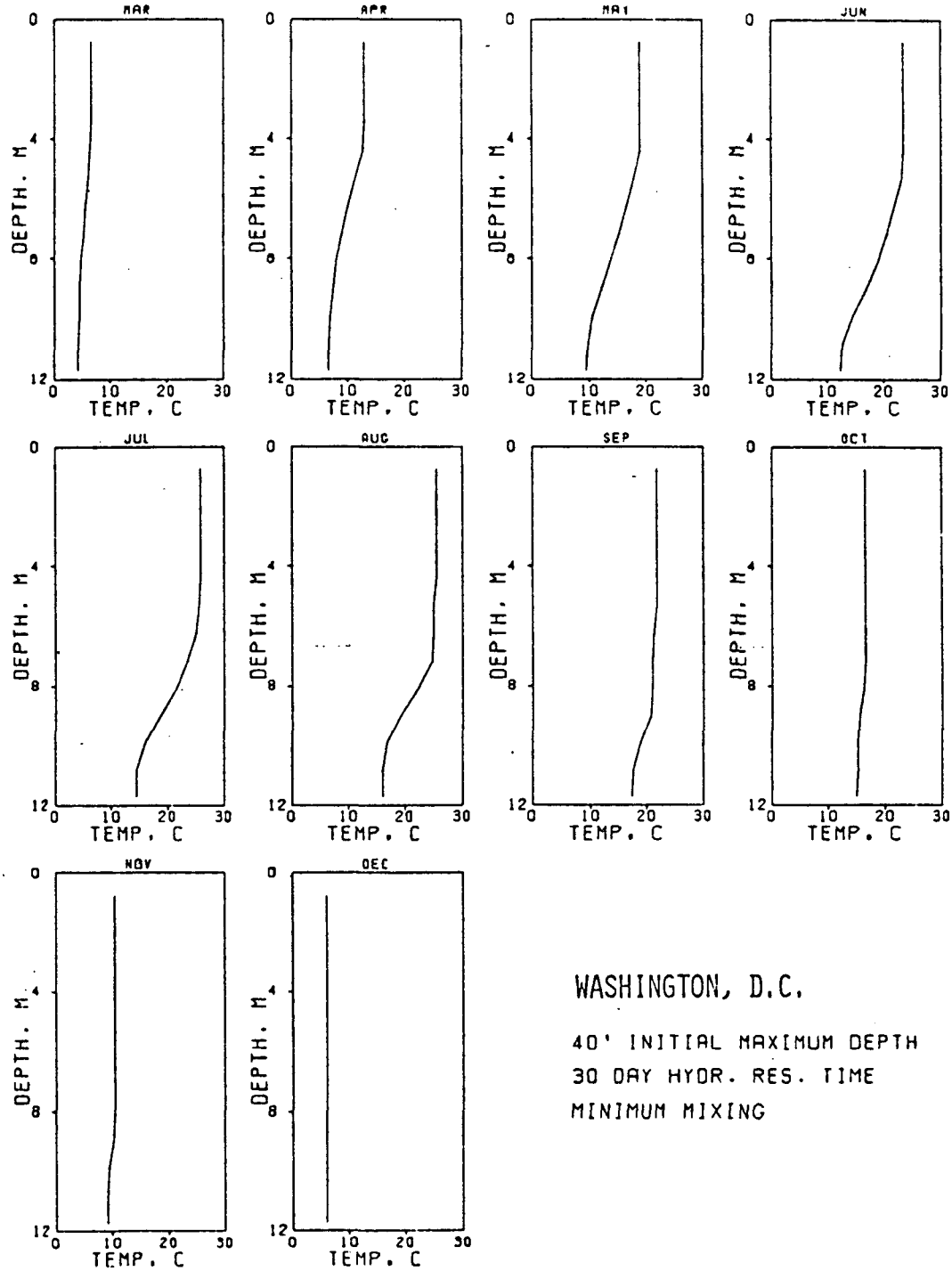

Figure 3.6-1. Thermal profile plots for Occoquan Reservoir.

TABLE 3.6-4. THERMAL PROFILE DATA FOR OCCOQUAN RESERVOIR[a)]

Location	Date	Depth (m)	Temperature (°C)
High Dam (upper end of reservoir)	6/11/70	0	26
		1.5	25
		3.0	22
		4.6	20
		5.8	16
High Dam	7/01/70	0	26
		3.0	23
		6.1	15
Occoquan Dam (Lower end of reservoir)	7/19/73	0	28.3
		1.2	26.8
		4.6	22.2
		7.6	19.1
		16.8	17.0

a) Source: U.S. EPA STORET System.

thermal plots do occur. The good agreement may be largely due to the fact that relatively low flows occurred during 1970. As a result, the mean hydraulic residence time increased to 26 days, a value much closer to the 30-day residence time Figure 3.6-1 is based on.

At the lower end of the reservoir (Occoquan Dam), the thermal gradient remains between 1.0 and 1.4°C m^{-1} from the surface to a depth of 7.6 meters. At greater depths, the gradient is very small. Although the initial gradient is steep enough to meet the criterion for stratification (thermal graident $\geq$ 1°C m^{-1}), it is not as steep as the thermal plots predict. The reason for the poor agreement in this case is probably that 1973 was a slightly wetter than average year. The mean hydraulic residence time using the annual flow for 1973, 20 days, was substantially lower than the value of 26 days that resulted in more strongly stratified conditions during 1970.

These two cases demonstrate that the thermal plots can be used successfully to predict the time and the degree of stratification in impoundments. The epilimnion depths predicted using the model are somewhat less reliable. In both cases, the model did not predict the observed 1°C m^{-1} gradient beginning at the surface.

The temperatures predicted by the thermal plots match those actually measured in the reservoir quite closely. A comparison of predicted and observed monthly mean temperatures (1974-1976) in both the epilimnion and hypolimnion can be made using data in Table 3.6-5. The difference between the two epilimnion temperatures averages 1.0°C and varies between 0.2 and 1.8°C. The difference in the hypolimnion temperatures averages 1.0°C and ranges from 0.2 to 2.7°C.

The close agreement of the predicted and observed impoundment temperatures probably results from the relatively long hydraulic residence times observed in two of the three years on which the averages are based.

TABLE 3.6-5. COMPARISON OF MODELED THERMAL PROFILES TO OBSERVED TEMPERATURES IN OCCOQUAN RESERVOIR

Month	Mean Epilimnion Temp. 40-foot Plot (°C)[a]	Mean Epilimnion Temp. Observed[c]	Mean Hypolimnion Temp. 40-foot Plot (°C)[b]	Mean Hypolimnion Temp. Observed[c]	Epilimnion Depth (m) 40-foot Plot[b]
March	7	8.4	6	6.3	--
April	13.5	12.6	10	9.2	--
May	19	20.5	15	14.4	4.5
June	24	24.8	18	17.2	5.0
July	26	26.6	20	21.2	6.5
August	26	26.5	21	23.7	7
September	22	23.8	20	20.2	--
October	17	17.2	16	15.8	--
November	11	12.2	10	11.6	--
December	7	6.2	7	5.8	--

[a] Mean temperatures in epilimnion from thermal plots with τ_w = 30 days and a maximum depth of 40 feet.

[b] Mean temperatures in thermocline and hypolimnion from thermal plots with τ_w = 30 days and a maximum depth of 40 feet.

[c] Means of observed temperatures in "upper" and "lower" layers of Occoquan Reservoir for 1974-1976, at Sandy Run.

Source: Northern Virginia Planning District Commission, January , 1979.

In 1974, 1975, and 1976, the mean hydraulic residence times were 31, 18, and 25 days, respectively. The 30-day thermal plots should predict results relatively close to the two low-flow years. The differences expected for 1975 would be less pronounced when averaged with the other two.

3.6.2 Sedimentation

The second step in the water quality screening method is to estimate the sedimentation rate in the impoundment. The computations used here require knowledge of sediment loading rates, the sediment size distribution, and the physical properties of the sediment and water. Using this information, the trap efficiency of the impoundment is computed which, along with the annual load, determines the amount of sediment accumulation.

A number of simpler methods of computing trapping efficiences and sediment loads are contained in the screening manual. The alternative means of computing trapping efficiencies will not be used in this demonstration due to their lower accuracy. Since the MRI loading functions provide sediment loads, other load estimation procedures given in the manual will only be used for comparisons.

The necessary sediment loading estimates were provided by the Midwest Research Institute's nonpoint source calculator. Table 3.6-6 contains the sediment and pollutant loads carried by major rivers and streams in the Occoquan watershed. Before they are used in further computations, a delivery factor must be applied to these values. This factor (the sediment delivery ratio or SDR) accounts for the fact that not all the sediment removed from the land surface actually reaches the watershed outlet. Additional nonpoint loads from urban sources are listed in Table 3.6-7. They are presumed to enter the reservoir through Bull Run River since most of the urbanized portion of the watershed lies in

TABLE 3.6-6. ANNUAL SEDIMENT AND POLLUTANT LOADS IN OCCOQUAN WATERSHED IN METRIC TONS PER YEAR[a)]

Type of Load	Kettle Run	Cedar Run	Broad Run	Bull Run	Occoquan River
Sediment	46,898	396,312	142,241	232,103	139,685
Total Nitrogen	164.46	1,457.42	518.91	789.24	469.46
Available Nitrogen	16.45	145.74	51.89	78.92	46.05
Total Phosphorus	39.01	341.95	114.22	202.71	119.42
Available Phosphorus	2.18	14.95	5.57	12.50	8.43
BOD_5	328.92	2,925.63	1,042.45	1,578.47	925.85
Rainfall Nitrogen	0.72	5.50	2.00	3.92	2.48

[a)] Estimates provided by Midwest Research Institutes Nonpoint Source Calculator. These values have not yet had a sediment delivery ratio (SDR) applied to them. We will use 0.1 and 0.2 as lower and upper bounds. The SDR does not apply to rainfall nitrogen.

Note: A large number of significant figures have been retained in these values to ensure the accuracy of later calculations.

TABLE 3.6-7. ANNUAL URBAN NONPOINT LOADS IN OCCOQUAN WATERSHED IN METRIC TONS PER YEAR[a]

Suspended Sediment	Total Nitrogen	Available Nitrogen	Total Phosphorus	Available Phosphorus	BOD_5
12,699	12.88	5.38	2.59	1.270	77.47

[a] Estimates provided by Midwest Research Institute's Nonpoint Source Calculator.

this sub-basin. Pollutant loadings from sewage treatment plants are shown in Table 3.6-8.

Computing the annual sediment load into Occoquan Reservoir is complicated by the presence of Lake Jackson immediately upstream from the reservoir. The trap efficiency must be computed for Lake Jackson as well in order to determine the amount of sediment entering the Occoquan Reservoir from Lake Jackson.

The calculation of the trap efficiency of a reservoir requires first that the fall velocities of sediment particles be computed and, second, that the flow pattern be modeled. Fall velocities for spherical particles can be computed using Stokes' law:

$$v_{max} = 4.71 \times 10^4 \times \frac{(D_p - D_w)\, d^2}{\mu}$$

where v_{max} = settling velocity, m day^{-1}

μ = viscosity of water, centipoise

D_p = density of sediment particle, g cm^{-3}

D_w = density of water, g cm^{-3}

d = diameter of sediment particle, mm

Stokes' law holds satisfactorily for Reynolds' numbers between 0.0001 and 0.5. Generally this requirement is met for particles less than 0.7 in diameter. Corrections for larger particles are unnecessary since impoundment residence times are rarely so small that particles in the range of 0.7 mm or greater are not trapped completely.

TABLE 3.6-8. SEWAGE TREATMENT PLANT POLLUTANT LOADS IN BULL RUN SUB-BASIN IN METRIC TONS PER YEAR[a)]

Total Nitrogen	Total Phosphorus	BOD_5
108.0	11.92	54.80

[a)] Averages for July 1974 - December 1977
Source: Northern Virginia Planning District Commission, March 1979.

Soil types provide an indication of the particle sizes in the basin under study. Soils in the Occoquan basin are predominately silt loams. Particle size data on the principal variety, Penn silt loam, are given in Table 3.6-9. (The size fractions of water-borne sediments would be more appropriate than in situ size fractions. This information should be used if available.)

Some effort can be conserved by first calculating the smallest particle size that will be completely trapped in the impoundment. To do so, P, the trap efficiency, must first be computed. Because both reservoirs are long and narrow and have relatively small residence times, the flow will be assumed to approximate vertically mixed plug flow. In this case, P is found from the expression:

$$P = \frac{v_{max}\ \tau_w}{D'}$$

where D' = mean flowing layer depth, m.

To calculate the smallest particle that is trapped in the impoundment, P is set equal to unity and the above equation is solved for v_{max}. This expression for v_{max} is then substituted into the fall velocity equation (Stokes' law), which in turn is solved for d. The resulting expression is:

$$d = \sqrt{\frac{D'\ \mu}{4.71 \times 10^4\ (D_p - D_w) \cdot \tau_w}}$$

The trap efficiency of Lake Jackson is calculated first. The data required for these calculations are:

TABLE 3.6-9. PARTICLE SIZES IN PENN SILT LOAM

Particle Size (mm)	% of Particles Smaller Than (By Weight)
4.76	100
2.00	99
0.42	93
0.074	84
0.05	78
0.02	50
0.005	26
0.002	16

$V = 1.893 \times 10^6\ m^3$

$Q = 12.37\ m^3\ sec^{-1}$

$\bar{D} = 3.34\ m$

$\mu = 1.11\ cp$ (Assuming $T = 16^oC$ as in Occoquan Reservoir)

and $\tau_w = \frac{V}{Q} = 1.77$ days.

The minimum particle size for 100 percent trapping is computed as:

$$d = \sqrt{\frac{3.34\ m \times 1.11}{4.71 \times 10^4\ (2.66 - 1.0) \cdot 1.77}} = 5.18 \times 10^{-3}\ mm$$

Sediment size fractions for *in situ* soils are known. However, particle sizes delivered to the reservoir via the stream channels are not determined by the screening methods, therefore, a composite trap efficiency for all particle sizes is needed. This is computed as follows:

$$P_c = 1 - \left\{W_I - \sum_d \left(P_d \times W_d\right)\right\}/100$$

where W_I = weight percent of sediment entering the reservoir in incompletely trapped particle size range (i.e., below minimum particle size 100% trapped)

P_d = trap efficiency for particle size range d

W_d = weight percent of particle size range d entering the reservoir

Weight fractions in each size range are estimated from data in Table 3.6-9 using linear interpolation. It is assumed that virtually all of the sediment mass consists of particles greater than 0.001 mm in diameter. For each size range, a mean trapping efficiency is calculated. The sedimentation calculations for Lake Jackson are summarized in Table 3.6-10.

Substituting the values from Table 3.6-10 into the above equation yields $P_c = 0.80$.

The total sediment accumulation in Lake Jackson i determined from the expression:

$$S_t = d_F \cdot P_c \sum_i S_i$$

where d_F = sediment delivery ratio from USLE

P_c = composite trap efficiency

S_i = sediment load from tributary i.

$$S_t = (0.1, 0.2) \times 0.8 \left[46898 + 396312 + 142241\right] \text{ metric tons/year}$$

$$= (46836, 93672) \text{ metric tons/year}.$$

Data listed in Appendix F of the screening manual show that the rate of sedimentation in Lake Jackson is 56153 metric tons/year.

The next step is to compute the sedimentation in Occoquan Reservoir. The minimum particle size that is completely trapped is computed using the following values:

TABLE 3.6-10. TRAP EFFICIENCY CALCULATIONS FOR LAKE JACKSON

Particle Size (mm)	Settling Velocity ($m\ day^{-1}$)	P	$\bar{P}$ [a]	Wt. % Particles in Size Range Into Lake Jackson	Wt. % Particles in Size Range Out of Lake Jackson
0.00518	1.89	1.00			
			0.966	.288	.05
0.005	1.76	0.932			
			.694	5.0	7.81
0.0035	0.861	0.456			
			.303	5.0	17.78
0.002	0.281	0.149			
			.117	8.0	36.04
0.0015	0.158	0.084			
			.061	8.0	38.32
0.001	0.070	0.037			

a) $\bar{P}$ represents the mean trap efficiency for the given size range.

D' = 5.29 m

μ = 1.1111 cp (@ T = 16°C, mean of Table 3.6-5)

D_p = 2.66 g cm^{-3}

D_w = 1.0 g cm^{-3}

Under stratified conditions, the epilimnion thickness should be used for D'. Since stratification is uncertain in this case and the predicted hypolimnion thickness, 5.75 m, is greater than the mean depth, the latter value will be used. All particles with diameter, d, such that:

$$d = \sqrt{\frac{5.29 \times 1.11}{4.71 \times 10^{4} (2.66 - 1.0) \cdot 21.54}} = 1.87 \times 10^{-3} \text{ mm}$$

will be completely trapped in the Occoquan Reservoir. By the same techniques utilized for Lake Jackson, the trap efficiency of the Occoquan Reservoir may be computed. The calculations are summarized in Table 3.6-11. The fraction of material from each source can now be evaluated. For the sediment from Lake Jackson:

$$P_c = 1 - (64.99 - .822 \times 26.67 - .465 \times 38.32)/100 = .748$$

And for the sediment from the Bull Run and Occoquan rivers:

$$P_c = 1 - (13.92 - .822 \bar{x} 5.92 - .286 \times 8.)/100 = .932$$

Finally, the total annual sediment accumulation in Occoquan Reservoir may be estimated. Using equation 2:

TABLE 3.6-11. TRAP EFFICIENCY CALCULATIONS FOR OCCOQUAN RESERVOIR

Particle Size (mm)	Settling Velocity (m day^{-1})	P	$\bar{P}$ [a]	Wt. % Particles in Size Range	
				From Lake Jackson	From Bull Run and Occoquan Rivers
0.00187	.246	1.00	.822	26.67	5.92
0.0015	0.158	0.644	.465	38.32	8.0
0.001	0.070	.286			

[a] $\bar{P}$ represents the mean trap efficiency for the given size range.

$$S_t = (0.1, 0.2) \times \left[\underbrace{(46898 + 396312 + 142241)\ (1 - .80)}_{\text{sediment from Lake Jackson}} \times .748 + \underbrace{(232103 + 139685)}_{\substack{\text{sediment from} \\ \text{Bull Run and} \\ \text{Occoquan}}} \times 0.932\right]$$

$$+ \underbrace{12699}_{\substack{\text{urban} \\ \text{load}}} \times 0.932$$

$$S_t = (55200, 98700) \text{ metric tons/year}$$

3.6.3 Eutrophication

In addition to the assessment of impoundment thermal characteristics and sedimentation rates, estimating nutrient levels is a major concern. The concentrations of nutrients directly affect plant growth rates, which in turn affect dissolved oxygen levels and impoundment aging. Since nitrogen and phosphorus are the macronutrients most commonly in limited supply, the screening methods focus on them. Nutrient concentrations depend primarily on the amounts of each carried into the reservoir by tributaries and point sources. Several assumptions concerning pollutants in the watershed-reservoir system are necessary in order to calculate the desired annual loads:

- The unavailable phosphorus is adsorbed on sediment particles. Therefore, of the unavailable forms coming into Lake Jackson, only the fraction $(1\text{-}P_{c[\text{Jackson}]})$ is delivered to the Occoquan Reservoir;
- All of the rainfall nitrogen is in available form;
- All of the phosphorus and nitrogen from the sewage treatment plants (STPs) is in available form;
- The output of STPs outside the Bull Run sub-basin is negligible compared to that of the STPs in Bull Run. This is justified by the fact that during the period under study, the plants in Bull Run had a combined capacity several times larger than the few plants outside the sub-basin.

By applying these assumptions to nonpoint source data generated by the MRI loading function and point source data reported in the literature (see Tables 3.6-6, 3.6-7, and 3.6-8) the total load of each pollutant type may be calculated. The computation for the total annual phosphorus load in Occoquan Reservoir is shown below. First, the quantity of total phosphorus coming into the Occoquan Reservoir through Lake Jackson is calculated by:

$$TP_{Jackson} = (1 - P_{c_{Jackson}}) \times [\text{Total P} - \text{Available P}] + \text{Available P}$$

The total phosphorus from Broad Run, Cedar Run, and Kettle Run are summed and the available phosphorus loads are subtracted to give the unavailable load. This load is multiplied by the trap efficiency of the lake, P_c, which yields the unavailable load passing through. This value, plus the available load, is an estimate of the total phosphorus entering Occoquan Reservoir from Lake Jackson. This quantity is 117.2 metric tons yr^{-1}. This value is added to the non-urban, nonpoint source loads from Bull Run and areas adjacent to the Occoquan Reservoir (see Table 3.6-6):

$$TP_{NPNU} = 202.71 + 119.42 + 117.21$$
$$= 439.34 \text{ metric tons } yr^{-1}.$$

This quantity is modified by the sediment delivery ratio. The urban nonpoint loads and STP loads are added to complete the calculation:

$$TP = (0.1, 0.2)\ (439.34) + 2.59 + 11.92$$
$$= (58.44, 102.38) \text{ metric tons } yr^{-1}.$$

The results of load calculations are summarized in Table 3.6-12.

The calculated annual total phosphorus and nitrogen loads may be compared with the observed loads listed in Table 3.6-13. The loads observed

TABLE 3.6-12. CALCULATED ANNUAL POLLUTANT LOADS TO OCCOQUAN RESERVOIR

	Sediment Delivery Ratio					
	0.1			0.2		
	% of Load From Source			% of Load From Source		
	Nonpoint	Point	Load[a]	Nonpoint	Point	Load[a]
Total Nitrogen	77	23	474.56	87	13	813.61
Available Nitrogen	33	67	161.91	45	55	195.82
Total Phosphorus	80	20	58.44	88	12	102.38
Available Phosphorus	32	68	17.56	46	54	21.92
BOD_5	93	7	812.40	96	4	1492.53

[a] Units of metric tons $year^{-1}$

Note: A large number of significant figures have been retained in these values to ensure the accuracy of later calculations.

TABLE 3.6-13. OBSERVED ANNUAL POLLUTANT LOADS TO OCCOQUAN RESERVOIR

Period	Mean Flow[a] Rate (m^3 sec^{-1})	Total Nitrogen Load (metric tons $year^{-1}$)	Total Phosphorus Load (metric tons $year^{-1}$)
10/74 - 9/75	24.7	805[b]	110[b]
7/75 - 6/76	24.0	1905[c]	188[c]
7/76 - 6/77	10.4	4763[c]	454[c]

[a] Source: USGS Regional Office, Richmond, Virginia.

[b] Grizzard et al., 1977

[c] Northern Virginia Planning District Commission, March, 1979. Data gathered by Occoquan Watershed Monitoring Laboratory.

by Grizzard et al., (1977) are within seven percent of those calculated using a delivery ratio of 0.2. On the other hand, the Occoquan Watershed Monitoring Laboratory (OWML) reported values 1.9 to 5.9 times higher than highest calculated loads. Comparison of loadings (kg/ha year) with literature values suggest that Grizzard is most accurate (Likens et al., 1977).

By dividing the total annual load by the total annual flow rate, the pollutant concentrations may be estimated. For example, the available phosphorus concentration is:

$$P_{AV} = \text{Annual Available Phosphorus Load/Annual Flow}$$

$$= \frac{(17.56,\ 21.92) \times 10^6 \frac{g}{yr}}{20.09 \frac{m^3}{sec} \times 86400 \frac{sec}{day} \times \frac{365\ day}{yr}} = (.028,\ .035)\ g\ m^{-3}$$

Calculated and observed pollutant concentrations are listed in Table 3.6-14. The mean summer concentrations of phosphorus and nitrogen are closer to the concentrations calculated using a delivery ratio of 0.1 than 0.2, although this would not be expected on the basis of the previous comparison of annual loads. The discrepancy could arise from a large seasonal variation in concentrations or processes such as adsorption onto settling sediment that reduce the water column concentrations.

The screening manual does present a relationship to compute the water column total phosphorus level, C_w:

$$C_w = \frac{C_{in}}{1 + \frac{k_1 k_3 A}{Q}}$$

(See the screening manual section 5.4.5, p. 348.)

Since the model has not been widely tested and the values of k_1 and k_3 are unknown, no attempt will be made to refine the previous calculation

TABLE 3.6-14. CALCULATED AND OBSERVED MEAN ANNUAL POLLUTANT CONCENTRATIONS IN OCCOQUAN RESERVOIR

	Total Nitrogen ($g\ m^{-3}$)	Available Nitrogen ($g\ m^{-3}$)	Total Phosphorus ($g\ m^{-3}$)	Available Phosphorus ($g\ m^{-3}$)	BOD_5 ($g\ m^{-3}$)
Delivery Ratio					
0.1	0.76	0.26	0.093	0.028	1.3
0.2	1.3	0.31	0.16	0.035	2.4
Observed Values[a)]					
Mean	0.88	0.16	0.08		
Max.	1.50	0.24	0.12		
Min.	0.35	0.10	0.04		

[a)] Averages for April-October between 1973 and 1977.
Source: Northern Virginia Planning District Commission, March, 1979.

by using this method. If the product k_1k_3 is in the range expected under steady state conditions, between 20 and 40, the actual concentrations will be 18 to 30 percent lower than that calculated without this correction. Thus, the result obtained by dividing the annual load by the annual flow should be considered an upper bound to the actual concentration.

The ratio of nitrogen to phosphorus concentration in the reservoir can be used to estimate which nutrient will limit the rate of plant growth. For the Occoquan Reservoir, the N:P ratios are shown in Table 3.6-15. The calculated nutrient ratios care between 5 and 10, where either nutrient could be considered limiting. The N:P ratio of the observed data indicates more conclusively that phosphorus is growth limiting.

TABLE 3.6-15. NITROGEN:PHOSPHORUS RATIOS IN OCCOQUAN RESERVOIR

	Delivery Ratio		
	0.1	0.2	Observed
Total N:Total P	8.1	7.9	11.0
Available N:Available P	9.2	8.9	

The first method of predicting algal growth is known as the Vollenweider Relationship. In the graph of total phosphorus load ($g\ m^{-2}\ yr^{-1}$) versus mean depth (m) divided by hydraulic retention time (yrs) (see Figure 3.6-2), areas can be defined that roughly correspond to the nutritional state of the impoundment. For the Occoquan Reservoir, the values of the parameters are:

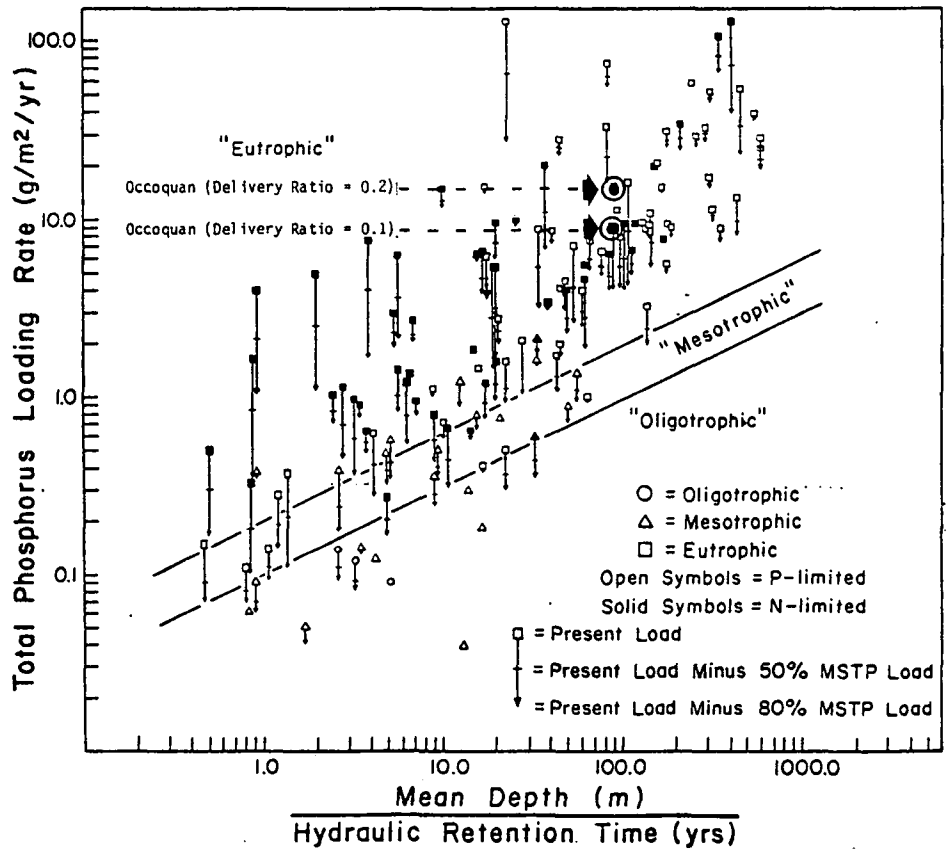

Figure 3.6-2. Plot of the Vollenweider relationship showing the position of Occoquan Reservoir using calculated total phosphorus loads (Source: Zison et al., 1977).

$$L_P = \frac{(58.4,\ 102.4) \times 10^6 \text{ g/yr}}{7.01 \times 10^6 \text{ m}^2} = \left(8.3,\ 14.6\right) \text{ g m}^{-2} \text{ yr}^{-1}$$

$$\frac{\overline{D}}{\tau_w} = \frac{5.29 \text{ m}}{21.4 \text{ days}} \times \frac{365 \text{ days}}{1 \text{ yr}} = 90 \text{ m yr}^{-1}$$

According to the Vollenweider Relationship, Occoquan Reservoir is well into the eutrophic region for both estimates of the total phosphorus load (see (Figure 3.6-2). Based on these predictions a more in-depth study of the algal productivity seems to be in order.

The available data also permits the estimation of the maximal primary production of algae from the Chiaudani and Vighi Curve (Figure 3.6-3). The theoretical phosphate (available phosphorus) concentration should be between .028 and .035 g m^{-3} according to these calculations. The maximal primary production of algae is found from Figure 3.6-3 to be between 1850 and 2000 mgC m^{-2} day^{-1}, or 1.85 and 2.0 gC m^{-2} day^{-1}. This level of algal production is roughly 75 to 80 percent of the maximum production shown on the curve. Both this method and the Vollenweider Relationship suggest algal growth will contribute significantly to the BOD load in the impoundment (see section 3.6.5).

3.6.4 Water Quality High Flow Events

A substantial fraction of the pollutant loads into the Occoquan Reservoir come from nonpoint sources. Seventy-seven percent or more of the total nitrogen and total phosphorus loads to the reservoir are derived from nonpoint sources (Table 3.6-12). Since most of the nonpoint loads into the reservoir are carried by runoff, it is important to determine the magnitude of nonpoint source pollutants, especially nutrients, during or immediately following a high flow event.

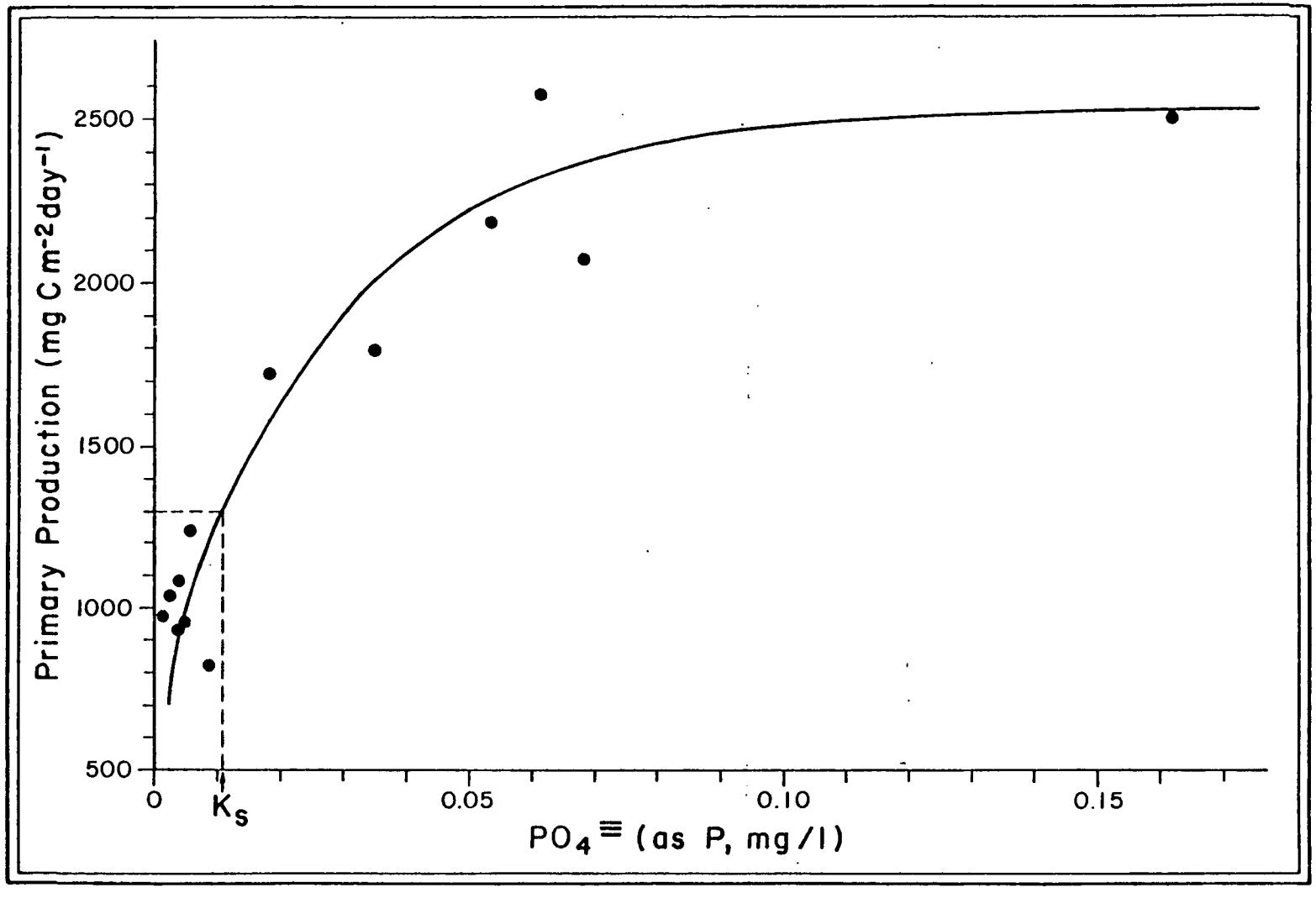

Figure 3.6-3. Maximal primary productivity as a function of phosphate concentration (Source: Zison et al., 1977).

To accomplish this, 15 seven-day high flow events between October 1978 and September 1976 were selected. The Midwest Research Institute's nonpoint source calculator was used to estimate the loads to the reservoir during these events. These results are summarized in Table 3.6-16.

Loads during the seven-day high flow event from urban nonpoint an point sources may be estimated by taking a fraction $\frac{7}{365}$ of the annual loads. As in the calculations of the annual average loads, unavailable phosphorus is assumed to be adsorbed on the sediment. Because of flow differences, it is necessary to determine the trapping efficiency of Lake Jackson during high flow events. Because of the lake's long, shallow geometry, the fluid motion is assumed to be approximated by vertically mixed plug flow.

Computation of trapping efficiencies requires that hydraulic residence times be known. The average inflow rates during the selected high flow periods are listed in Table 3.6-17.

The hydraulic residence time of Lake Jackson is:

$$\tau_w = \frac{1.893 \times 10^6 \text{ m}^3}{40.10 \frac{\text{m}^3}{\text{sec}} \times 86400 \frac{\text{sec}}{\text{day}}} = 0.546 \text{ days}$$

The second step in the compuation of trap efficiencies involves determining the minimum sediment size that is completely trapped in the reservoir. The values of constants used to determine this are:

$\tau_w = 0.546$ day = hydraulic residence time

$\overline{D} = 3.34$ m = mean depth

$\mu = 1.11$ cp = viscosity

$D_p = 2.66$ g cm^{-3} = particle density

$D_w = 1.0$ g cm^{-3} = water density

TABLE 3.6-16. HIGH FLOW EVENT POLLUTANT LOADS IN OCCOQUAN WATERSHED FROM NON-URBAN NONPOINT SOURCES[a)]

Type of Load	SUB-BASIN Kettle Run	Cedar Run	Broad Run	Bull Run	Occoquan River
Sediment, (metric tons/event)	2981	25758	9211	14207	8622
Total Nitrogen, (metric tons/event)	10.52	95.08	33.75	48.48	28.58
Available Nitrogen, (kg/event)	1050	9508	3375	4848	2858
Total Phosphorus, (kg/event)	3046	26718	8937	15813	9295
Available Phosphorus, (kg/event)	170.4	1168.8	436.6	975.2	657.1
BOD_5, (metric tons/event)	21.04	190.16	67.50	96.98	57.17

[a)] These values are gross loads (i.e., delivery ratio has not been applied). Values supplied by Midwest Research Institutes Nonpoint Event Load Calculator.

TABLE 3.6-17. STREAM FLOWS INTO OCCOQUAN RESERVOIR DURING HIGH FLOW EVENTS[a)]

Tributary	Flow Rate, (m^3 sec^{-1})
Bull Run @ Clifton	28.40
Occoquon River @ Manassas	40.10
TOTAL	68.50

[a)] Averages of 15 high flow events from October, 1968 to September, 1976.
Source: USGS Regional Office, Richmond, VA.

Substitution of these constants into the following equation:

$$d = \sqrt{\frac{\mu \bar{D}}{4.71\ 10^{4}\ (D_p - D_w)\tau_w}}$$

yields a minimum diameter of:

$$d = 9.32 \times 10^{-3} \text{ mm.}$$

The fraction of the total load in size ranges smaller than the minimum diameter is estimated by interpolation between values listed in Table 3.6-18. The computations for the trap efficiency in each size range are also summarized in Table 3.6-18.

The composite trap efficiency is:

$$P_c = 1 - \left(32.9 - 6.9 \times .64 - 5.(.21 + .093) - 8.(.036 + .019)\right) / 100$$
$$= 0.735$$

There is now sufficient information to calculate the total sediment and pollutant loads to Occoquan Reservoir during high flow events. The computational steps for the total phosphorus load are shown below:

$$TP_{Jackson} = (1 - 0.735) \times \Big[\overbrace{(3046 + 26718 + 8937)}^{\text{Total Phosphorus}} \frac{kg}{event} - \overbrace{(170.4 + 1168.8 + 436.6)}^{\text{Available Phosphorus}} \frac{kg}{event} \Big]$$

Unavailable Phosphorus

$$+ \underbrace{(170.4 + 1168 + 436.6)}_{\text{Available Phosphorus}} \frac{kg}{event}$$

$$= 11560 \frac{kg}{event}$$

TABLE 3.6-18. TRAP EFFICIENCY CALCULATIONS FOR LAKE JACKSON DURING HIGH FLOW EVENTS

Particle Size (mm)	Settling Velocity (m day^{-1})	P	$\overline{P}$ [a]	Wt. % Particles in Size Range
0.00932	6.11	1.00		
			0.64	6.9
0.005	1.76	0.287		
			.21	5.0
0.0035	0.861	0.141		
			0.093	5.0
0.002	0.281	0.046		
			0.036	8.0
0.0015	0.158	0.026		
			0.019	8.0
0.001	0.070	0.011		

[a] $\overline{P}$ represents the mean trap efficiency for the given size range.

Total Nonpoint Non-Urban Load:

$$TP_{NPNU} = (11560 + 15813 + 9295)\ \frac{kg}{event} \times \underbrace{(0.1,\ 0.2)}_{\substack{\text{Sediment}\\ \text{Delivery}\\ \text{Ratio}}}$$

$$TP_{NPNU} = (3667,\ 7334)\ \frac{kg}{event}$$

Urban Nonpoint Load:

$$TP_U = 2590\ kg\ yr^{-1} \times \frac{1\ yr}{365\ days} \times \frac{7\ days}{1\ event}$$

$$= 49.7\ kg\ event^{-1}$$

Point Source Load:

$$TP_{PS} = 11920\ kg\ yr^{-1} \times \frac{1\ yr}{365\ days} \times \frac{7\ days}{1\ event}$$

$$= 228.6\ kg\ event^{-1}$$

Total Load from All Sources:

$$TP = (3667,\ 7334) + 49.7 + 228.6$$

$$= (3945,\ 7612)\ kg\ event^{-1}.$$

The total load for each pollutant type is listed in Table 3.6-19.

Pollutant concentrations in the reservoir during high flow periods may be estimated by dividing the total event load by the total event flow. This is an accurate estimate if flow in the reservoir is characterized by vertically mixed plug flow. Otherwise, the estimate can be considered to be an upper bound for the concentration that would be attained in a partially or completely mixed impoundment.

TABLE 3.6-19. TOTAL POLLUTANT LOADS TO OCCOQUAN RESERVOIR DURING HIGH FLOW EVENTS

Pollutant, (metric tons event^{-1})	Sediment Delivery Ratio	
	0.1	0.2
Sediment	3532	6821
Total Nitrogen	23.96	45.60
Available Nitrogen	4.339	6.503
Total Phosphorus	3.945	7.612
Available Phosphorus	0.594	.935
BOD_5	45.8	89.1

Calculated maximum nitrogen and phosphorus concentrations for the Occoquan Reservoir during high flow events are given in Table 3.6-20.

TABLE 3.6-20. MAXIMUM CALCULATED POLLUTANT LEVELS IN OCCOQUAN RESERVOIR DURING HIGH FLOW EVENTS (g m^{-3})

Pollutant	Sediment Delivery Ratio 0.1	0.2
Total Nitrogen	0.58	1.1
Available Nitrogen	0.10	0.16
Total Phosphorus	0.095	0.18
Available Phosphorus	0.014	0.023

The total phosphorus concentration is one to 12 percent higher during high flow events than the annual means. However, the remaining nutrient concentrations are lower for high flows. In spite of the high nutrient loads during these events, most concentrations are lower because of the high flow rates. It may be safely concluded that water quality will not worsen during high flow events. Any planning for future water quality can be based on annual average loads.

3.6.5 Dissolved Oxygen

The final water quality parameter to be examined using the screening methods is hypolimnion dissolved oxygen. If stratification does not occur, reaeration of deep waters occurs via mixing with surface waters. When a hypolimnion exists, the deep waters are cut off from oxygen

sources, e.g., surface reaeration and inflowing water. Organic matter decay, benthic uptake, and other oxygen demands can seriously deplete dissolved oxygen levels. As was determined earlier, the Occoquan Reservoir may stratify during the months of May through August. The time period is long enough that hypolimnion oxygen depletion could be a problem.

The simplified model used to predict hypolimnion dissolved oxygen levels assumes that the only substantial dissolved oxygen sinks are water column and benthic deposit BOD. Additionally, all sources of oxygen, photosynthesis, etc., are neglected in the hypolimnion after the onset of stratification. Thus, the procedure requires that pre-stratification levels of BOD and dissolved oxygen be estimated in order to compute the post-stratification rate of oxygen disappearance. The pre-stratification concentration of water column BOD is determined first. A simple mass balance leads to the following relationship, if steady state conditions are assumed:

$$C_{ss} = - \frac{k_a}{k_b}$$

where C_{ss} = steady state concentration of BOD in water column, mg ℓ^{-1}

k_a = mean rate of BOD loading from all sources, g m^{-3} day^{-1}

$$k_b = - k_s - k_1 - \frac{Q}{V}$$

where $k_s = V_s / \overline{D}$ = mean rate of BOD settling out onto impoundment bottom, day^{-1}

k_1 = mean rate of decay of water column BOD, day^{-1}

Q = mean export flow rate, m^3 day^{-1}

V = impoundment volume, m^3

V_s = settling velocity, m day^{-1}

$\overline{D}$ = impoundment mean depth, m .

The BOD load to the impoundment originates in two principal sources: algal growth and tributary loads. The algal BOD loading rate is computed from the expression:

$$k_{a(algae)} = SMP / \overline{D}$$

S = stoichiometric conversion from algal biomass as carbon to BOD = 2.67

M = proportion of algal biomass expressed as oxygen demand

P = primary algal production, g m^{-2} day

$\overline{D}$ = mean impoundment depth, m

Since the Chiaudani curve (see section 3.6.3) gives the maximal algal production, a correction should be made for the actual epilimnion temperature. If the maximal rate occurs at 30°C and the productivity decreases by half for each 15°C decrease in temperature, the algal production can be corrected for temperature using the expression:

$$P_{(T)} = P_{(30)} \times 1.047^{(T-30°C)}.$$

According to the data in Table 3.6-5, the epilimnion temperature during the month prior to stratification is approximately 13°C. Thus:

$$P_{(13°)} = (1.85, 2.0)\ gC\ m^{-2}\ day^{-1} \times 1.047^{(13°C-30°C)}$$
$$= (0.85, 0.92)\ gC\ m^{-2}\ day^{-1}.$$

If M is assumed to have lower and upper limits of 0.7 and 1.0, then:

$$k_{a(algae)} = \frac{2.67 \times (0.7, 1.0) \times (.85, .92)\ gC\ m^{-2}\ day^{-1}}{5.293\ m}$$
$$= \left(0.30, 0.46\right)\ g\ m^{-3}\ day^{-1}$$

The BOD load borne by tributaries is found by the expression:

$$k_{a(trib)} = \frac{\text{Mean Daily BOD from Tributaries}}{\text{Impoundment Volume}}$$

$$= \frac{(812.40,\ 1492.53) \times 10^6 \text{ g yr}^{-1} \times \frac{1 \text{ yr}}{365 \text{ days}}}{3.71 \times 10^7 \text{ m}^3}$$

$$= \left(0.060,\ 0.11\right) \text{ g m}^{-3} \text{ day}^{-1} \quad .$$

The total BOD load to Occoquan Reservoir is then:

$$k_a = k_{a(algae)} + k_{a(trib)}$$

$$= (0.30,\ 0.460) \text{ g m}^{-3} \text{ day}^{-1} + (0.06,\ .11) \text{ g m}^{-3} \text{ day}^{-1}$$

$$= (0.36,\ 0.57) \text{ g m}^{-3} \text{ day}^{-1} \quad .$$

Before the water column BOD concentration can be computed, the constants comprising k_b must be evaluated. The first of these, k_s, requires knowledge of the settling velocities of BOD particles. Ideally these would be determined by using values of the physical properties of the particles and the water in the settling velocity equation, V-6 (screening manual section 5.3.3.1, page 398). Because such data are lacking, a settling velocity of 0.2 m day^{-1} reported for detritus will be substituted. The reported values lie between 0 and 2 meters day^{-1}, with most values close to 0.2 m day^{-1} (Zison et al., 1978). Then,

$$k_s = 0.2 \text{ m day}^{-1} / 5.29 \text{ m} = .0378 \text{ day}^{-1}$$

The second constant comprising k_b is the first-order decay rate constant for wtaer column BOD. Reported values of k_1 vary widely depending on the degree of waste treatment. Zison et al. (1978) presents data for rivers, but contains only two values for k_1 in lakes and estuaries. Both are $k_1 = 0.2\ day^{-1}$. Camp (1968) reports values from 0.01 for slowly metabolized industrial wastes to 0.3 for raw sewage. Because there is considerable sewage discharge into the Occoquan Reservoir, k_1 may be assumed to be in the upper range of these values, between 0.1 and 0.3 day^{-1}. Like the algal production rate, k_1 must be corrected for the water temperature. In April, the mean water temperature is about 11°C.

Then:

$$k_1 = (0.1, 0.3)\ day^{-1} \times 1.047^{(11°C-20°C)}$$
$$= (0.066, 0.20)\ day^{-1} \quad .$$

Finally, k_b is evaluated as follows:

$$k_b = -\ 0.0378\ day^{-1} - (0.066, 0.20) day^{-1} - \frac{m^{-3}\ sec^{-1} \times 86400\ sec\ day^{-1}}{3.71 \times 10^7\ m^3}$$
$$= -\ \left(0.15, 0.28\right) day^{-1} \quad .$$

Next, k_a and k_b may be substituted into equation V-27 (screening manual section 5.5.2.1, page 362) to obtain C_{ss}.

$$C_{ss} = \frac{(0.36, 0.57)\ g\ m^{-3}\ day^{-1}}{(0.15, 0.28)\ day^{-1}}$$

$$C_{ss} = \begin{matrix} (1.3, 2.0)\ g\ m^{-3} \sum k_{1(20°C)} = 0.3\ day^{-1} \\ (2.4, 3.8)\ g\ m^{-3} \sum k_{1(20°C)} = 0.1\ day^{-1} \end{matrix}$$

Once the water column BOD concentration is known, the benthic BOD is computed from the expression:

$$L_{ss} = \frac{k_s C_{ss} \bar{D}}{k_4}$$

where k_4 = mean rate of benthic BOD decay, day^{-1}.

Values for the benthic BOD decay rate constant span a greater range than those for water column BOD. Camp (1968), however, reports values of k_4 very near 0.003 day^{-1} for a range of benthic depth from 1.42 to 10.2 cm (see page 366 of the screening manual). Assuming this to be a good values, a temperature-corrected value of k_4 may be computed at an April hypolimnion temperature of 10°C:

$$k_4 = 0.003\ day^{-1} \times 1.047^{(10-20)} = 0.0019\ day^{-1} \quad .$$

Then,

$$L_{ss} = \frac{0.038\ day^{-1} \times (1.3,\ 2.0;\ 2.4,\ 3.8)\ g\ m^{-3} \times 5.29\ m}{0.0019\ day^{-1}}$$

$$= (138,212)\ g\ m^{-2} \quad \text{for } k_s = 0.3\ day^{-1}$$

$$(254,402)\ g\ m^{-2} \quad \text{for } k_s = 0.1\ day^{-1} \quad .$$

Prior to stratification the impoundment is assumed to be fully mixed and saturated with oxygen. During April, the hypolimnion temperature is 10°C. Saturated water at this temperature contains 11.17 ppm oxygen.

Finally, the dissolved oxygen level in the hypolimnion may be predicted during the period of stratification. The applicable expressions are:

$$O_t = O_o - \Delta O_L - \Delta O_c$$

$$\Delta O_L = \left(\frac{L_{ss}}{\bar{D}} + \frac{k_s C_{ss}}{k_s + k_1 - k_4}\right)\left(1 - e^{-k_4 t}\right) - \left(\frac{k_s C_{ss}}{k_s + k_1 - k_4}\right)\left(\frac{k_4}{k_s + k_1}\right)\left(1 - e^{-(k_s + k_1)t}\right)$$

$$\Delta O_c = \frac{k_1 C_{ss}}{k_1 + k_s}\left(1 - e^{-(k_1 + k_s)t}\right)$$

where O_t = dissolved oxygen at time t

O_o = dissolved oxygen at time t = 0

D = hypolimnion depth

In order to illustrate the use of these expressions, the computation of a dissolved oxygen concentration for the case $k_a = 0.57$ g m^{-3} day^{-1} and $k_{1(20°C)} = 0.1$ day^{-1} is shown below. First, the BOD decay rate constants must be adjusted to account for their temperature dependence. During the period from May through August, the mean temperature in the hypolimnion and thermocline is 19°C according to the thermal plots (see Table 3.6-5). The temperature-corrected rate constants are:

$$k_1 = 0.1 \text{ day}^{-1} \times 1.047^{(19-20)} = 0.096 \text{ day}^{-1}$$

$$k_4 = 0.003 \text{ day}^{-1} \times 1.047^{(19-20)} = 0.0029 \text{ day}^{-1}$$

Next, the settling coefficient, k_s, must be reevaluated using the mean depth of the hypolimnion and thermocline. The mean depth (3.38 m) was approximated by assuming the reservoir has a triangular cross section and an average maximum depth of 12.5 meters. Then:

$$k_s = 0.2 \text{ m day}^{-1}/3.38 \text{ m} = 0.06 \text{ day}^{-1}$$

Finally, the dissolved oxygen level 26 days after the onset of stratification is calculated by substituting these parameters into the oxygen uptake equations. The results are:

$$\Delta O_L = \left(\frac{402}{3.38 \text{ m}} + \frac{0.06 \times 3.8}{0.06 + 0.096 - 0.0029}\right)\left(1 - e^{-.0029 \times 26}\right)$$

$$- \left(\frac{0.06 \times 3.8}{0.06 + 0.096 - 0.0029}\right)\left(\frac{0.0029}{0.06 + 0.096}\right)\left(1 - e^{-(0.06 + .096)\times 26}\right) = 8.72 \text{ g m}^{-3}$$

$$\Delta O_c = \frac{0.096 \times 3.8}{0.096 + 0.06}\left(1 - e^{-(0.096 + 0.06)\times 26}\right) = 2.31 \text{ g m}^{-3}$$

$$O_t = 11.27 - 8.72 - 2.31 = 0.24 \text{ g m}^{-3}$$

By performing many similar calculations, the dissolved oxygen-time curves presented in Figure 3.6-4 were generated. Each of the four curves represents the predicted dissolved oxygen levels for one combination of values of the BOD loading rate, k_a, and water column BOD decay rate constant, k_1, expected in the Occoquan Reservoir. These curves indicate that the dissolved oxygen will be completely depleted in 25 to 100 days after the onset of stratification. If stratified conditions last four months, as predicted by the thermal plots, there could be as many as 20 to 95 days when water close to the reservoir bottom contains no oxygen.

The wide range of calculated times required to deplete the oxygen supply demonstrates the sensitivity of the oxygen level to the BOD loading and decay rates. This can also be seen from the equations used in the methodology presented here. The dissolved oxygen level has an exponential dependence on the first-order BOD decay rate constant in the water column, k_1, and the benthic layer, k_4. The decrease in the dissolved oxygen concentration at any time is directly proportional to the BOD loading rate, k_a. Because of the uncertainty inherent in the use of reported or calculated values of these constants, they should be measured in situ if quantitatively certain projections of dissolved oxygen levels are desired.

The accuracy of the hypolimnion dissolved oxygen model can be determined by a comparison of predicted and observed dissolved oxygen levels (see Table 3.6-21). At Occoquan Dam, the hypolimnion oxygen was depleted within 85 days of stratification in 1973. Since the reservoir is deepest at this location and a higher-than-average flow rate in 1973 resulted in weakly stratified conditions (see section 3.6.1)), the period in which oxygen is depleted in this case should be one of the longest likely to occur in the impoundment. The model predicted a maximum of 99 days would be required to consume the dissolved oxygen. Thus, the time required to consume the dissolved oxygen should fall below the predicted upper limit in nearly all cases.

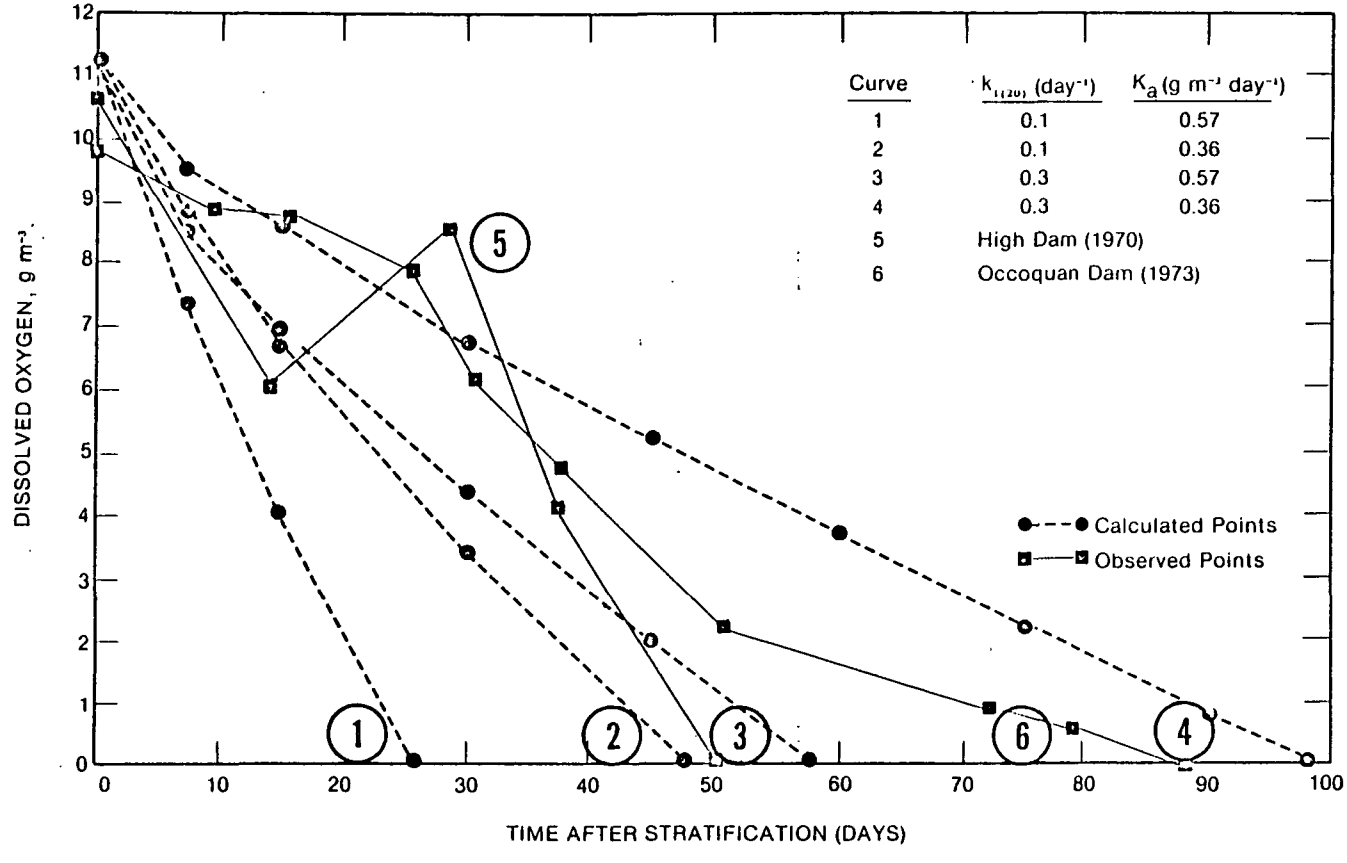

Figure 3.6-4. Dissolved oxygen depletion versus time in the Occoquan Reservoir

TABLE 3.6-21. HYPOLIMNION DISSOLVED OXYGEN IN OCCOQUAN RESERVOIR[a)]

Location	Depth (m)	Date	Dissolved Oxygen ($g\ m^{-3}$)
Occoquan Dam	7.6-16.8	4/9/73	9.9
		4/18/73	9.0
		4/24/73	8.7
		5/4/73	8.0
		5/9/73	6.3
		5/16/73	4.8
		5/29/73	2.3
		6/19/73	1.0
		6/26/73	0.6
		7/3/73	0.1
High Dam	4.3- 7.9	4/8/70	10.3
		4/16/70	10.7
		4/29/70	6.2
		5/14/70	8.6
		5/22/70	4.3
		6/5/70	0.1

[a)] Source: U.S. EPA STORET System.

Interpretation of the dissolved oxygen-time data at High Dam in 1970 presented in Table 3.6-21 is complicated by the introduction of fresh oxygen after the onset of stratification. Although a direct comparison of oxygen depletion times is not possible, the rates of oxygen level follows curve 2 of Figure 3.6-4 very closely, while during the second period of oxygen consumption the oxygen concentrations closely match those of curve 1. Since the reservoir is shallowest at High Dam and the substantially lower than average flow rate in 1970 resulted in strongly stratified conditions, the oxygen depletion rates in this case should be among the highest likely to be observed in the impoundment. Curve 1 represents the fastest decay rates predicted by the model. Thus, the observed oxygen consumption times should be greater than the lower limit predicted by the model in nearly all cases.

The above agreement of the observed with the predicted limits for the range of oxygen depletion times in Occoquan Reservoir implies that the typical or average time must also fall within the predicted range. Since it was for "average" conditions that the impoundment was modeled, it may be concluded that the model does accurately describe the behavior of the Occoquan Reservoir.

BIBLIOGRAPHY

Amy, G., et al., 1974. Water Quality Management Planning for Urban Runoff. EPA 440/9-75-004.

Camp, T. R. 1968. Water and Its Impurities. Reinhold Book Corporation. New York.

Delucia, R. and J. Smith. 1973. Effluent Charges: Is the Price Right? Meta Systems, Inc. September

Dyer, K.R. 1973. Estuaries: A Physical Introduction. John Wiley and Sons, London.

Eckenfelder, W.W. 1970. Water Quality Engineering for Practicing Engineers. Barnes and Noble, Inc., New York.

Grizzard, T.J., J.P. Hartigan, C.W. Randall, A.S. Librach, J.I. Kim, and M. Derewianka. 1977. Characterizing "Runoff Pollution - Land Use" Relationships in Northern Virginia's Occoquan Watershed. Presented at the MSDGC-AMSA Workshop on Water Quality Surveys for 208: Data Acquisition and Interpretation of Nonpoint Runoff. Chicago, IL. April 20-22, 1977.

Haan, C.T. 1977. Statistical Methods in Hydrology. The Iowa State University Press, Ames, Iowa 50010.

Likens, E., F. Bormann, S. Pierce, S. Eaton, M. Johnson. 1977. Biogeochemistry of a Forested Ecosystem. Springer-Verlag. New York, Heidelberg and Berlin.

Lippson, A.J. 1973. The Chesapeake Bay in Maryland. An Atlas of Natural Resources. The Johns Hopkins University Press. Baltimore and London.

Lorenzen, C.J. 1972. Extinction of Light in the Ocean by Phytoplankton. J. Cons. Int. Explor. Mer. 34:262-267.

McElroy, A.D., S.Y. Chiu, J.W. Nebgen, A. Aleti, F.W. Bennett. 1976. Loading Functions for Assessment of Water Pollution from Nonpoint Sources. EPA-600/2-76-151. U.S. Environmental Protection Agency, Washington, D.C.

Megard, R.O. 1979. Mechanisms and Models for the Transmission of Light Rates of Photosynthesis, and the Regulation of Phytoplankton Populations. In Phytoplankton-Environmental Interactions in Reservoirs (Lorenzen, M.W., ed.). Vol. I U.S. Army Corps of Engineers, Waterways Experiment Station, Vicksburg, MS. (In Press).

Midwest Research Institute. 1979. Personal Communication.

Northern Virginia Planning District Commission, Regional Resources Division. 1979a. Water Quality Goals for Nonpoint Pollution Management Program: Background Information. Falls Church, Virginia.

Northern Virginia Planning District Commission, Regional Resources Division. 1979b. Occoquon Basin Computer Model: Summary of Calibration Results. Falls Church, Virginia.

Officer, C.B. 1976. Physical Oceanography of Estuaries (and Associated Coastal Waters). John Wiley and Sons, Inc., New York.

Ohio Environmental Protection Agency. 1978. State Water Quality Management Plan, Sandusky River Basin Part II. Preliminary Report.

Pheiffer, T.H., L.J. Clark, and N.L. Lovelace. 1976. Patuxent River Basin Model Rates Study. Proceedings of the Conference on Environmental Modeling and Simulation, April 19-22, 1976, Cincinnati, Ohio. U.S. Environmental Protection Agency.

Porcella, D.B., A.B. Bishop. 1974. Comprehensive Management of Phosphorus Water Pollution. Ann Arbor Science, Ann Arbor, MI.

Pritchard, D.W. 1967. Observations of Circulation in Coastal Plain Estuaries. American Association for the Advancement of Science Publication No. 83, "Estuaries".

Schwab, G.O., R.K. Frevert, T.W. Edminster, K.K. Barnes. 1966. Soil and Water Conservation Engineering. John Wiley and Sons, New York, Second Edition.

State of Maryland and the Westinghouse (Electric) Corporation. 1972. Chester River Study. November.

State of Maryland. 1975. Maryland Water Quality 75. Joint Report of the Water Resources Administration, Environmental Health Administration and the Maryland Environmental Service.

Thompson, M.J., L.E. Gilliland, L.K. Rosenfeld. 1979. Light Scattering and Extinction in a Highly Turbid Coastal Inlet. Estuaries 2(3): 164-171. September.

Tsivoglou, E.C., J.R. Wallace. 1972. Characterization of Stream Reaeration Capacity. EPA-R3-72-012. U.S. Environmental Protection Agency, Washington, D.C. October.

U.S. Army Corps of Engineers, Baltimore District. 1977. Chesapeake Bay Future Conditions Report, Vol. 6, Water Quality. December.

U.S. Army Corps of Engineers, Buffalo District. 1978. Water Quality Data, Sandusky River Material Transport. Buffalo, N.Y.

U.S. Department of Commerce. 1965. Climatic Atlas of the United States. U.S. Dept. of Commerce, Environmental Science Services Administration, Environmental Data Service; Washington, D.C.

U.S. Environmental Protection Agency. 1973. Water Quality Criteria, 1972. EPA-R3-73-033, March, 1973. Washington, D.C.

Virginia Water Control Board, Tidewater Regional Office. 1977. Gloucester STP-Fox Mill Run/Ware River Special Studies #7-0178, October, 1977. Unpublished.

Zison, S.W., K. Haven, W.B. Mills. 1977. Water Quality Assessment: A Screening Methodology for Nondesignated 208 Areas. EPA-600/9-77-023. U.S. Environmental Protection Agency, Athens, GA.

Zison, S.W., W.B. Mills, D. Deimer, C. Chen. 1978. Rates, Constants, and Kinetics Formulations in Surface Water Quality Modeling. EPA-600/3-78-105. U.S. Environmental Protection Agency, Athens, GA.

APPENDIX A

MUNICIPAL DISCHARGE SUPPLEMENT

If effluent data is not available for sewage treatment plants in the study area waste loads can be roughly estimated by using survey data and reducing influent concentrations by knowledge of the type of treatment that the facility applies. In addition to the raw sewage data presented in the screening manual the following are also shown. Table A-1 is taken from Eckenfelder (1970) and shows typical municipal sewage characteristics. Once the influent characteristics of raw sewage to the treatment plant have been determined some effluent concentrations may be estimated by the following method.

Assume, for instance that the reduced nitrogen load for medium strength municipal sewage is 40 mg ℓ^{-1}. The BOD_5 of medium strength sewage is about 200 mg ℓ^{-1}. The ratio of the two times the influent BOD_5 (x) gives an estimated reduced nitrogen load (y) in the unknown influent.

$$\frac{40 \text{ mg-N } \ell^{-1}}{200 \text{ mg-BOD}_5 \ \ell^{-1}} \left(x \text{ mg-BOD}_5 \ \ell^{-1}\right) = y \text{ mg-N } \ell^{-1}$$

By multiplication by the stoichiometric factor for converting total oxidizable nitrogen to biochemical oxygen demand the $NBOD_5$ for the influent is estimated. Then, consulting Table A-2 (Delucia and Smith, 1973) a treatment efficiency for the particular type of treatment can be ascertained for BOD_5. Subtracting this fraction from unity and multiplying by the influent $NBOD_5$ gives an estimate of the effluent $NBOD_5$ from the sewage treatment plant. This proportioning procedure can be used for any of the parameters listed in Table A-2 (BOD_5, COD, suspended solids, total phosphorus, total nitrogen) to estimate effluent concentrations.

TABLE A-1. AVERAGE CHARACTERISTICS OF MUNICIPAL SEWAGE

Characteristics	Maximum	Mean	Minimum
pH	7.5	7.2	6.8
Settleable solids, mg ℓ^{-1}	6.1	3.3	1.8
Total solids, mg ℓ^{-1}	640	453	322
Volatile total solids, mg ℓ^{-1}	388	217	118
Suspended solids, mg ℓ^{-1}	258	145	83
Volatile suspended solids, mg ℓ^{-1}	208	120	62
Chemical oxygen demand, mg ℓ^{-1}	436	288	159
Biochemical oxygen demand, mg ℓ^{-1}	276	147	75
Chlorides, mg ℓ^{-1}	45	35	25

After Eckenfelder (1970)

TABLE A-2. MUNICIPAL WASTEWATER TREATMENT -- SYSTEM PERFORMANCE[a)]

Scheme Number[c)]	Effluent Concentrations (mg ℓ^{-1}) (% Total Removal Efficiencies[b)]) BOD_5	COD	SS	P_T, (mgP ℓ^{-1})	N_T, (mgN ℓ^{-1})
0, Raw Wastewater	200 (0%)	500 (0%)	200 (0%)	10 (0%)	40 (0%)
1	130 (35%)	375 (25%)	100 (50%)	9 (10%)	32 (20%)
2	40 (80%)	125 (75%)	30 (85%)	7.5 (25%)	26 (35%)
3	25 (88%)	100 (80%)	12 (94%)	7 (30%)	24 (40%)
4	18 (91%)	70 (86%)	7 (96%)	1 (90%)	22 (45%)
5	18 (91%)	70 (86%)	7 (96%)	1 (90%)	4 (90%)
6	13 (94%)	60 (88%)	1 (99.5%)	1 (90%)	3 (92%)
7	2 (99%)	15 (97%)	1 (99.5%)	1 (90%)	2 (95%)

a) Influent is assumed to be raw-medium strength domestic sewage. See scheme number 0 for characteristics.

b) Efficiencies for wastewater treatment are for the approximate concentration range, as measured by BOD_5, of $100 \leq BOD_5 \leq 400$ (mg ℓ^{-1}).

c) Scheme No. — Process

- 0..... No treatment
- 1..... Primary
- 2..... Primary, plus Activated Sludge (Secondary Treatment)
- 3..... Primary, Activated Sludge, plus Polishing Filter (High Efficiency or Super Secondary)
- 4..... Primary, Activated Sludge, Polishing Filter, plus Phosphorus Removal and Recarbonation
- 5..... Primary, Activated Sludge, Polishing Filter, Phosphorus Removal, plus Nitrogen Stripping and Recarbonation
- 6..... Primary, Activated Sludge, Polishing Filter, Phosphorus Removal, Nitrogen Stripping Recarbonation, plus Pressure Filtration
- 7..... Primary, Activated Sludge, Polishing Filter, Phosphorus Removal, Nitrogen Stripping Recarbonation, Pressure Filtration, plus Activated Carbon Adsorption